NASA/TM-2016-219177

Parametric Analysis of Surveillance Quality and Level and Quality of Intent Information and their Impact on Conflict Detection Performance

Nelson M. Guerreiro, Ricky W. Butler, George E. Hagen,
Jeffrey M. Maddalon, and Timothy A. Lewis
Langley Research Center, Hampton, Virginia

March 2016

NASA STI Program . . . in Profile

Since its founding, NASA has been dedicated to the advancement of aeronautics and space science. The NASA scientific and technical information (STI) program plays a key part in helping NASA maintain this important role.

The NASA STI program operates under the auspices of the Agency Chief Information Officer. It collects, organizes, provides for archiving, and disseminates NASA's STI. The NASA STI program provides access to the NTRS Registered and its public interface, the NASA Technical Reports Server, thus providing one of the largest collections of aeronautical and space science STI in the world. Results are published in both non-NASA channels and by NASA in the NASA STI Report Series, which includes the following report types:

- TECHNICAL PUBLICATION. Reports of completed research or a major significant phase of research that present the results of NASA Programs and include extensive data or theoretical analysis. Includes compilations of significant scientific and technical data and information deemed to be of continuing reference value. NASA counter-part of peer-reviewed formal professional papers but has less stringent limitations on manuscript length and extent of graphic presentations.

- TECHNICAL MEMORANDUM. Scientific and technical findings that are preliminary or of specialized interest, e.g., quick release reports, working papers, and bibliographies that contain minimal annotation. Does not contain extensive analysis.

- CONTRACTOR REPORT. Scientific and technical findings by NASA-sponsored contractors and grantees.

- CONFERENCE PUBLICATION. Collected papers from scientific and technical conferences, symposia, seminars, or other meetings sponsored or co-sponsored by NASA.

- SPECIAL PUBLICATION. Scientific, technical, or historical information from NASA programs, projects, and missions, often concerned with subjects having substantial public interest.

- TECHNICAL TRANSLATION. English-language translations of foreign scientific and technical material pertinent to NASA's mission.

Specialized services also include organizing and publishing research results, distributing specialized research announcements and feeds, providing information desk and personal search support, and enabling data exchange services.

For more information about the NASA STI program, see the following:

- Access the NASA STI program home page at http://www.sti.nasa.gov

- E-mail your question to help@sti.nasa.gov

- Phone the NASA STI Information Desk at 757-864-9658

- Write to:
  NASA STI Information Desk
  Mail Stop 148
  NASA Langley Research Center
  Hampton, VA 23681-2199

NASA/TM–2016-219177

Parametric Analysis of Surveillance Quality and Level and Quality of Intent Information and their Impact on Conflict Detection Performance

Nelson M. Guerreiro, Ricky W. Butler, George E. Hagen,
Jeffrey M. Maddalon, and Timothy A. Lewis
Langley Research Center, Hampton, Virginia

National Aeronautics and
Space Administration

Langley Research Center
Hampton, Virginia 23681-2199

March 2016

Available from:

NASA STI Program / Mail Stop 148
NASA Langley Research Center
Hampton, VA 23681-2199
Fax: 757-864-6500

Table of Contents

Acronyms and Abbreviations

ADS-B	-	Automatic Dependent Surveillance-Broadcast
BOC	-	bottom of climb
BOD	-	bottom of descent
BOT	-	beginning of turn
CD	-	conflict detection
CONUS	-	Continental United States
CTAS	-	Center/TRACON Automation System
EOT	-	end of turn
FA	-	false alert
FAA	-	Federal Aviation Administration
FL	-	flight level
ICAO	-	International Civil Aviation Organization
IFR	-	instrument flight rules
IQ1	-	intent information quality test matrix 1
IQ2	-	intent information quality test matrix 2
LOI	-	level of intent
LOS	-	loss-of-separation
MA	-	missed alert
MASPS	-	Minimum Aviation System Performance Standards
MD	-	missed detection
NACp	-	Navigation Accuracy Category for position
NACv	-	Navigation Accuracy Category for velocity
NAS	-	National Airspace System
PDF	-	probability density function
QOI	-	quality of intent
SA	-	Separation Assurance
SQ1	-	surveillance quality test matrix 1
SQ2	-	surveillance quality test matrix 2
SQ3	-	surveillance quality test matrix 3
SSR	-	Secondary Surveillance Radar
TC	-	trajectory change
TOC	-	top of climb
TOD	-	top of descent
TRACON	-	Terminal Radar Approach Control (Facility)
VFR	-	visual flight rules
WPT	-	fly-by waypoint

Nomenclature

alt	=	altitude, as a function of time
$\boldsymbol{C}$	=	single conflict or conflict set, true
$\widehat{\boldsymbol{C}}$	=	single conflict or conflict set, predicted
$\boldsymbol{d}_{GCD}$	=	great-circle distance function
D_H	=	horizontal distance
D_V	=	vertical distance
δ_t	=	time tolerance for conflict comparison criteria
δ_H	=	horizontal distance tolerance for conflict comparison criteria
δ_V	=	vertical distance tolerance for conflict comparison criteria
Δalt_{Q4}	=	altitude interval for intent quality 4 vertical points
Δt_{LOS}	=	relative time-to entry into loss-of-separation
$\Delta t_{LOS,mean}$	=	mean time-to loss-of-separation at first detection
Δt_{Q4}	=	time interval for intent quality 4 horizontal points
Δt_{traj}	=	track data and trajectory prediction time interval
$\boldsymbol{\varepsilon}$	=	error vector
$\boldsymbol{f}_{GCD}$	=	great-circle projection function
IQ_H	=	horizontal quality of intent
IQ_V	=	vertical quality of intent
Γ	=	Gamma function
gs	=	groundspeed, as a function of time
H_{sep}	=	horizontal separation criterion
lat	=	latitudinal position, as a function of time
lon	=	longitudinal position, as a function of time
$N_{\widehat{\boldsymbol{C}}}$	=	number of predicted conflicts
$N_{\boldsymbol{C}}$	=	number of true conflicts
$N_{\boldsymbol{C},sim}$	=	number of true losses-of-separation in one simulation run
N_{FA}	=	number of false conflict alerts
N_{MA}	=	number of missed conflict alerts
N_{MD}	=	number of loss-of-separation missed detections
P_{FA}	=	probability of false alert
P_{MA}	=	probability of missed alert
P_{MD}	=	probability of missed detection
R_s	=	surveillance range
$\boldsymbol{s}$	=	position state vector
$\hat{\boldsymbol{s}}$	=	position state vector estimate
SQ_{model}	=	surveillance quality parameter set
σ_r	=	surveillance horizontal position error standard deviation
σ_a	=	surveillance altitude error standard deviation
σ_{gs}	=	surveillance groundspeed error standard deviation
σ_{vs}	=	surveillance vertical speed error standard deviation
σ_{trk}	=	surveillance track angle error standard deviation
t	=	time
$\boldsymbol{T}$	=	true trajectory
$\widehat{\boldsymbol{T}}$	=	predicted trajectory
t_{cd}	=	conflict detection time
T_{det}	=	conflict detection cycle period
T_{int}	=	time horizon for intent information

t_{LOS}	=	time at entry into loss-of-separation
T_{pred}	=	time horizon for trajectory prediction and conflict detection
t_s	=	surveillance time
$t_{shift,max}$	=	maximum track time shift
t_{sl}	=	surveillance lag time
trk	=	track angle, as a function of time
$\boldsymbol{v}$	=	velocity state vector
$\hat{\boldsymbol{v}}$	=	velocity state vector estimate
vs	=	vertical speed, as a function of time
V_{sep}	=	vertical separation criterion

Abstract

A loss-of-separation (LOS) is said to occur when two aircraft are spatially too close to one another. A LOS is the fundamental unsafe event to be avoided in air traffic management and conflict detection (CD) is the function that attempts to predict these LOS events. In general, the effectiveness of conflict detection relates to the overall safety and performance of an air traffic management concept. An abstract, parametric analysis was conducted to investigate the impact of surveillance quality, level of intent information, and quality of intent information on conflict detection performance. Surveillance quality was represented by a surveillance error model of current and proposed surveillance technologies through a set of position and velocity state accuracy standard deviations. Level of intent information was represented by an intent time horizon and quality of intent information was represented by various levels of intent data, each providing incrementally more information to define the vertical and horizontal components of a kinematic trajectory. CD performance was measured using the primary metrics of false alert probability, missed alert probability, missed detection probability, and mean time-to-LOS at first detection. Two complementary analysis methods were used to conduct the analysis runs; one method used time-shifted, recorded traffic data from the National Airspace System (NAS) as the source for scenarios while the second used circular traffic scenarios with flight plans randomly-generated using the characteristics observed in the NAS traffic data. Three surveillance quality test matrices were implemented to investigate: (1) the CD performance impact of a set of surveillance technologies and several variations of conflict detection and trajectory prediction parameters, (2) the sensitivity of the performance metrics to each of the surveillance error and trajectory prediction and conflict detection parameters, and (3) the variability of the performance metrics to different random traffic scenarios and to Monte Carlo sampling. Two level and quality of intent information test matrices were implemented to investigate: (1) the CD performance impact of different levels of intent and different qualities of intent information with several variations of trajectory prediction and conflict detection parameters, (2) the variability of the performance metrics to different random traffic scenarios and the sensitivity of the performance metrics to the time and altitude interval parameters used to represent the highest quality of intent information modeled.

The surveillance quality analysis runs quantified the conflict detection performance of some expected trends. State-projection trajectory prediction, used in the surveillance quality runs, exhibits poor performance, even in the presence of no surveillance error and with a short trajectory prediction and CD horizon. As the trajectory prediction and CD horizon increases, the false alert probability, missed alert probability, and mean time-to-LOS increase while the missed detection probability decreases. Surveillance technologies with high position and velocity state accuracies result in better CD performance than those with low position and velocity state accuracies. The sensitivity curves indicate that false alert and missed alert probabilities are most sensitive to CD and trajectory prediction horizon and vertical speed errors. Missed detection probability is sensitive to most of the parameters tested, with the lowest sensitivity being due to vertical position error. The mean time-to-LOS metric is most sensitive to CD cycle period, CD and trajectory prediction horizon, and surveillance range. The variability of the CD performance metrics to different traffic scenarios with the same input parameters and to Monte Carlo sampling is small based on the parameters and scenarios tested.

The conflict detection performance generally improves as the level and quality of intent information is increased. The level of intent trends indicate that conflict detection performance is improved as the intent horizon approaches the trajectory prediction and CD horizon. When the CD horizon is equal to the intent horizon, CD performance is improved by a shorter detection horizon for the metrics of false alerts, missed alerts, and missed detections but there is a negative impact on the mean time-to-LOS metric. The use of shorter conflict detection cycle periods has a positive impact on CD performance, primarily by reducing the missed detection rate. The variability of the CD performance metrics due to different traffic scenarios in the presence of intent information is small based on the parameters and scenarios tested.

The data collected in this parametric analysis can be used to estimate the conflict detection performance under alternative future scenarios or alternative allocations of the conflict detection function, based on the quality of the surveillance and intent data under those conditions. Alternatively, this data could also be

used to estimate the surveillance and intent information quality required to achieve some desired CD performance as part of the design of a new separation assurance system.

I. Introduction

Separation Assurance (SA) has been an area of study for government agencies, research institutions, and Universities for a few decades [1]. The motivation for that work stems from the need to provide higher levels of automation for the separation assurance functions in order to increase the capacity of the National Airspace System, while retaining or increasing the level of safety of the system. Some research has explored the potential allocation of the separation assurance functions amongst different agents in the system, including air traffic controllers, flight crews, and automation systems. In a broader sense, this area of research is called Function Allocation.

Function Allocation research is focused on understanding the impacts of allocating the separation assurance functions between air and ground agents and between human and automation systems in different ways. All separation assurance systems are comprised of two primary functions: conflict detection and conflict resolution. However, other functions may also be provided, such as conflict prioritization, conflict prevention, complexity avoidance, etc. The performance of a specific allocation of the separation assurance functions has typically been studied as a complete system. In this work, the performance impact of only one of the primary functions is investigated, namely, the performance of the conflict detection function. More specifically, this work is focused on measuring the performance of conflict detection as a function of parameters directly related to the air-ground allocation.

The objective of this work was to develop a set of data characterizing the performance of conflict detection in a parametric way as a function of the quantity and quality of data available to perform that function. Differences in the quantity and quality of data available to the conflict detection function could be considered the primary distinguishing features between an airborne or ground-based allocation of that function. Thus, the parametric set of data generated by this work can be used to support the analysis of the performance of a complete separation assurance function allocation scheme, or to make recommendations regarding the quantity and quality of data that should be used to perform conflict detection with some required minimum level of performance.

The organization of this document is as follows: Section II provides some background on conflict detection and prior work as it relates to the current work. Section III describes the analysis models used to collect the parametric performance data and the specifics of some of the modeling elements. Section IV describes the input data used in the analysis and the method used for creating traffic scenarios. Section V presents the metrics and definitions used to characterize conflict detection performance. In section VI, the analysis test matrices are presented. The results of the analysis runs are presented and discussed in section VII. Finally, the Appendix describes additional modeling details.

II. Background

Conflict detection refers to the identification or prediction of a future loss-of-separation between two aircraft based on the predicted futures states of those aircraft. The conflict detection function is a core function of any separation assurance system, as shown in the simplified separation assurance system diagram in Figure 1. Its performance has a direct impact on the effectiveness of the conflict resolution function. If the CD function provides an alert to a conflict that does not exist (false alert), then the conflict resolution function may compute an unnecessary resolution maneuver. If the CD function does not provide an alert for a LOS that does exist (missed alert), then safety issues may result. For these reasons, it is important to understand the performance characteristics of the conflict detection function independent from other separation assurance functions.

The conflict detection function is often tightly integrated with a trajectory prediction function, which can be considered to be the largest contributor to CD performance. The trajectory prediction function and the CD performance function define the domain for analysis in this work. The inputs to this sub-system are the surveillance information for relevant traffic, the intent information that may be available for that traffic, and any other sources of information relevant to trajectory prediction, such as wind information or aircraft performance parameters. The outputs of this sub-system are the detected conflicts. Figure 1 shows

the input/output diagram and the trajectory prediction and conflict detection relationship in a separation assurance system and also highlights the CD performance analysis domain explored here.

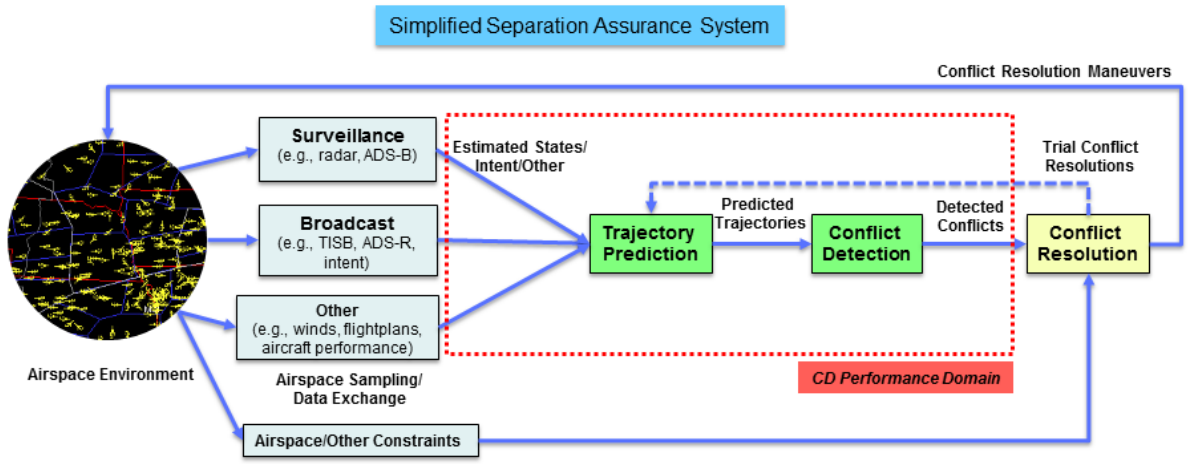

Figure 1. Simplified separation assurance diagram and the CD performance analysis domain for this work.

An abstract, parametric approach to analyze conflict detection performance aids in the analysis of fundamental large-scale system trade studies of air traffic management concepts. Thus, general trends can be evaluated without requiring the detail of particular algorithms, communication technologies, etc. This type of analysis is particularly appropriate for analyzing different conflict detection function allocations. For example, airborne allocation of conflict detection may have very good information about the ownship's current state and intent but little information about the surrounding traffic's intent. Similarly, an automated conflict detection system running on a centralized server may have a good level of intent information about all nearby traffic, based on flight plan information, but may have less accurate current state information for any single aircraft. Rather than studying only two specific allocation schemes, an abstract, parametric analysis enables the estimation of conflict detection performance for many allocation schemes. Data interpolation is one possible approach that can be used when the input data characteristics can be cast into a parameterization consistent with that used in this analysis.

A. Prior Conflict Detection Research

An extensive body of work exists in the literature with respect to trajectory prediction [2, 3] and conflict detection [4-6]. A large portion of prior work is focused on the design of conflict detection algorithms and the performance of those implementations in simulation. Additionally, a significant amount of work has been done to study human performance in performing separation assurance functions in the face of different conflict alerting systems [7, 8].

The performance of various conflict detection algorithms (sometimes called alerting algorithms) has been analyzed in prior work [9-13]. Paglione [9] evaluated the performance of the Federal Aviation Administration's (FAA) Host computer detection algorithms while Bilimoria [10] performed a similar evaluation for the NASA Center/TRACON Automation System's (CTAS) detection algorithms. Prior work has also studied conflict detection independent of an algorithm. This research has shown that a conflict detection algorithm can be developed that is correct, within a given approximation bound, for an arbitrary trajectory [14]. Therefore, if a correct algorithm is used, the performance of the CD function is dominated by factors such as trajectory prediction sophistication, alerting buffers, and other heuristics.

The impact of data quality (described in terms of surveillance quality and navigation error) and data content have been discussed in prior work [15, 16]. The impact of intent availability has also been studied [17-20] in the context of separation assurance. Chung [15] discusses the implication of surveillance delays and how these could be used to determine buffers for the trajectory prediction of future states. Finkelsztein [18] has looked at the sensitivity of the range at closest point of approach in a parametric analysis.

Our investigation of the prior work in conflict detection performance revealed that more work was needed to provide a parametric and broadly-applicable characterization of conflict detection performance, which was the focus of this work. In much of the prior work, it is difficult to separate the performance of the entire SA system, which is typically measured by observed losses-of-separation, from the performance of conflict detection alone, which is typically characterized by false and missed alert rates. Many of these studies were performed using a conflict resolution algorithm which had the consequence of directly impacting the key performance metrics. Also, prior work consisted of algorithm design, human factors implications, and full SA system performance, whereas this work is focused on the performance of conflict detection as a function of the quality and content of the input data.

B. Research Questions

This study was focused on collecting the data needed to answer two fundamental questions:

1. ***What are the impacts of surveillance quality on conflict detection performance?***
2. ***What are the impacts of level and quality of intent information on conflict detection performance?***

Surveillance quality has a direct impact on the accuracy of the flight state estimate available for trajectory prediction. Flight state information received from a radar system will have different accuracy than that received from an ADS-B system, primarily due to the differences in the sensing and transmission mechanisms. To answer question 1, the parametric impact of flight state accuracy on conflict detection was analyzed in a way that allows for the evaluation of the performance under various surveillance systems and data exchange scenarios.

Flight intent information can have an even more significant impact on trajectory prediction accuracy and conflict detection performance. To answer question 2, the impact of the amount of intent information available for trajectory prediction and the quality of that intent information on conflict detection performance was analyzed. The level of intent information is related to the time horizon for which intent information is provided while the quality of intent information is related to the amount of information that is contained in that intent for the purposes of re-creating a trajectory. Quality of intent information can range from simple target-state information to a more detailed kinematic representation of the trajectory.

III. Analysis Model

The conflict detection performance analysis was completed using two analysis methods. The first analysis methodology (Method 1) involved the use of recorded traffic tracks time-shifted to create NAS-wide scenarios with losses-of-separation. Similar analysis approaches with time-shifted recorded data have been used in the past by other researchers [21]. The recorded traffic data contains much of the complexity that is typically difficult to replicate in a fast-time simulation, such as the airspace structure and routings, the varying performance of many aircraft types, and step climbs and descents. The primary disadvantage of using real aircraft traces is that losses of separation are rare events in the airspace system. The only appropriate modification that can increase the number of LOS events while maintaining the real-world nature of this data is temporal shifting. Method 1 leverages this temporal shifting to create losses-of-separation that did not exist in the as-flown track data as targets for the conflict detection function.

The second analysis methodology (Method 2) uses randomly generated flight plan scenarios over a generic volume of airspace. A circular region of airspace is defined and flight plans are randomly generated using a set of distributions for parameters such as track angle change, flight segment length, average groundspeed, and others, to traverse the circular region. To retain some level of credibility for the flight plans randomly generated, the sampling distributions used for the parameters were derived from the observed characteristics in the NAS-recorded traffic data. The advantage of using this second analysis methodology is that scenarios can be simulated with conditions that can further stress test the conflict detection function, such as with geometries or conditions that may not be present in the time-shifted,

recorded data. Also, method 2 had shorter scenario execution times that allowed analysis runs to be completed more quickly.

The two analysis methods had the same basic functionality: traffic simulation/playback, trajectory prediction, conflict detection, and metrics collection. A scenario of traffic was simulated within some airspace region (NAS-wide for method 1 and regional for method 2) and conflict detection and trajectory prediction was executed at a given interval or period within that simulation. For method 1, the simulation was simply a time-shifted play-back of the recorded track data while in method 2 a kinematic trajectory generation step was used to simulate the flight plan prescribed in the scenario. During each CD cycle, a trajectory prediction was created for each aircraft using the quantity and quality of data specified by a set of input parameters, the predictions were compared pair-wise to determine a set of predicted conflicts, the true or simulated aircraft tracks were compared pair-wise to determine the set of true conflicts, and, finally, the comparison of the true versus predicted conflicts constituted the metrics collection.

The use of two analysis methods allowed for the cross-validation of results and for balancing of the advantages and disadvantages of each method. The assumptions used in both methods were verified through a common set of inputs that produced a comparable set of metrics results. The impact of modeling differences between the two analysis methods are highlighted throughout this document.

A. Simulation Control

The traffic simulation was implemented as a simple execution loop that advanced each aircraft to the appropriate position in the recorded or emulated track data at each simulation time, until all aircraft tracks had completed. The simulation step size was determined by the desired conflict detection cycle period, T_{det}. The simulation times where trajectory prediction, conflict detection, and metrics collection would occur were integer multiples of this parameter.

B. Trajectory Prediction

Trajectory propagation methods for conflict detection can be classified as deterministic, probabilistic, and worst-case. In a deterministic case, a single trajectory prediction is assumed to have a 100% probability of occurring. In the probabilistic case, each possible trajectory prediction for an aircraft has a probability of occurring. Finally, a worst-case approach assumes 100% probability on any possible trajectory for an aircraft, thereby defining a bounded region ahead of the aircraft that encompasses all possible future trajectories. Each of these methods requires its own set of assumptions for implementation; the choice can be made based on the use case. Because, for this study, the results are intended to apply NAS-wide and many probabilistic effects are explored through the Monte Carlo approach used, the deterministic trajectory propagation method was chosen.

At each conflict detection time, t_{cd}, a deterministic trajectory prediction, $\hat{\boldsymbol{T}}_i(t)$, was created for each aircraft i, for all times, t, between t_{cd} and $t_{cd} + T_{pred}$, where T_{pred} is the trajectory prediction and CD time horizon. In the case where no intent information was available, a simple state-projection trajectory prediction was used whereby, the current position vector of each aircraft was projected from time t_{cd} to time $t_{cd} + T_{pred}$ using the current velocity vector. In the runs where intent information was available, constant velocity or constant acceleration segments were used to build a piece-wise trajectory prediction up to a future time given by $t_{cd} + T_{int}$ (using constant radius turn geometry and constant vertical acceleration regions, where T_{int} is the intent horizon time). Separate lateral and vertical trajectory profiles were generated and these were synchronized using the time elements of the two predictions. For cases where the trajectory prediction horizon was longer than the intent horizon ($T_{pred} > T_{int}$), a state projection was used to estimate the states beyond the intent horizon point.

Analysis method 1 used a discretized representation for track data and trajectory predictions, with discrete state information at every five seconds ($\Delta t_{traj} = 5$ s). In contrast, analysis method 2 used a kinematic description of a trajectory, with state information given as the start or end point of a constant velocity or constant acceleration segment – a more concise trajectory representation.

C. Conflict Detection

A conflict is a future LOS between two aircraft based on some model of their trajectories. There are two types of conflicts and LOS's reported in this paper: true and predicted, so careful terminology is required. The major contribution of this paper is a parametric analysis of the information types and error sources going into different trajectory predictions and comparing the conflict detection effectiveness based on these predictions to the ideal conflict detection effectiveness based on true trajectories. A predicted LOS may never manifest itself because the true trajectories of the aircraft may be different from the trajectory predictions. Or, the LOS may not manifest because of a maneuver issued by a conflict resolution function. We do not consider this case, because this work is not concerned with conflict resolution.

A *true conflict*, denoted $\boldsymbol{C}_{m,i,j}$, is when a future LOS occurs in the true trajectories of the aircraft, denoted, $\boldsymbol{T}_i(t)$ and $\boldsymbol{T}_j(t)$. A *predicted conflict*, denoted $\widehat{\boldsymbol{C}}_{n,i,j}$, is when a future LOS occurs in the predicted trajectories of the aircraft, denoted, $\widehat{\boldsymbol{T}}_i(t)$ and $\widehat{\boldsymbol{T}}_j(t)$. Formally, a LOS is when, simultaneously, the horizontal distance between the aircraft trajectories (either true or predicted) is less than the horizontal separation criterion, H_{sep}, and the vertical distance is less than the vertical separation criterion, V_{sep}. Given a pair of trajectories (either true or predicted), a conflict (respectively either true or predicted) exists at t_{cd} if there exists some time, t, within the time horizon ($t_{cd} < t \leq t_{cd} + T_{pred}$), where those trajectories have a LOS.

Conflict detection was executed at a specified time interval, T_{det}, during the simulation/playback of the traffic in a given scenario. During each conflict detection cycle, the trajectory predictions of all aircraft were compared pair-wise to identify the set of *predicted* conflicts, $\widehat{\boldsymbol{C}}$, for that detection cycle. The true losses-of-separation between all aircraft, which were pre-processed from the true aircraft tracks at the beginning of the scenario run, were used to identify the set of *true* conflicts, $\boldsymbol{C}$, for that conflict detection cycle.

Surveillance range was simulated during each conflict detection cycle by not performing conflict detection between specific pairs of aircraft. If the distance from current position of an aircraft j to the current position of another aircraft i was greater than the surveillance range parameters, R_s, then conflict detection was not executed for that aircraft pair.

In analysis method 1, conflict detection was performed over a discretized trajectory whereas, in analysis method 2, conflict detection was performed by comparing linear trajectory segments. These modeling assumptions are one reason for the differences in the results between the two analysis methods, but the differences were small. Method 1 could not identify instances of LOS that last less than the trajectory sampling interval (5 seconds) and that occur between trajectory sample points whereas method 2 did not have this limitation.

D. Metrics Collection

Metrics collection was done during each conflict detection cycle. The primary metrics (e.g., false alerts (FA) and missed alerts (MA)) were collected by comparing the predicted and true conflict sets during each detection cycle. FA and MA counts were aggregated over all conflict detection cycles of a single analysis scenario run. More details on the full set of metrics used in this analysis can be found in section V.

E. Surveillance Quality

The impacts of surveillance quality (research question 1) on conflict detection performance were analyzed using a surveillance error model. The model implements an un-compensated surveillance lag time parameter, t_{sl}, as well as a set of standard deviation parameters, (σ_r, σ_a, σ_{gs}, σ_{vs}, σ_{trk}), for the Gaussian distributions of error on the position and velocity states of aircraft. The position errors were modeled via a range error parameter, σ_r, and an altitude error parameter, σ_a, while the velocity errors were modeled via vertical speed, groundspeed, and track angle error parameters, σ_{gs}, σ_{vs}, σ_{trk}, respectively. Figure 2 shows a graphical representation of the surveillance error modeling approach, while a more detailed description of the surveillance error modeling approach can be found in the Appendix.

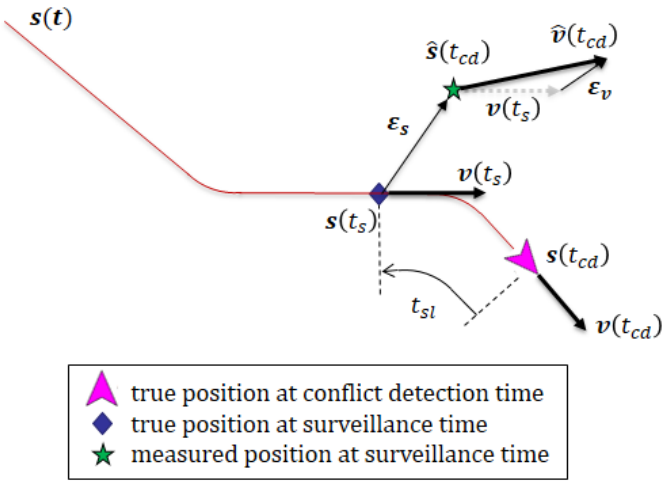

Figure 2. Position and velocity error components for surveillance modeling (horizontal profile).

Three surveillance technologies were simulated in the analysis discussed here, as well as the baseline case with no added surveillance error. One of the surveillance technologies analyzed was the current-day secondary surveillance radar (SSR). The parameter values for the modeling of the position error for this surveillance technology are described in an ICAO document [22]. The velocity error parameters were obtained from a study that compared Data Link-provided (considered truth) state information with that being obtained from ATC data feeds [23].

The second surveillance technology analyzed was Automatic Dependent Surveillance-Broadcast (ADS-B), in two variations. One of the challenges in defining the ADS-B parameters for the surveillance error model is the uncertainty of the accuracy of future avionics equipment over a diverse aircraft fleet. The Minimum Aviation System Performance Standards (MASPS) for ADS-B, DO-242A [24], defines the accuracy levels that the position and velocity values can have in terms of a 95% error bound and the associated, reported NACp and NACv values, but does not make recommendations about which accuracy levels to use for any given application. Instead, the MASPS for Airborne Surveillance Applications, DO-289 [25], was used to select the parameter values for ADS-B. DO-289 provides a minimum recommendation for the position and velocity error bounds (NACp>=5, NACv>=2) as well as desired values (NACp>=9, NACv>=3) for conflict detection applications. For the purposes of this study, we refer to the minimum ADS-B requirements as ADSB_1 and the desired requirements as ADSB_2 and both were simulated in this analysis.

Table 1 lists the values chosen for these three technology levels. The lag time parameter is a fixed value that was applied across all surveillance samples in each simulation scenario while the remaining parameters are standard deviation of the modeled Gaussian error distributions, each with an assumed zero mean value. The parameter SQ_{model} was used to denote a set of surveillance error parameters (the columns of Table 1) for each of the three surveillance error models and the baseline case of no surveillance error; possible values for this parameters were: None, Radar, ADSB_1, or ADSB_2.

Table 1. Surveillance error parameters for the simulated technologies.

Error Parameter	None	Radar	ADSB_1 (NACp=5,NACv=2)	ADSB_2 (NACp=9,NACV=3)
lag time (t_{sl})	0 seconds	12 seconds	1 second	1 second
horizontal position (σ_r)	0.0 NM	0.3 NM	0.25 NM	0.0081 NM
altitude (σ_a)	0.0 ft	127.5 ft	108.8 ft	73.8 ft
groundspeed (σ_{gs})	0.0 NM/hr	17.4 NM/hr	2.9 NM/hr	1.0 NM/hr
vertical speed (σ_{vs})	0 ft/min	495 ft/min	450 ft/min	150 ft/min
track angle (σ_{trk})	0 deg	3.73 deg	1 deg	1 deg

F. Level and Quality of Intent Information

The impacts of intent information on conflict detection performance (research question 2) were investigated using a representation of level of intent (LOI) and a representation of quality of intent (QOI). In this analysis, level of intent refers to the relative time horizon over which intent information is available and is denoted by the parameter T_{int}. For example, intent information may be available for trajectory prediction for the next five minutes from the current time. LOI parameter values for short, medium, and long time horizons (5, 10, and 20 minutes) were used in this analysis. Instead of a time horizon, some studies [18] represent the level of intent by the number of communication transmissions, e.g., number of trajectory change points [24]. The appeal of using number of communication transmissions is that this parameter closely relates to the load on the communication system, which is a significant cost driver. On the other hand, the number of conflicts and losses, which are the primary metrics of this study, are more closely tied to the time horizon than the number of points; for instance, five trajectory change points could represent one minute of a trajectory, or one hour of a trajectory. More pointedly, the number of communication transmissions alone cannot be used to determine communication load; the content of the message must also be defined. One message with five points is equivalent to five messages with one point each; the content of a message mixes parametric variables. In our study, the content of a message is described as the quality of intent. To maintain this separation of concerns, only the time horizon is used in LOI.

The quality of intent (QOI) representation refers to the amount of information that is contained in the available intent. This representation was partially inspired by the ADS-B MASPS definition of a trajectory change (TC) report [24], whereby a lateral TC point, for example, includes a reference point and may contain information about the turn geometry, such as turn radius and the track into and out of that reference point. The representation differs from the ADS-B MASPS definition in the use of five levels that contain more or less information than the proposed MASPS. Quality of intent information was further broken down into the vertical and horizontal components and was represented by the parameters IQ_V and IQ_H, respectively. The separation of the horizontal and vertical components of intent information allowed us to perform analysis runs with a DO-242A-equivalent representation of intent information, specifically, with IQ_{V1} and IQ_{H2}. Table 2 shows the quality of intent representations used in this analysis and the information associated with each lateral and vertical intent point.

The vertical intent information available for trajectory prediction ranges from target altitude only to fully-defined altitude change points. Vertical intent quality of zero (IQ_{V0}) specifies that target altitude information will be available during an altitude change maneuver. Vertical quality of one (IQ_{V1}) adds to the vertical quality of zero by providing 2-dimensional (time and altitude) information for any bottom-of-climb (BOC) or top-of-climb (TOC) points within the intent horizon, for any climb maneuver. With vertical quality two (IQ_{V2}), each BOC and TOC point also contains the target climb rate out-of or into those points, respectively. Vertical quality of three (IQ_{V3}) adds a constant acceleration value used to transition from the BOC point to the target climb rate or to transition from the target climb rate to the TOC point. Finally, vertical intent quality of four (IQ_{V4}) adds additional 2-dimensional vertical profile points at a specified altitude interval (Δalt_{Q4}) between any BOC and TOC points. The same set of information hierarchy applies to the top-of-descent (TOD) and bottom-of-descent (BOD) intent points and the vertical profile of any descent maneuver.

A similar quality of intent scheme was used for the lateral intent information that ranged from target track to fully-defined track change points. Lateral/horizontal intent quality of zero (IQ_{H0}) specifies the target track that is available during a turning maneuver. Lateral quality of intent one (IQ_{H1}) adds the 3-dimensional reference point (time, latitude, longitude) for the turn, which is assumed to be the equivalent of a fly-by waypoint. With lateral quality level two (IQ_{H2}), the radius for an assumed constant radius turn for the fly-by maneuver is provided. The trajectory prediction function uses the turn radius information, along with an estimated groundspeed, to determine the turn rate for the turn maneuver. Lateral quality of intent three (IQ_{H3}) includes a turn rate value which, combined with the turn radius, defines the groundspeed for the constant turn rate and constant radius turn. Finally, lateral intent quality of four (IQ_{H4}) adds

additional 3-dimensional points at a specified time interval (Δt_{Q4}) between subsequent turn reference points.

Additional details regarding the methods used to obtain intent information from the recorded traffic data for this study are provided in section IV, sub-section A.

Table 2. Quality of intent (QOI) values on the horizontal and vertical profiles.

Horizontal/ Vertical Quality	Target State	Position 2-D/3-D	Target Rates	Acceleration
IQ_{V0}	Target altitude			
IQ_{V1}	Target altitude	Time, altitude		
IQ_{V2}	Target altitude	Time, altitude	Target climb rate	
IQ_{V3}	Target altitude	Time, altitude	Target climb rate	Vertical acceleration
IQ_{V4}	Includes all IQ_{V3} points plus additional IQ_{V1} points added based on refined vertical profile requirements (Δalt_{Q4})			
IQ_{H0}	Target track			
IQ_{H1}	Target track	Time, latitude, longitude[1]		
IQ_{H2}	Target track	Time, latitude, longitude	Turn radius[2]	
IQ_{H3}	Target track	Time, latitude, longitude	Turn radius	Turn rate[3]
IQ_{H4}	Includes all IQ_{H3} points plus additional IQ_{H1} points added based on refined horizontal profile requirements (Δt_{Q4})			

Notes: *[1] Track in and track out are available with all intent waypoints for horizontal quality levels of 1 and above. [2]Combine with estimated turn speed to estimate turn rate. [3]Combined with radius provides turn speed and centripetal acceleration.*

G. Analysis Parameters

A comprehensive set of the parameters used in this analysis of conflict detection performance is presented in Table 3, along with the nominal values used for each parameter. The nominal values were used in each scenario unless otherwise specified in the experiment test matrices in section VI. Note that the horizontal and vertical separation criteria (H_{sep} and V_{sep}) were held constant for all analysis runs. Similarly, all track data and trajectory predictions used a single resolution (Δt_{traj}) of five seconds for analysis method 1.

Table 3. Analysis input parameters.

Parameter	*Description*	*Nominal Value*	*Units*
T_{det}	conflict detection cycle period	60	seconds (s)
T_{pred}	trajectory prediction and conflict detection time horizon	1200	seconds (s)
Δt_{traj}	trajectory sampling interval	5	seconds (s)
H_{sep}	horizontal separation criterion	5	nautical miles (NM)
V_{sep}	vertical separation criterion	800	feet (ft)
R_s	surveillance range	1500	nautical miles (NM)
SQ_{model}	surveillance quality parameter set	None	-
t_{sl}	surveillance lag time	0	seconds (s)
σ_r	surveillance horizontal position error standard deviation	0	nautical miles (NM)
σ_a	surveillance altitude error standard deviation	0	feet (ft)
σ_{gs}	surveillance groundspeed error standard deviation	0	knots (kn)
σ_{vs}	surveillance vertical speed error standard deviation	0	feet/minute (ft/min)
σ_{trk}	surveillance track angle error standard deviation	0	degrees (deg)
T_{int}	intent horizon time (level of intent)	0	seconds (s)
IQ_V	vertical quality of intent	None	-
IQ_H	horizontal quality of intent	None	-
Δt_{Q4}	time interval for intent quality 4 horizontal points	120	seconds (s)
Δalt_{Q4}	altitude interval for intent quality 4 vertical points	1000	feet (ft)
δ_t	time tolerance for conflict comparison criteria[1]	120	seconds (s)
δ_H	horizontal distance tolerance for conflict comparison criteria[1]	10	nautical miles (NM)
δ_V	vertical distance tolerance for conflict comparison criteria[1]	2000	feet (ft)

H. Assumptions and Scope

The scope and assumptions used in this analysis help to define the realm of applicability of the results obtained. The scope of this analysis was limited to the evaluation of en-route conflict detection performance in an architecture- and algorithm-agnostic way. The analysis does not include conflict resolution nor does it explore the development of any new, or the refinement of any existing, conflict detection algorithms.

The primary assumptions used in the analysis modeling are listed below. Note that some assumptions are also inherent to the data processing algorithms used and are described later in this document.

- Conflict detection is being performed by automation
- Conflict detection uses deterministic trajectory predictions
- Conflict detection performance is dependent on the assumptions used in trajectory prediction
- The true trajectory flown by each aircraft is known perfectly and *a priori*
- No added atmospheric disturbances, such as wind, are used in simulation or in trajectory prediction
- Only trajectory data above flight level (FL) 180 are used for the recorded traffic tracks
- A horizontal separation criterion of 5 nautical miles is used for CD
- A vertical separation criterion of 800 feet is used for CD[1]
- The surveillance range is assumed to be aircraft-centric with respect to the first aircraft in the aircraft pair
- The surveillance error model assumes zero-mean, Gaussian error distributions

[1] This value was used instead of 1000 ft to prevent spurious detections caused by small fluctuations and noise in the altitude data.

- The intent information was inferred from the track data using a custom curve-fitting algorithm developed for this project[2]
- There is no lag in the intent information at conflict detection time
- Blunders in the form of missing intent or non-conformance to intent are not considered
- An intent point is added at the intent horizon time if another intent point does not already exist close to that horizon

IV. Input Data

The CD performance analysis leveraged a set of recorded traffic tracks from the NAS. The source data is a fused, NAS-wide data set that covers 45 days in 2013 and is stored in the Data Warehouse at the NASA Ames Research Center. Surveillance radar and ADS-B feeds from multiple facilities are fused to create full visual- and instrument-flights-rules (VFR and IFR) track profiles (latitude, longitude, altitude, and time) for flights within the Continental United States (CONUS), and partial track profiles for flights entering and exiting the NAS.

A representative day of traffic was chosen from this data set for use in this analysis. Figure 3 shows the Federal Aviation Administration's Aviation System Performance Metrics (ASPM77) database [26] values for total daily operations and total daily delayed operations for one portion of the available data days. The representative day of traffic was chosen to be March 28th, 2013 due to the high demand and low level of delayed operations, likely indicating a day with low weather impacts on the flown tracks. A 36-hour window was selected to capture 6 hours of traffic prior to and 6 hours of traffic after the selected date. This allowed for the inclusion of the complete track profile for flights that were already airborne before the start of the selected date and those that were still airborne at the conclusion of the selected date.

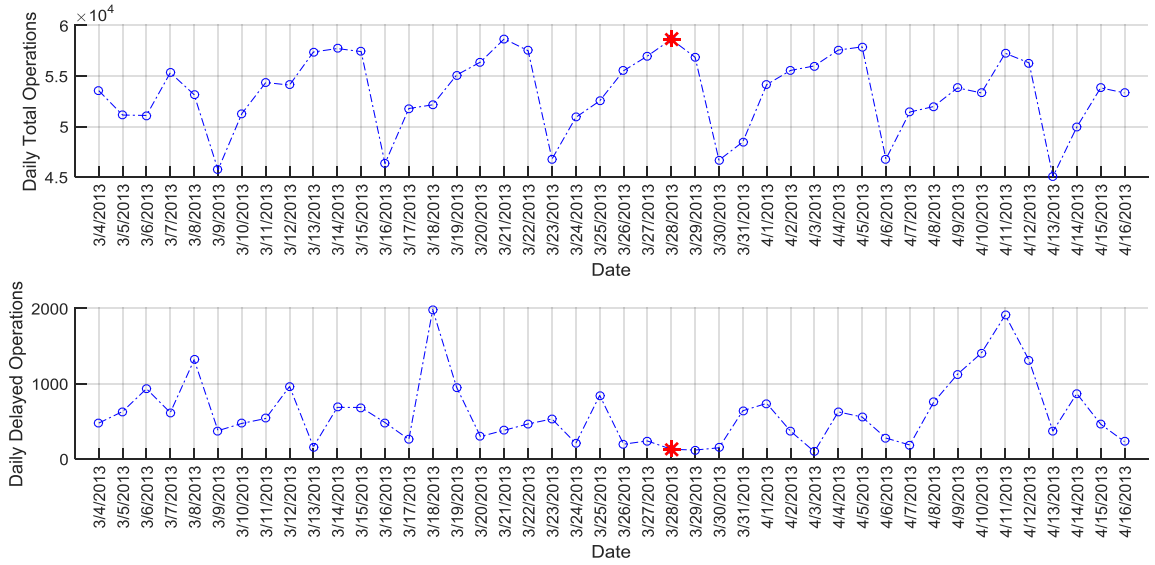

Figure 3. ASPM77 daily total operations (top), and ASPM daily delayed operations (bottom). March 28, 2013 was chosen as a high volume and low delay day from the recorded traffic data available.

The sample set of traffic tracks were used in three different ways within this analysis, after some initial processing and conditioning. First, the traffic tracks were used in analysis method 1 as the playback or true tracks flown by aircraft within those scenarios. Second, the conditioned track data was processed within a custom algorithm to process or infer the intent information for each track. Third, the inferred intent

[2] The extraction of intent information from track data was much more difficult than originally envisioned. Several different algorithms were created and compared. We note that our intent results are strongly connected to the goodness of the fit of the intent model to the track data.

information was used to build distributions of parameters such as track angle change, average groundspeed, average climb rates, and others that were used in the generation of random flight plans for the circular scenarios used in analysis method 2. A total of 30,799 recorded flight tracks (time, latitude, longitude, altitude) for flights into, within, and out of the Continental United States were used in this analysis.

A. Data Processing

Track Data Processing

The raw track data required pre-conditioning and filtering before it could be used to conduct this analysis. The tracks inherently contain the noise from the surveillance sensors that captured the data. Additionally, the fusion of multiple data sources can introduce an artificial noise due to the various sampling frequencies and timestamps. Figure 4 and Figure 5 show the track and altitude profiles, respectively, for a randomly selected flight before and after data processing. Note that, using these figures alone, it is difficult to spot the noisy characteristics of the data. However, an inspection of the velocity profiles for this example flight computed using a simple finite difference (estimating the derivative) reveals the noise characteristics. Figure 6-Figure 8 show the groundspeed, vertical speed, and track angle profiles, respectively, for the same sample flight before and after the processing step. Note the high level of noise in these velocity profiles. In each of the figures for the sample flight, the raw track data is shown in blue and the final processed track data for use in this analysis is shown in red.

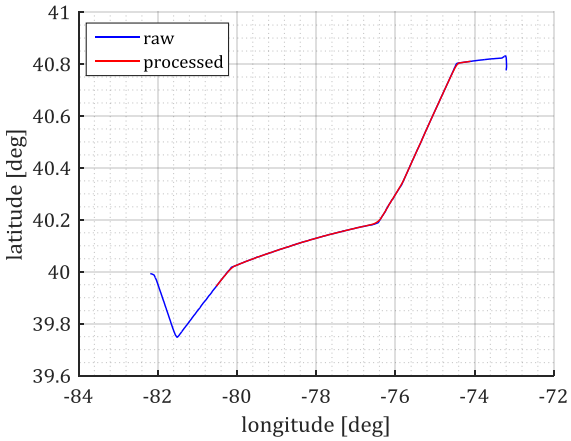

Figure 4. Raw and processed track profile for a randomly-selected sample flight.

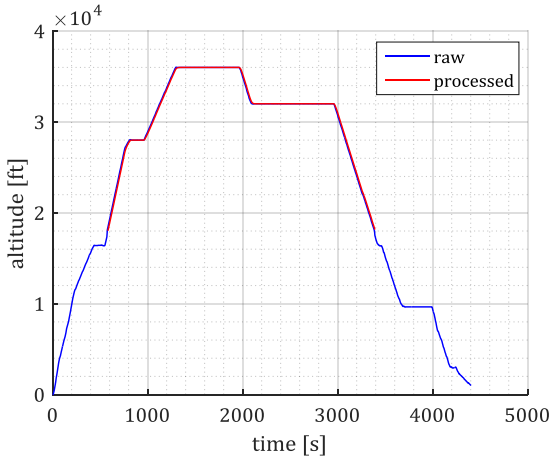

Figure 5. Raw and processed altitude profile for a randomly-selected sample flight.

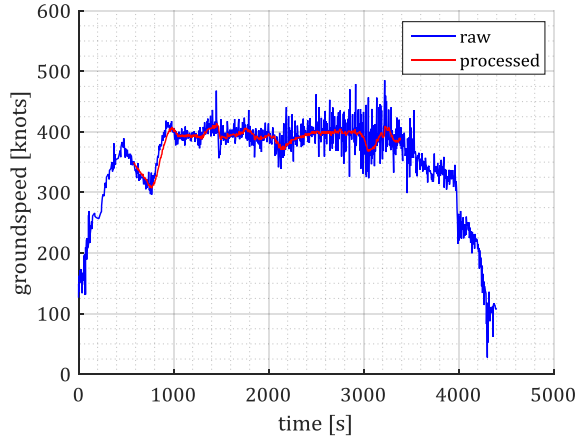

Figure 6. Raw and processed groundspeed profile for a randomly-selected sample flight.

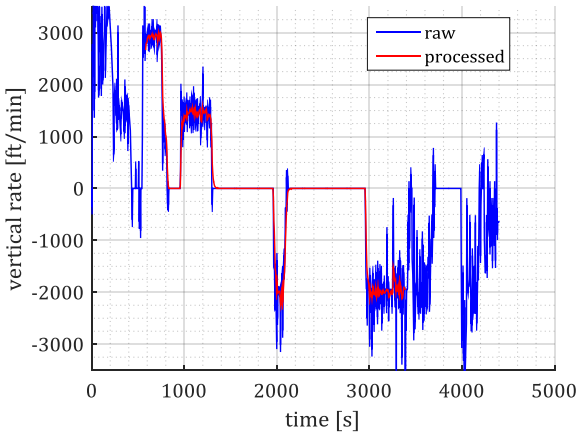

Figure 7. Raw and processed vertical speed profile for a randomly-selected sample flight.

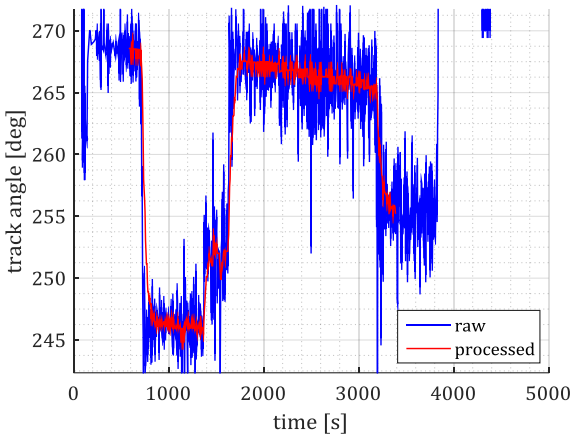

Figure 8. Raw and processed track angle profile for a randomly-selected sample flight.

The processing of the track data was completed in three basic steps. First, a pre-screening step was used to discard flights that did not have sufficient data useful for this analysis. This included discarding flights with no track data above FL180, discarding flights fully outside the time window of interest, and discarding flights with anomalous track data. Next, a conditioning step was used to correct any data drop-outs and to trim the flight track data to the portion above FL180. Flight segments below FL180 include VFR flights with altitude separations in 500 foot increments and traffic entering or exiting the terminal airspace environment where the separation standards are different from the en-route environment and special separation rules exist; these conditions were observed in a few preliminary test runs of the analysis model. Finally, a filtering step was used to remove the surveillance and data fusion noise in order to create a baseline set of track data. A combination of excessive groundspeed and vertical speed data point removal, followed by a one-dimensional Kalman Filter [27], generated the final processed track data that can be seen in Figure 4-Figure 8. The thresholds and algorithms used for the processing of the raw data were developed largely by observations drawn from the raw data. The following is a list of the pre-processing and filtering steps that were applied to the raw data:

Pre-screening:

- Discard all flights with no data points above FL180
- Discard all flights with the same origin and destination airport
- Discard flights with un-identified origin or destination airport
- Discard any flights already airborne at the beginning of the 36 hour sample window
- Discard any flights still airborne at the end of the 36 hour sample window
- Discard any flights with data gaps in time greater than 5 minutes
- Discard any flights with a processed track time less than 10 minutes
- Discard any flights with incomplete track data (missing descent or climb portion but fully within the CONUS)

Conditioning:

- Trim all track data to retain only the portion above FL180
- Remove any duplicated time data points
- Remove any data drop-outs (identified via vertical speeds in excess of 10,000 ft/min)

Filtering:

- Remove any data points producing excessive groundspeeds and vertical speeds
  - Groundspeeds greater than 590 knots
  - Vertical speeds greater than 10,000 ft/min
- Remove any data points with large groundspeed and vertical speed deviations away from a 9-point centered moving average
  - Groundspeed differences larger than 100 knots

- Vertical speed differences larger than 100 ft/min
- Interpolate the track data for a uniform time sampling of 5 seconds
- Apply a one-dimensional Kalman Filter to the track data (altitude, latitude, and longitude)

The selected traffic demand day of March 28th, 2013, with the additional 6 hours of pre- and 6 hours of post-traffic, contained a total of 72,769 recorded traffic tracks. After the processing steps above were implemented, the remaining traffic set contained 30,799 recorded traffic tracks.

Intent Information Processing

The intent information used in the conflict detection performance study was inferred from the recorded track data using a custom curve-fitting program developed for this project. Flight plan and flight plan amendment information was available for the recorded tracks but using that information as source for intent would likely lead to un-realistic intent information. For example, if an aircraft had been vectored for traffic, or some other reason, for a brief period of time, that vector information would not have been present in the flight plan amendments. It was decided that the scope of this analysis should not include erroneous intent information or blunder scenarios, which led to the decision to infer the intent information from the track data.

The vertical and lateral components of intent information were identified separately. The lateral intent was identified by searching for the start and end of non-turning flight segments using significant changes in track rate as the trigger. The track angle was computed using the track positions and the track rate was computed as the differential of the track angle. Moving average filters were used to mitigate the noisy differential derivatives. A tuned threshold limit for track rate of +/-0.03 deg/s was used to identify the lateral states (turning, not turning) of each track data point, thereby creating the boundaries between straight and turning flight segments, or the estimated beginning-of-turn (BOT) and end-of-turn (EOT) locations. By considering only the non-turning flight segments, the projected intersection of subsequent segments constituted the notion of a fly-by waypoint along a flight plan. These identified waypoints are the lateral intent points inferred from the track data. Figure 9 shows an example of a recorded lateral profile and the identified lateral intent points; note that these waypoints are the intersections of the non-turning segments and, thus, do not overlay on the track data.

Inferring the vertical intent information involved identifying the level flight segments from each vertical profile (time, altitude). The differential vertical speed was first used to initialize the states (climb, descent, level) at each track data point using a threshold limit of +/-100 ft/min. Moving average filters were used to mitigate the noisy differential vertical speed while heuristics were used to handle consecutive segments of the same type and to fine tune the location of the start and end points of the level flight segments. Finally, the start and end of each level flight segment was labeled as a BOC, TOC, TOD, or BOD altitude intent point based on the preceding or subsequent segment type. Figure 10 shows a sample vertical profile with and the identified altitude change points.

The intent information generation process also included the identification of the data elements required to support the various qualities of intent modeled in this study. For the lateral intent points, the turn radius was determined using the distance from the identified waypoint to the BOT or EOT, whichever was smallest, and the track angle change from the BOT to the EOT. The average groundspeed between the BOT and EOT, the track angle change, and the radius were then used to compute a constant turn rate for the turn. Figure 11 shows a sample lateral profile, including the constant rate turns that were estimated for those track changes. Note that the BOT and EOT points are not part of the intent information that was available for trajectory prediction and are just depicted here for reference[3]. For the vertical data elements, an optimization routine was used to fit two acceleration regions and a constant vertical rate region for any altitude change maneuver by minimizing the mean squared error between the recorded data and the modeled

[3] We decided to follow DO-242 as much as possible. The DO-242 approach uses other parameters which enable a calculation of the BOT and EOT locations. With full information, the BOT and EOT locations can be accurately calculated. With less information, they can only be estimated.

maneuver. Figure 12 shows a sample altitude change with the TOD point, a constant vertical acceleration region, followed by a constant vertical rate region, then another constant vertical acceleration region, and finally the BOD point. Note that the acceleration regions are properties of the intent point that they begin from or end at and that each intent point has a vertical rate into and a vertical rate out of that point.

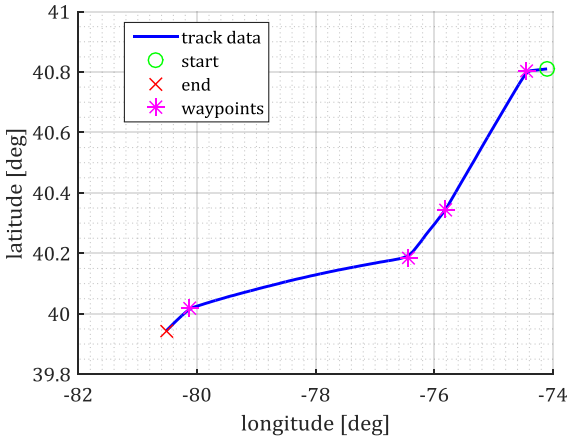

Figure 9. Sample recorded track horizontal profile with identified waypoints.

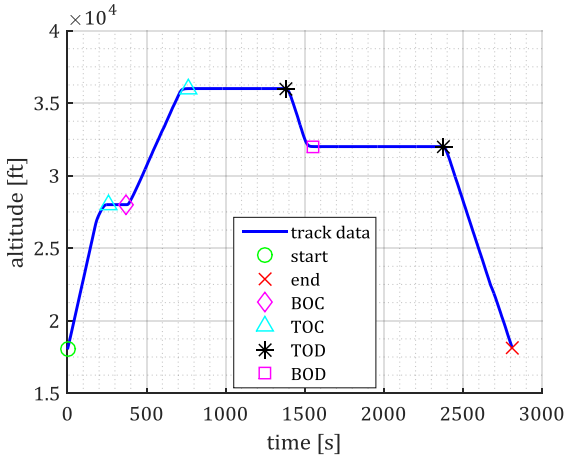

Figure 10. Sample recorded track vertical profile with identified altitude change points.

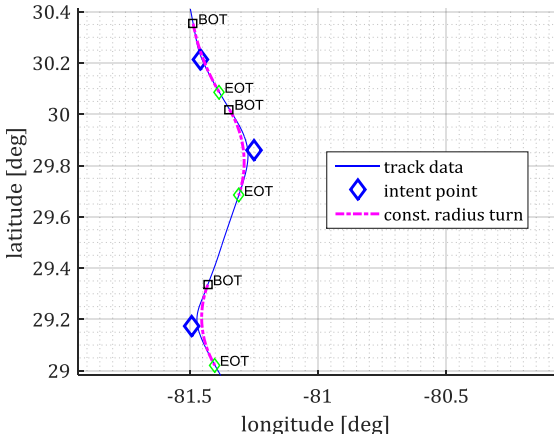

Figure 11. Example identified turn intent and fitted constant radius turns.

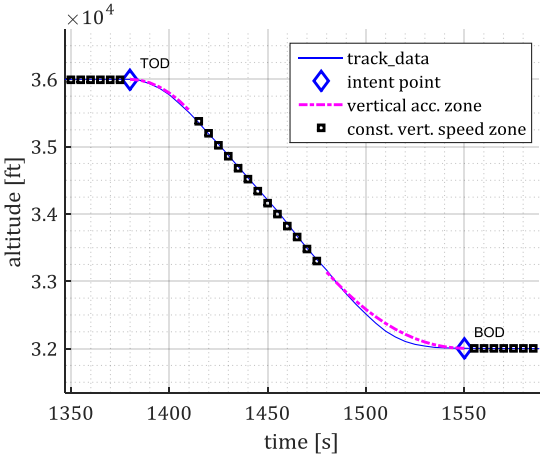

Figure 12. Example identified vertical intent points with vertical acceleration zones and constant vertical speed segments.

Table 4 shows the identified horizontal intent information that was available for trajectory prediction for the sample track shown in Figure 9 at the horizontal quality level of three. Similarly, Table 5 shows the identified vertical intent information that was available for trajectory prediction for the sample vertical profile shown in Figure 10 at the vertical quality level of three. These two tables constitute one kinematic representation of the recorded track data that was estimated or fitted algorithmically and was used as the method for describing intent information in this analysis.

Table 4. Identified horizontal intent data for sample profile shown in Figure 9.

time [s]	latitude [deg]	longitude [deg]	trackIn [deg]	trackOut [deg]	turnRadius [NM]	turnRate [deg/s]	type [unitless]
0	40.8102	-74.1015	268.6	268.6	0	0	START
169.7	40.80281	-74.4436	268.4	246.6	32.4	-0.1558	WPT
810.81	40.34498	-75.8101	245.8	251.8	85.4	0.0755	WPT
1082.7	40.18667	-76.4341	251.5	267.6	64.3	0.0980	WPT
2641.5	40.01759	-80.1314	265.5	256.2	72.7	-0.0872	WPT
2810	39.9442	-80.5185	255.3	255.3	0	0	END

Note: *trackOut is the same as target track for intent level 0.*

Table 5. Identified vertical intent data for sample profile shown in Figure 10.

time [s]	altitude [ft]	targetAltitude [ft]	climbRateIn [ft/min]	climbRateOut [ft/min]	verticalAcceleration [ft/s^2]	type [unitless]
0	18028	28000	2664	2973	0.1187	START
260	28000	28000	2973	0	-0.4385	TOC
370	28000	35998	0	1459	0.6194	BOC
765	35998	35998	1459	0	-0.2615	TOC
1380	36000	32005	0	-2072	-1.0191	TOD
1550	32005	32005	-2072	0	0.4618	BOD
2375	32000	18161	0	-1968	-1.4486	TOD
2810	18161	18161	-1968	-1944	0.0014	END

B. Scenarios

Scenarios for Analysis Method 1

The traffic scenarios for this analysis were generated in two ways. For method 1, scenario generation was done by randomly time-shifting the original start time of each flight track within some specified limits. A test set of ten different scenarios using the full recorded traffic data were generated with a maximum time shift parameter, $t_{shift,max}$, of zero, two, five, and fifteen minutes, and one, two, four, six, twelve, and twenty-four hours. These scenarios were analyzed with the nominal analysis model parameter values and helped to identify the time shift that produced the highest number of true losses-of-separation. As seen in Figure 13, the peak number of true LOS was achieved with a time shift close to fifteen minutes or one hour. At these time shift values, the full day of time-shifted traffic produced over 15,000 true LOS. The increase followed by a decrease in the number of true LOS is the result of the small increase in time shift values that increasingly create LOS events in the recorded tracks until such point as the peaks of traffic start to flattens out and the density of traffic is reduced, as shown by the number of simulated traffic over the simulation time in Figure 14.

All scenarios for analysis method 1 consisted of the full 30,799 recorded traffic tracks and a random time shift of up to one hour for each track. Ten different randomized scenarios were created and used to investigate the variability due to the randomization. One of these ten scenarios was selected as the baseline scenario for all other analysis runs.

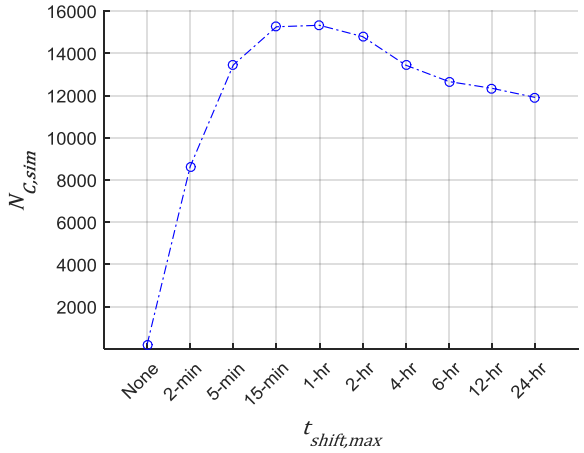

Figure 13. Number of true LOS, $N_{C,sim}$, created as a function of the maximum time shift parameter, $t_{shift,max}$.

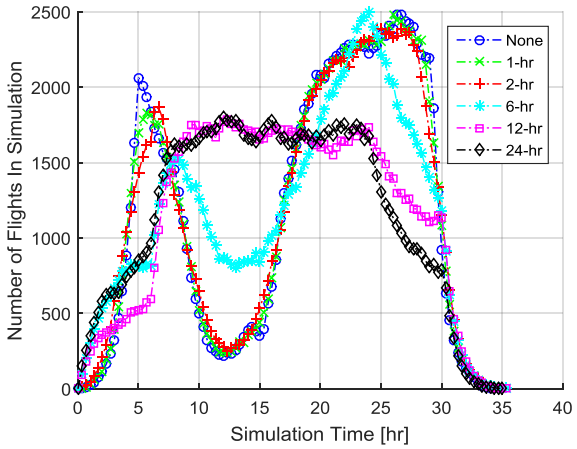

Figure 14. Number of flights as a function of the simulation clock time for a few of the time shift scenarios.

Scenarios for Analysis Method 2

The scenario generation approach for analysis method 2 was to generate flight plans that traverse a circular region of airspace, where the flight plan characteristics were generated using distributions obtained from the recorded traffic tracks. After selecting the number of aircraft and the radius of the circular region of airspace, flight plans were randomly generated by sampling from a set of distributions for: initial heading angle deviation, groundspeed, horizontal leg time, turn angle magnitude, number of altitude segments, vertical speed, and level flight segment time. Each flight plan was initialized at the boundary of the circular region. An initial heading offset was selected from a uniform distribution and added as a deviation away from a heading towards the center of the circular region. A horizontal profile was created by successively sampling from a horizontal leg time and a turn angle until the flight plan exited the circular region. A vertical profile was created by subsequently sampling a level segment time, an altitude change of 1000 or 2000 feet up or down, and a vertical speed for that altitude change until the time required to exit the circular region was achieved. The fitted distributions derived from the characteristics of the recorded traffic data and used in the scenario generation are shown in Figure 16 - Figure 21 below and the associated probability density functions defined in equations (1)-(3). The horizontal profile of a 100 aircraft scenario is shown in Figure 15.

A LOS-maximizing approach was used in creating the set of scenarios for analysis method 2. A set of preliminary runs were used to calibrate the parameters for: number of aircraft, circular region radius, and initial heading angle deviation. The analysis results presented in this paper used a set of scenarios with 1500 aircraft over a circular region with a radius of 300 nautical miles and a uniform distribution of initial heading angle deviation within +/-40 degrees.

$$PDF_{Normal}(x|\mu,\sigma) = \frac{1}{\sigma\sqrt{2\pi}} e^{-\frac{(x-\mu)^2}{2\sigma^2}} \quad \textbf{(1)}$$

$$PDF_{InverseGaussian}(x|\mu,\lambda) = \left[\frac{\lambda}{2\pi x^3}\right]^{1/2} e^{-\frac{\lambda(x-\mu)^2}{2x\mu^2}} \quad \textbf{(2)}$$

$$PDF_{Gamma}(x|a,b) = \frac{1}{b^a \Gamma(a)} x^{(a-1)} e^{-x/b} \quad \textbf{(3)}$$

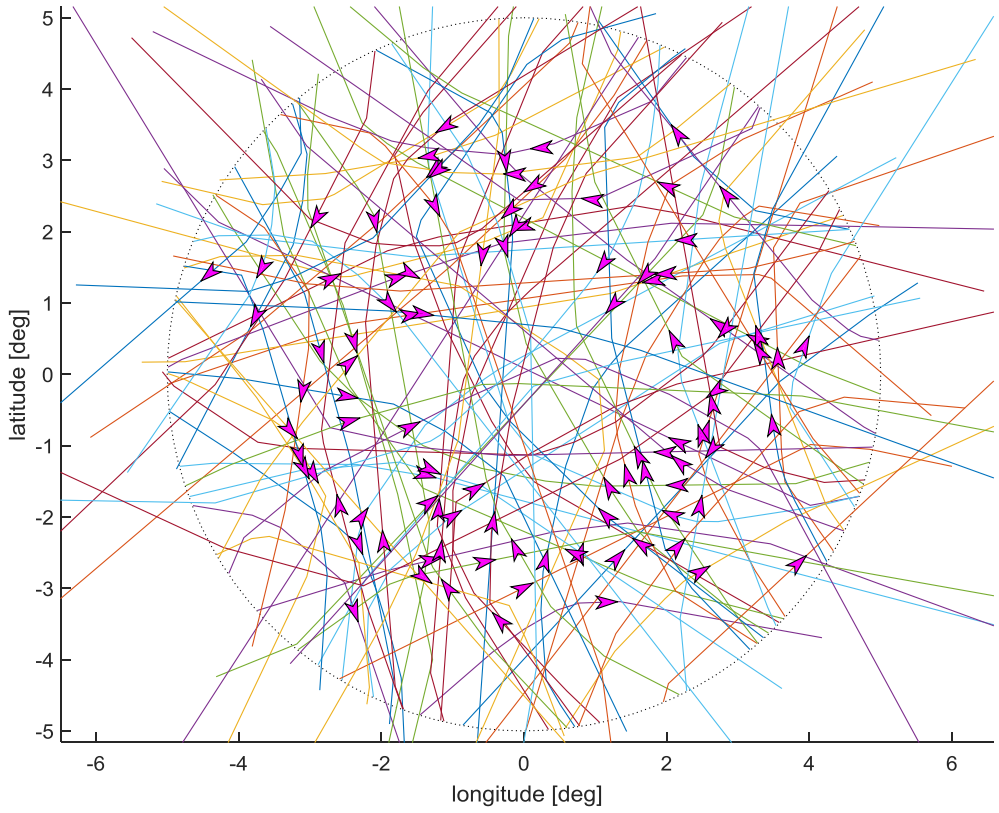

Figure 15. Example circular scenario horizontal profile with 100 aircraft.

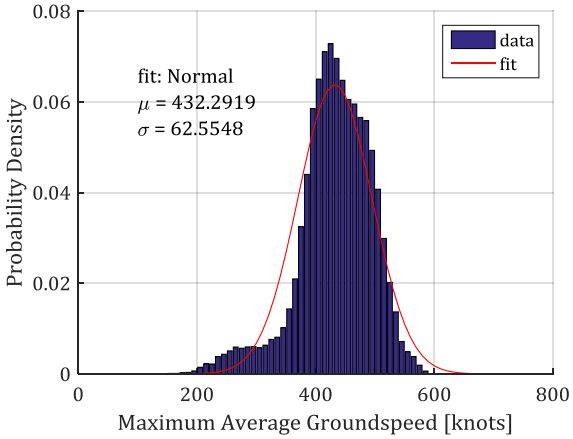

Figure 16. Distribution of the maximum average groundspeed for all recorded traffic tracks.

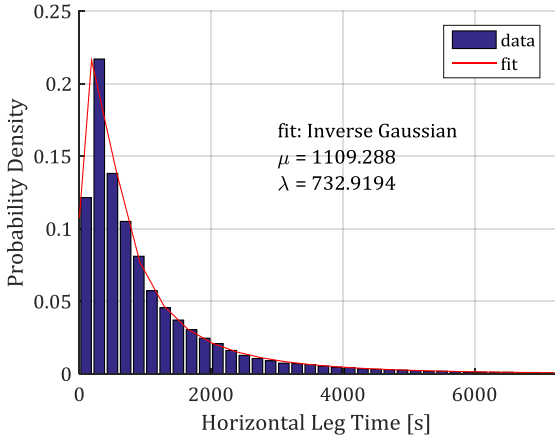

Figure 17. Distribution of the time for all horizontal flight segments over all recorded tracks.

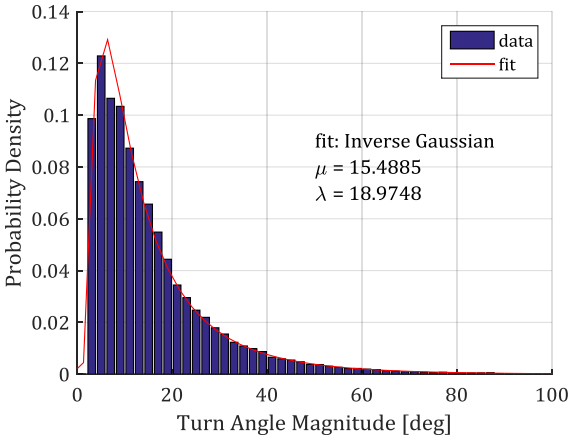

Figure 18. Distribution of the magnitude of the turn angle between horizontal flight segments for all tracks and all segments.

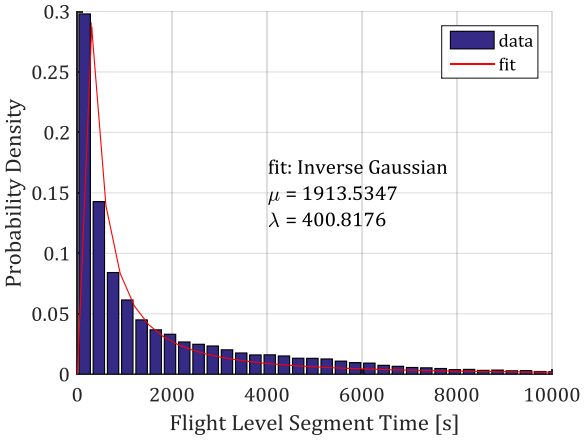

Figure 19. Distribution of the time in level flight over all tracks and all level altitude segments.

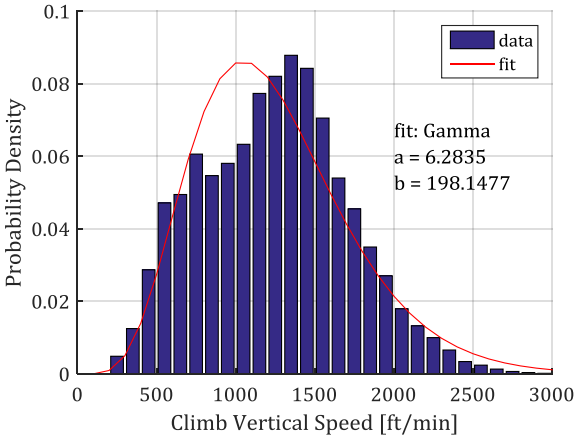

Figure 20. Distribution of the average vertical speed between vertical level segment changes in climbs for all tracks.

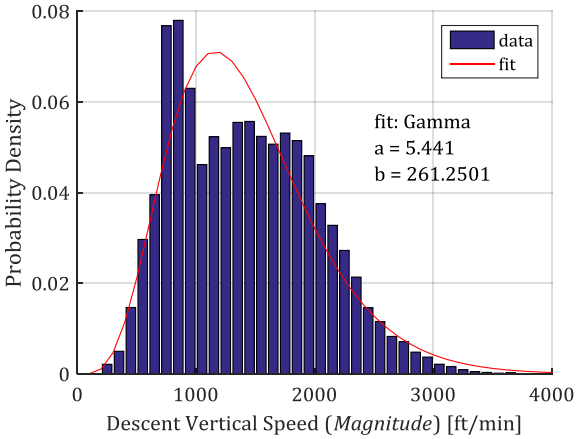

Figure 21. Distribution of the average vertical speed magnitude between vertical level segment changes in descents for all tracks.

V. Metrics

A. Definitions

In conflict detection, the primary concern is in the accuracy of the alerts provided. An alert is a warning provided by the conflict detector at some time regarding the potential for a LOS between two aircraft at some future time. The correctness of these alerts has typically been characterized using false alert and missed alert statistics. A false alert is an issued alert where there is no corresponding LOS. This kind of alert is sometimes described as a nuisance alert because it can lead to unnecessary actions by the agent receiving it. A missed alert is the lack of an alert to a LOS that will occur between two aircraft within a specified look-ahead time. In most air traffic concepts, a missed alert means that the action to resolve the conflict will be delayed, which could result in significant safety issues. Correct alerts are alerts that are neither missed alerts nor false alerts.

Table 6 provides a set of definitions for conflict detection-related terms used throughout this document. In particular, it's important to note the difference between an alert and a detection. An alert is a warning provided by the conflict detector at any given time or any conflict detection cycle. Conversely, a detection is the successful identification of a true LOS event over all time or over all conflict detection cycles. A

missed detection means that conflict resolution will never occur because the conflict is never detected; this is an important safety consideration. A LOS event in this study is characterized by the position of both aircraft at initial entry into LOS and the time at which that entry occurs.

The idea of a *"true conflict"* was used in the analysis and is possible because of the availability of truth track data that is known *a priori*. A true conflict exists if there is a LOS between the true tracks of two aircraft; however, in a real world environment, no such true data exists because the future tracks can change for a variety of reasons (e.g., to resolve a conflict). Nonetheless, the idea of a true conflict is a useful concept when measuring the performance of trajectory prediction and conflict detection in the absence of conflict resolution. One true LOS can correspond to multiple true conflicts depending on the number of conflict detection cycles that contain that LOS within the conflict detection horizon.

The true and predicted conflicts identified in this study were based on separation criteria that are different from the separation standard for en-route airspace [28]. The horizontal separation criterion of 5 nautical miles was used but a reduced vertical separation criterion of 800 feet was chosen for this study. In the track data processing step, and in preliminary analysis runs, it was observed that the Mode-C resolution of +/-100 feet altitude of some of the track data had a significant impact on the number of predicted conflicts, thereby justifying the use of a reduced vertical separation criterion.

Table 6. Conflict detection terms and definitions.

Term	Definition
loss(es)-of-separation *(LOS)*	violation(s) of the minimum separation criteria between two aircraft trajectories
separation criteria	vertical and horizontal distances that identify the boundary for a LOS event between two trajectories
conflict	two aircraft are in conflict if there exists a time, *t*, with a LOS in their true or predicted trajectories
detection	the identification of a true LOS event
true conflict	a conflict that exists between the true trajectories of two aircraft and that is within the conflict detection horizon, in the absence of a resolution maneuver
predicted conflict	a conflict that exists between the predicted trajectories of two aircraft and that is within the conflict detection horizon
alert	a warning provided by the conflict detector
false alert *(FA)*	an alert regarding a LOS *that is not* present in the true aircraft trajectories within the conflict detection horizon
missed alert *(MA)*	the lack of an alert regarding a LOS *that is* present in the true aircraft trajectories within the conflict detection horizon
missed detection *(MD)*	over all detection attempts, the absolute failure to detect a true LOS event

The metrics for this study were collected in terms of absolute counts, ratios or probabilities, or mean values. Table 7 lists the primary conflict detection metrics for this study while Table 8 lists the secondary metrics. The secondary metrics are absolute counts of quantities such as false alerts and missed alerts and are required to compute the observed probabilities and mean values in the primary metrics. The number of false alerts, the number of missed alerts, the number of predicted conflicts, and the number of true conflicts were each obtained using the size of the true and predicted conflict sets, $\boldsymbol{C}$ and $\widehat{\boldsymbol{C}}$, respectively, identified during each conflict detection cycle and aggregated over all detection cycles in a simulation run. For each simulation run, the total number of LOS and, of those, the number that were never detected in any detection cycle (the number of missed detections) were also collected. Only the primary metrics are reported in the results tables for this study.

The primary metrics collected for this study were: probability of false alert, P_{FA}, probability of missed alert, P_{MA}, probability of missed detection, P_{MD}, and mean time-to-LOS at first detection, $\Delta t_{LOS,mean}$. The probability of false alert represents the observed ratio of total false conflict alerts to the total number of conflict alerts and indicates the likelihood that any alert provided by the conflict detector could be false. Missed alert probability represents the observed ratio of the total number of missed alerts to the total number

of true conflicts and indicates the likelihood that, at any detection cycle, there is a true LOS present within the conflict detection horizon that is not alerted. The missed detection probability represents the observed ratio of total LOS that were not detected as a true conflict in any detection cycle to the total number of LOS present in a given simulation run and indicates the likelihood that the conflict detector will fail to provide any alert for a given true LOS. Finally, the mean time-to-LOS represents the average time to entry into LOS at the first successful detection for those losses-of-separation that were successfully detected within a simulation run; losses-of-separation that were never detected do not contribute to this mean value.

Table 7. Conflict detection performance primary metrics.

Metric	Definition
$P_{FA} = N_{FA}/N_{\widehat{C}}$	the false alert ratio or **false alert probability**
$P_{MA} = N_{MA}/N_{\boldsymbol{C}}$	the missed alert ratio or **missed alert probability**
$P_{MD} = N_{MD}/N_{\boldsymbol{C},sim}$	the missed detection ratio or **missed detection probability**
$\Delta t_{LOS,mean} = \sum_{m=1,2,\ldots}^{M} \frac{\Delta t_{LOS,m}}{M}$	**mean time-to loss-of-separation at first detection** for all M successfully detected true conflicts

Table 8. Conflict detection performance secondary metrics.

Metric	Definition
$N_{FA} = \sum_{sim\_run} \sum_{t_{cd}} \lvert\widehat{\boldsymbol{C}} \setminus \boldsymbol{C}\rvert$	the **number of false alerts** from the set of predicted conflicts (conflict alerts), $\widehat{\boldsymbol{C}}$, identified during each detection cycle, summed over every detection cycle and over an entire simulation run
$N_{\widehat{C}} = \sum_{sim\_run} \sum_{t_{cd}} \lvert\widehat{\boldsymbol{C}}\rvert$	the **number of predicted conflicts** (conflict alerts), $\widehat{\boldsymbol{C}}$, identified during each detection cycle, summed over every detection cycle and over an entire simulation run
$N_{MA} = \sum_{sim\_run} \sum_{t_{cd}} \lvert\boldsymbol{C} \setminus \widehat{\boldsymbol{C}}\rvert$	the **number of missed alerts** from the set of true conflicts, $\boldsymbol{C}$, within the time horizon of each detection cycle, summed over every detection cycle and over an entire simulation run
$N_{\boldsymbol{C}} = \sum_{sim\_run} \sum_{t_{cd}} \lvert\boldsymbol{C}\rvert$	the **number of true conflicts** present during each conflict detection cycle, summed over every detection cycle and over an entire simulation run
$N_{\boldsymbol{C},sim} = \lvert\boldsymbol{C}\rvert$	the number of unique true conflicts (**number of LOS**) in a simulation run
$N_{MD} = \lvert\boldsymbol{C} \setminus \widehat{\boldsymbol{C}}\rvert$	the **number of missed detections** – from the set of all true conflicts, $\boldsymbol{C}$, not in the set of predicted conflicts (conflict alerts), $\widehat{\boldsymbol{C}}$, over an entire simulation run

B. Same Conflict Comparison

The notion of two conflicts being the "same conflict" or not was developed for this study in order to properly characterize conflict detection performance. The traditional definition of a false alert, as it is most commonly defined in other examples of conflict detection-related literature, is that, an alert is false when *there exists a predicted conflict* between the predicted trajectories of two aircraft but *there does not exist a true conflict* between the true trajectories of those same two aircraft, within the same time horizon. Similarly, the traditional definition of a missed alert is that, an alert is missed when *there does not exist a predicted conflict* between the predicted trajectories of two aircraft but *there does exist a true conflict* between the true trajectories of those same two aircraft, within the same time horizon. Given that conflict detection is done with imperfect trajectory predictions, these definitions can lead to the characterization of a conflict alert as a correct alert even if the predicted and true conflicts are far from each other in space and/or time. The false alert and missed alert definitions need to contain criteria to evaluate whether a predicted conflict and a true conflict are "the same;" that is, that their respective losses-of-separation occur roughly in the same place and at the same time.

The schematic in Figure 22 depicts two aircraft with both a predicted conflict *and* a true conflict. The traditional definitions for false alert and missed alert would indicate that there is no false alert and no missed alert; that is, this example would be considered a correct alert due to the presence of both a predicted and a

true conflict. However, the scale of the diagram in Figure 22 might be large and the location of the LOS in the two conflicts may be many nautical miles apart. This difference in location is important for functions such as conflict resolution where the difference between a conflict ahead-of-track and a conflict to the right-of-track is important. Using the traditional definitions for false alert and missed alert results in artificially better conflict detection performance. This is because, if some criteria for evaluating whether two conflicts are "the same" is applied to the diagram of Figure 22, either of two conditions would occur: the two conflicts are considered to be the same and the false alerts and missed alerts are both zero, just as the traditional definitions indicate, or, the two conflict are not the same, in which case, the predicted conflict is considered to be a false alert to a non-existent LOS, and the true conflict is considered to be a missed alert of a true LOS. Therefore, using criteria for evaluating whether two conflicts are the same within each conflict detection cycle, the revised definitions of a false and a missed alert are:

- a false alert is a *predicted conflict* between the predicted trajectories of two aircraft where *the same true conflict* in the true trajectories of those aircraft *does not exist*, within the conflict detection time horizon, and
- a missed alert is a *true conflict* between the true trajectories of two aircraft where *the same predicted conflict* in the predicted trajectories of those aircraft *does not exist*, within the conflict detection time horizon.

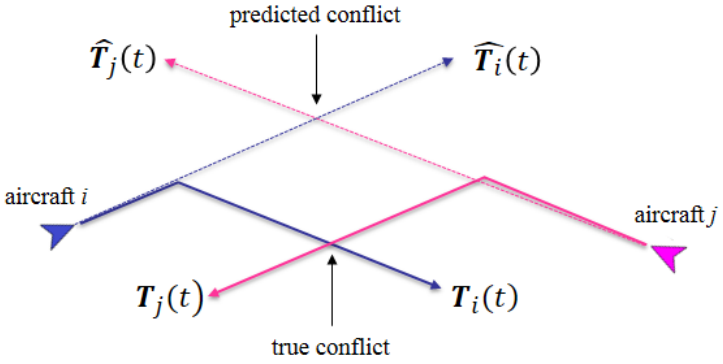

Figure 22. Example predicted and true conflicts between a pair of aircraft (20 minute long prediction arrows).

The criteria chosen to evaluate whether two conflicts are "the same" involves comparing the time and position of both aircraft at the entry into LOS. This is an appropriate method to use, given that a LOS event in this study is a reference to the time and position of first entry into LOS for a pair of aircraft. A conflict comparison for an example such as the one in Figure 22 should determine that the two conflicts are not the same because, even though the temporal location of the LOS for the predicted and true LOS events may be very close, the spatial location of the two LOS is significantly different. Define a conflict vector, $\boldsymbol{C}_{m,i,j}$, for conflict m between aircraft i and aircraft j as:

$$\boldsymbol{C}_{m,i,j} := [t_{LOS,m}, \boldsymbol{s}_{i,m}(t_{LOS,m}), \boldsymbol{s}_{j,m}(t_{LOS,m})] \quad \textbf{(4)}$$

where the first element is the absolute entry time into LOS, $t_{LOS,m}$, for conflict m, the next element is the 3-dimensional position of aircraft i at $t_{LOS,m}$, and the last element is the 3-dimensional position of aircraft j at $t_{LOS,m}$. Figure 23 shows the actual positions of aircraft i and j at the time-in to LOS, $t_{LOS,n}$, of the true conflict n, and the predicted positions of those aircraft at the time-in to LOS, $t_{LOS,m}$, of the predicted conflict m.

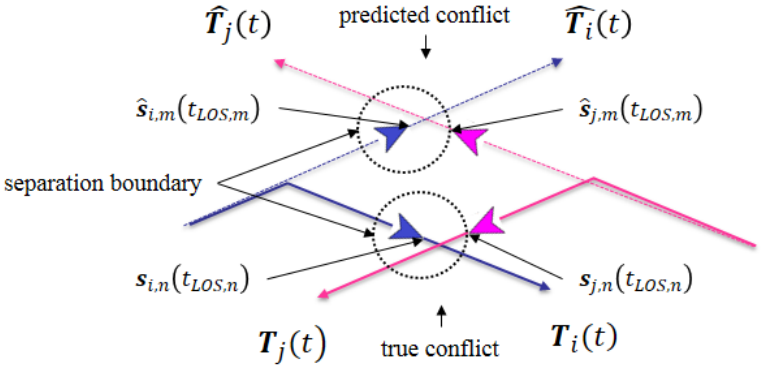

Figure 23. True aircraft positions at time-in to LOS, $t_{LOS,n}$, for a true conflict, n, and predicted aircraft positions at, $t_{LOS,m}$, for a predicted conflict, m.

Comparison of two conflicts is done by evaluating the space/time differences between the conflict vectors against a set of threshold values. Let,

$$D_{H,i,m,n} = \boldsymbol{d}_{GCD}\left(lat_{i,m}(t_{LOS,m}), lon_{i,m}(t_{LOS,m}), lat_{i,n}(t_{LOS,n}), lon_{i,n}(t_{LOS,n})\right) \quad \textbf{(5)}$$

be the horizontal arc-distance between the positions of aircraft i in conflicts m and n, where $\boldsymbol{d}_{GCD}$ is a function that computes the great-circle distance between two points on a sphere. Let,

$$D_{V,i,m,n} = \left|alt_{i,m}(t_{LOS,m}) - alt_{i,n}(t_{LOS,n})\right| \quad \textbf{(6)}$$

be the magnitude of the difference between the altitude of aircraft i in conflict m, and the altitude of the same aircraft i in conflict n. Then, two conflicts m and n are said to be <u>*the same*</u> ($\boldsymbol{C}_{m,i,j} \approx \boldsymbol{C}_{n,i,j}$) if and only if <u>*all*</u> of the conditions in equations (7)-(11) are satisfied:

$$\left|t_{LOS,m} - t_{LOS,n}\right| \leq \delta_t \quad \textbf{(7)}$$

$$D_{H,i,m,n} \leq \delta_H \quad \textbf{(8)}$$

$$D_{H,j,m,n} \leq \delta_H \quad \textbf{(9)}$$

$$D_{V,i,m,n} \leq \delta_V \quad \textbf{(10)}$$

$$D_{V,j,m,n} \leq \delta_V \quad \textbf{(11)}$$

where δ_t, δ_H, and δ_V, are threshold values selected for the maximum allowable time difference between two LOS entry times, the maximum allowable horizontal distance between the position of each aircraft in both conflicts, and the maximum allowable vertical distance between the altitudes of each aircraft in both conflicts, respectively. The following logic was used in determining a set of reasonable threshold values, based on a lateral separation standard of 5 NM and a vertical separation standard of 1000 ft:

- $\delta_t = 120$ s : the time it takes to traverse 10 NM at an assumed groundspeed of 300 knots
- $\delta_H = 10$ NM : the horizontal position of an aircraft i can vary by as much as 10 NM and still be in LOS with an aircraft j
- $\delta_V = 2000$ ft : the vertical position of an aircraft i can vary by as much as 2000 ft and still be in LOS with an aircraft j

The comparison criteria defined by equations (7)-(11) lead directly to the computation of the primary metrics. At any conflict detection time, a false alert was identified when a predicted conflict was not the same as any true conflict within the same conflict detection horizon. Similarly, at any conflict detection time, a missed alert was identified when a true conflict was not the same as any predicted conflict within the same conflict detection horizon. A missed detection was identified by a true LOS that was not predicted

in any conflict detection cycle over an entire simulation run. The time-to entry into loss-of-separation at first detection, $\Delta t_{LOS,m}$, for any true conflict, m, was given by:

$$\Delta t_{LOS,m} = t_{LOS,m} - t_{cd} \quad \textbf{(12)}$$

and was recorded at the earliest detection cycle in which a correct alert is issued for that LOS.

VI. Test Matrices

The analysis runs for conflict detection performance using method 1 were divided into five test matrices. Analysis runs using method 2 were conducted where appropriate for comparison. In the three surveillance quality test matrices, the current state of each aircraft was subjected to the surveillance error parameters being analyzed and state-projections were used for trajectory predictions. In the two level and quality of intent test matrices, no surveillance error was added to the aircraft states and the available intent information was used to inform the trajectory predictions.

A. Surveillance Quality Test Matrix 1 (SQ1)

Surveillance quality test matrix 1 is a full factorial combination of the primary input parameters for surveillance quality and conflict detection. The conflict detection cycle period (T_{det}) was tested at 15 and 60 seconds. Conflict detection and trajectory prediction horizon (T_{pred}) was tested at short, medium, and long values of 5, 10, and 20 minutes, respectively. The surveillance range (R_s) was also tested at short, medium, and long values of 50, 250, and 1500 (conservative surrogate for infinite surveillance range) nautical miles, respectively. Each combination of the three different surveillance error model parameter sets (SQ_{model}), including the baseline model with no surveillance error, was tested. Trajectory prediction was exercised using symmetric and asymmetric approaches where, for the asymmetric cases, perfect trajectory prediction was assumed for the first aircraft in the conflict pair where the predicted trajectory was equal to the true trajectory of that aircraft, and for the symmetric cases, both aircraft had the same quality of imperfect trajectory predictions. A single, time-shifted, recorded traffic scenario with 30,799 aircraft tracks was used for all runs. Table 9 lists the parameter values analyzed, which correspond to a total of *144 analysis runs*.

Table 9. Surveillance quality test matrix SQ1 (full-factorial; 144 runs).

Parameter	Values	Units
CD Period (T_{det})	15, 60	sec
Prediction Horizon (T_{pred})	300, 600, 1200	sec
Surveillance Range (R_s)	50, 250, 1500	NM
Surveillance Error Source (SQ_{model})	None, Radar, ADSB_1, ADSB_2	-
Trajectory Prediction Symmetry	Symmetric, Asymmetric	-

B. Surveillance Quality Test Matrix 2 (SQ2)

Surveillance quality test matrix 2 provides a set of sensitivity data for each of the conflict detection and surveillance quality parameters in the model. The sensitivity runs were conducted with respect to two baseline conditions selected from the SQ1 test matrix. Baseline condition 1 had no surveillance error while baseline condition 2 implemented the ADSB_2 surveillance error parameters set. For each sensitivity run only a single parameter value was changed relative to the corresponding baseline run and that parameter was constant over the entire run. Suitable parameter values were selected for conflict detection cycle period, detection and prediction horizon, and the various surveillance error model parameters. The conflict comparison criteria ($\delta_t, \delta_H, \delta_V$) were investigated at multiplier values of 0.5, 1.0, 2.0, and infinity (disables conflict comparison) with respect to their baseline values. Table 10 lists the parameter values that were analyzed in this test matrix for a total of *208 analysis runs*.

Table 10. Surveillance quality test matrix SQ2 (sensitivity runs; 208 runs).

Parameter	Values	Units
Nominal Parameter Values	***baseline 1***: $T_{det} = 60, T_{pred} = 600, R_s = 1500, SQ_{model} = None$ ***baseline 2***: $T_{det} = 60, T_{pred} = 600, R_s = 1500, SQ_{model} = ADSB\_2$	-
CD Period (T_{det})	15, 30, 60, 120, 300	s
Prediction Horizon (T_{pred})	60, 120, 300, 600, 900, 1200	s
Surveillance Range (R_s)	20, 40, 80, 100, 200, 300, 500, 1500	NM
Surveillance Lag (t_{sl})	0, 1, 2, 5, 10, 15	s
Horizontal Position Error (σ_r)	0.001, 0.01, 0.1, 0.5	NM
Vertical Position Error (σ_a)	1, 10, 25, 50, 100, 150	ft
Groundspeed Error (σ_{gs})	0.1, 1, 5, 10, 20, 50	NM/hr
Vertical Speed Error (σ_{vs})	10, 25, 50, 100, 500, 1000	ft/min
Track Angle Error (σ_{trk})	0.1, 0.5, 1, 2, 5	deg
Same Conflict Tolerance ($\delta_t, \delta_H, \delta_V$) Multiplier	0.5X, 1.0X, 2.0X, Inf	-
Trajectory Prediction Symmetry	Symmetric, Asymmetric	-

C. Surveillance Quality Test Matrix 3 (SQ3)

Surveillance quality test matrix 3 was implemented to investigate the variability in the analysis metrics due to different traffic scenarios and due to Monte Carlo sampling of the surveillance error parameters. A set of 10 different traffic scenario randomizations, each with 30,799 aircraft and using the one hour maximum time shift, were used in this test matrix. For scenario variability, the baseline 1 and 2 case runs from the SQ2 test matrix were each analyzed using the 10 different scenarios with symmetric and asymmetric trajectory predictions. For Monte Carlo sampling variability, the baseline 2 case run (with ADSB_2) was run with 10 different random seeds and the same traffic scenario both with symmetric and asymmetric trajectory predictions. Table 11 shows the *60 analysis runs* conducted to investigate variability.

Table 11. Surveillance quality test matrix SQ3 (variability; 60 runs).

Variability Test	Baseline Run	Trajectory Prediction Symmetry	Number of Scenarios	Number of Runs Per Scenario
Scenario Variability	*baseline 1*	Symmetric	10	1
	baseline 1	Asymmetric	10	1
	baseline 2	Symmetric	10	1
	baseline 2	Asymmetric	10	1
Sampling Variability	*baseline 2*	Symmetric	1	10
	baseline 2	Asymmetric	1	10

baseline 1: $T_{det} = 60, T_{pred} = 600, R_s = 1500, SQ_{model} = None$
baseline 2: $T_{det} = 60, T_{pred} = 600, R_s = 1500, SQ_{model} = ADSB\_2$

D. Level and Quality of Intent Information Test Matrix 1 (IQ1)

Level and quality of intent information test matrix 1 is a partial factorial exploration of the conflict detection and level and quality of intent input parameters. The partial factorial matrix is the result of the full-factorial matrix with the reduction of the parameter combinations that do not provide meaningful results. For example, there was no need to analyze a level of intent (intent horizon) parameter of 20 minutes if trajectory prediction was only being performed on a 10 minute horizon; intent information beyond 10

minutes would have been ignored. The purpose of this test matrix was to generate a family of CD performance curves for the level of intent information and quality of intent information parameters.

Table 12 shows the parameter values that were investigated in the IQ1 test matrix. Conflict detection cycle period (T_{det}) was analyzed at short and long values of 15 and 60 seconds, respectively. The conflict detection and trajectory prediction horizon (T_{pred}), and the level of intent (T_{int}), were each examined at the short, medium and long horizon levels of 5, 10, and 20 minutes. The vertical and horizontal quality of intent values were combined at the levels that provide equivalent information along the vertical and horizontal profiles (e.g., IQ_{V1}+IQ_{H1}) with the addition of the IQ_{V1}+IQ_{H2} quality combination that is the equivalent of the ADS-B trajectory change report definition in the ADS-B MASPS. Trajectory prediction symmetry was again investigated using the symmetric and asymmetric approaches where, for the asymmetric cases, perfect trajectory prediction was assumed for the first aircraft in the conflict pair by setting the predicted trajectory equal to the true trajectory of that aircraft, and for the symmetric cases, both aircraft had the same quality of imperfect trajectory predictions. Table 12 lists the test matrix parameters, which constitute a total of *132 analysis runs* from the meaningful parameter combinations.

Table 12. Level and quality of intent test matrix IQ1 (partial-factorial; 132 runs).

Parameter	Values	Units
CD Period (T_{det})	15, 60	s
Prediction Horizon (T_{pred})	300, 600, 1200	s
Level of Intent (T_{int})	300, 600, 1200	s
Quality of Intent	IQ_{V0}+IQ_{H0}, IQ_{V1}+IQ_{H1}, IQ_{V1}+IQ_{H2}[1], IQ_{V2}+IQ_{H2}, IQ_{V3}+IQ_{H3}, IQ_{V4}+IQ_{H4}[2]	-
Trajectory Prediction Symmetry	Symmetric, Asymmetric	-

Note: [1] Represents the closest equivalent to the ADS-B MASPS definition of a trajectory change report. [2] Default quality 4 intervals of 120 seconds and 1000 ft, per Table 3*.*

E. Level and Quality of Intent Information Test Matrix 2 (IQ2)

Level and quality of intent information test matrix 2 investigated the impact of different traffic scenarios on the variability of the output metrics and the sensitivity of the metrics to the parameters associated with vertical and horizontal intent quality 4. The same set of 10 random traffic scenarios used in the SQ2 test matrix were used in test matrix IQ2a to investigate the variability of the output metrics with respect to 3 baseline scenario runs, with symmetric and asymmetric trajectory predictions. Baseline runs 3-5 represent the conditions of an intent information quality at level 3 and with long, medium, and short intent horizons, respectively. Table 13 lists the details of the scenario variability runs for a total of *60 analysis runs*.

Test matrix IQ2b, shown in Table 14, lists the parameter settings of baseline run 6 with medium prediction and medium intent horizons, and the intent information quality 4 parameters variations. The time interval for the horizontal points that the intent information quality 4 adds to the horizontal intent information quality 3 points was varied from 15 seconds to 300 seconds. The altitude interval for the vertical points that the vertical intent information quality 4 adds to the intent information quality 3 points was varied from 100 feet to 5000 feet. The analysis runs of test matrix IQ2b were run with symmetric and asymmetric trajectory predictions for a total of *36 analysis runs*.

Table 13. Level and quality of intent test matrix IQ2a (scenario variability; 60 runs).

Variability Test	Baseline Run	Trajectory Prediction Symmetry	Number of Scenarios	Number of Runs Per Scenario
Scenario Variability	*baseline 3*	Symmetric	10	1
	baseline 3	Asymmetric	10	1
	baseline 4	Symmetric	10	1
	baseline 4	Asymmetric	10	1
	baseline 5	Symmetric	10	1
	baseline 5	Asymmetric	10	1

baseline 3: $T_{det} = 60, T_{pred} = 1200, T_{int} = 1200, IQ_{V3}, IQ_{H3}$
baseline 4: $T_{det} = 60, T_{pred} = 1200, T_{int} = 600, IQ_{V3}, IQ_{H3}$
baseline 5: $T_{det} = 60, T_{pred} = 1200, T_{int} = 300, IQ_{V3}, IQ_{H3}$

Table 14. Level and quality of intent test matrix IQ2b (Q4 sensitivity runs; 36 runs).

Parameter	Values	Units
Nominal Parameter Values	***baseline 6***: $T_{det} = 60, T_{pred} = 600, T_{int} = 600, IQ_{V4}, IQ_{H4}$	-
Time Interval for Intent Quality 4 Horizontal Points (Δt_{Q4})	15, 30, 45, 60, 75, 90, 120, 180, 300	s
Altitude Interval for Intent Quality 4 Vertical Points (Δalt_{Q4})	100, 200, 300, 400, 500, 750, 1000, 2000, 5000	ft
Trajectory Prediction Symmetry	Symmetric, Asymmetric	-

VII. Results and Discussion

The use of two separate conflict detection performance analysis methods required that some additional steps be taken to reconcile any differences in assumptions inherent in the analysis codes. Several comparison runs were made and the primary metrics compared in order to identify and correct these differences. The two analysis methods were shown to produce nearly identical results when run under the same input parameters and the same traffic scenarios. Table 15 shows the CD performance metrics for methods 1 and 2, and their differences, for a sample set of ten traffic scenarios. Each of the ten traffic scenarios is a random sample of 100 aircraft pairs with known LOS events from the set of time-shifted, recorded NAS traffic. Note that analysis method 2 was run with the recorded traffic data for these comparisons, as opposed to random circular scenarios.

Table 15. Comparison results for analysis methods 1 and 2 using the same 10 sample scenarios.

	Method 1				Method 2				Difference			
Sample Run	P_{FA}	P_{MA}	P_{MD}	$\Delta t_{LOS,mean}$ [s]	P_{FA}	P_{MA}	P_{MD}	$\Delta t_{LOS,mean}$ [s]	P_{FA}	P_{MA}	P_{MD}	$\Delta t_{LOS,mean}$ [s]
1	0.068	0.323	0.042	641	0.065	0.316	0.050	644	0.003	0.007	-0.008	-3
2	0.077	0.287	0.033	650	0.081	0.286	0.010	637	-0.004	0.001	0.023	13
3	0.081	0.319	0.030	648	0.083	0.321	0.030	632	-0.002	-0.002	0.000	16
4	0.064	0.296	0.053	661	0.074	0.298	0.040	646	-0.010	-0.002	0.013	15
5	0.103	0.348	0.043	613	0.098	0.335	0.060	619	0.005	0.013	-0.017	-6
6	0.083	0.318	0.034	647	0.080	0.307	0.050	658	0.003	0.011	-0.016	-11
7	0.075	0.339	0.008	649	0.075	0.334	0.010	656	0.000	0.005	-0.002	-7
8	0.076	0.290	0.016	605	0.077	0.293	0.020	606	-0.001	-0.003	-0.004	-1
9	0.065	0.305	0.009	678	0.065	0.304	0.020	677	0.000	0.001	-0.011	1
10	0.091	0.321	0.053	689	0.090	0.317	0.030	678	0.001	0.004	0.023	11

Note: analysis method 1 and 2 were both run with recorded traffic data scenarios; random circular scenarios were not used with analysis method 2 in these comparison runs.

Although the two analysis methods produced nearly identical results under the same parameter and scenario conditions, the two methods were expected to produce somewhat different results under the same parameter conditions when comparing recorded traffic scenarios to circular traffic scenarios. The primary reason for this difference is due to the fact that the recorded data has a small level of surveillance and sensor noise remaining even after the processing and filtering steps taken to clean the data. This small level of noise can have a significant impact on trajectory prediction accuracy, particularly in state-projection trajectory predictions where the predictions rely on velocity states obtained from differential derivatives. The second reason for the differences is that, for the circular scenarios, the intent information is perfect (the intent is identical to the kinematic flight plan and it is flown perfectly using kinematics). The significance of these differences is that, in general, the results produced using the circular scenarios of method 2 show better CD performance (lower false alert, missed alert, and missed detection probabilities, and higher values for mean time-to-LOS) than the results for the scenarios using recorded traffic data and analysis method 1. In some sense, the results from method 2 could be considered the upper bounds of CD performance since the conditions are more idealized, whereas, the results from method 1 could be considered closer to what could be expected in a real environment with noisy or imperfect data.

The following sections present the full set of results tables for the surveillance quality and intent information quality test matrices and the figures for a subset of those results, along with some discussion of the results. Comparison data runs using the analysis method 2 and random circular traffic scenarios are also presented and compared where applicable.

A. Surveillance Quality Results and Discussion

The results of the analysis runs for surveillance quality test matrix 1 (SQ1) are listed in Table 16-Table 19. The figures associated with test matrix SQ1 are Figure 24-Figure 29. Figure 24 illustrates that the absence of intent information, or the reliance on state-projection trajectory predictions, produces poor conflict detection performance in all of the primary metrics. In addition, if surveillance error is present at the quality of current surveillance radar technologies, the performance is reduced by 50% or more in terms of false alerts and missed detections. Even at short trajectory prediction and conflict detection horizons of 5 minutes, the CD performance in the absence of surveillance noise is poor with 48% false alerts, 46% missed alerts, 7% missed detections, and 158 seconds average time-to-LOS at first detection (Figure 25). There is a trade-off between trajectory prediction and the conflict detection horizon because higher detection horizons produce worst false alert, missed alert, and mean time-to-LOS metrics while missed detections are reduced. A surveillance range beyond 250 nautical miles appears to have minimal impact in improving the CD performance (Figure 26 and Figure 27), further solidifying the poor quality of state-projection trajectory predictions. Conflict detection cycle periods of 15 and 60 seconds (Figure 28) produced nearly identical false alert and missed alert metrics for the same input parameters but missed detection were reduced by ~60% and mean time-to-LOS at first detection was increased by ~25% by using 15 seconds instead of 60 seconds. Conflict detection performance using asymmetric predictions (perfect prediction for aircraft 1 in a pair) versus symmetric predictions had a positive impact on CD performance for all metrics (Figure 29).

The results of the analysis runs for surveillance quality test matrix 2 (SQ2) are listed in Table 20-Table 23. Table 24 shows the results of a set of comparison runs using circular scenarios and analysis method 2. The figures associated with test matrix SQ2 are Figure 30-Figure 40. The comparison results of Table 24 are shown in Figure 31 and Figure 33. The sensitivity curves indicate that false alert and missed alert probabilities are most sensitive to conflict detection and trajectory prediction horizon (Figure 31) and vertical speed errors (Figure 37). Missed detection probability, in terms of percent change, is sensitive to most of the parameters tested, with the lowest sensitivity being to the vertical position error (Figure 35). The mean time-to-LOS metric is most sensitive to CD cycle period (Figure 30), conflict detection and prediction horizon (Figure 31), and surveillance range (Figure 32). The comparison results from analysis method 2 for conflict detection and trajectory prediction horizon sensitivity show trends that are in agreement with the results of analysis method 1 (Figure 31). A similar agreement in sensitivity curves between the two analysis methods can be seen in Figure 33 for the sensitivity of the metrics to the

surveillance lag time parameter. The impact of the conflict comparison criteria on the CD performance metrics versus the conventional metrics definitions is that the conventional measurement would produce a less conservative performance (~4% lower false alert probability, ~6% lower missed alerts, ~3% lower missed detection, and ~60 second longer mean time-to-LOS metrics). Figure 40 confirms the improved conflict detection performance when using asymmetric trajectory predictions.

The results of the analysis runs for surveillance quality test matrix 3 (SQ3) are listed in Table 25 and Table 26. Table 27 and Table 28 present the summary statistics for the variability in the metrics due to different traffic scenarios and due to Monte Carlo sampling of the surveillance error parameters, including one case using analysis method 2. The variability of the CD performance metrics to different traffic scenarios with the same input parameters appears to be small with ~0.33% or less of standard deviation in the false alert probability, less than 0.3% of standard deviation in missed alert probability, less than 0.5% of standard deviation in the missed detection probability, and approximately 2 seconds of standard deviation for the mean time-to-LOS metric (Table 27). The variability of the CD performance metrics to the Monte Carlo sampling of the surveillance error parameters using the same traffic scenario is also small, with less than 0.1% of standard deviation in the false and missed alert probabilities, less than 0.25% of standard deviation in the missed detection probability, and less than 1.5 seconds of standard deviation for the mean time-to-LOS metric (Table 28). The variability is likely dependent on the number of LOS and the number of alerts identified during each scenario run; all of the variability scenario runs using the recorded traffic data had ~15,000 true LOS and between 135,000 and 237,000 conflict alerts.

Surveillance Quality Results Tables

Table 16. Surveillance quality run data with symmetric predictions and 60 second CD cycle period.

Run	T_{det} [s]	T_{pred} [s]	SQ_{model}	R_s [NM]	P_{FA}	P_{MA}	P_{MD}	$\Delta t_{LOS,mean}$ [s]
sq1_001	60	1200	none	1500	0.752	0.742	0.063	277
sq1_002	60	1200	radar	1500	0.931	0.905	0.182	134
sq1_003	60	1200	ADSB_1	1500	0.914	0.878	0.103	172
sq1_004	60	1200	ADSB_2	1500	0.881	0.810	0.065	259
sq1_005	60	1200	none	250	0.741	0.743	0.063	275
sq1_006	60	1200	radar	250	0.929	0.905	0.184	135
sq1_007	60	1200	ADSB_1	250	0.912	0.879	0.110	169
sq1_008	60	1200	ADSB_2	250	0.875	0.810	0.061	255
sq1_009	60	1200	none	50	0.576	0.803	0.069	188
sq1_010	60	1200	radar	50	0.865	0.910	0.193	109
sq1_011	60	1200	ADSB_1	50	0.833	0.887	0.115	133
sq1_012	60	1200	ADSB_2	50	0.734	0.837	0.069	176
sq1_013	60	600	none	1500	0.647	0.624	0.064	214
sq1_014	60	600	radar	1500	0.904	0.838	0.186	125
sq1_015	60	600	ADSB_1	1500	0.879	0.792	0.109	154
sq1_016	60	600	ADSB_2	1500	0.815	0.687	0.067	211
sq1_017	60	600	none	250	0.647	0.624	0.064	214
sq1_018	60	600	radar	250	0.902	0.835	0.191	129
sq1_019	60	600	ADSB_1	250	0.879	0.793	0.111	156
sq1_020	60	600	ADSB_2	250	0.815	0.686	0.065	211
sq1_021	60	600	none	50	0.523	0.677	0.069	172
sq1_022	60	600	radar	50	0.854	0.844	0.192	109
sq1_023	60	600	ADSB_1	50	0.815	0.805	0.115	129
sq1_024	60	600	ADSB_2	50	0.698	0.721	0.070	167
sq1_025	60	300	none	1500	0.483	0.460	0.069	148
sq1_026	60	300	radar	1500	0.851	0.708	0.193	104
sq1_027	60	300	ADSB_1	1500	0.814	0.641	0.118	119
sq1_028	60	300	ADSB_2	1500	0.703	0.502	0.070	147
sq1_029	60	300	none	250	0.483	0.460	0.069	148
sq1_030	60	300	radar	250	0.851	0.710	0.195	103
sq1_031	60	300	ADSB_1	250	0.812	0.641	0.120	120
sq1_032	60	300	ADSB_2	250	0.702	0.503	0.072	147
sq1_033	60	300	none	50	0.433	0.482	0.070	139
sq1_034	60	300	radar	50	0.830	0.714	0.193	100
sq1_035	60	300	ADSB_1	50	0.783	0.650	0.118	112
sq1_036	60	300	ADSB_2	50	0.644	0.522	0.073	137

Table 17. Surveillance quality run data with symmetric predictions and 15 second CD cycle period.

Run	T_{det} [s]	T_{pred} [s]	SQ_{model}	R_s [NM]	P_{FA}	P_{MA}	P_{MD}	$\Delta t_{LOS,mean}$ [s]
sq1_037	15	1200	none	1500	0.751	0.742	0.003	316
sq1_038	15	1200	radar	1500	0.929	0.903	0.022	220
sq1_039	15	1200	ADSB_1	1500	0.914	0.878	0.015	278
sq1_040	15	1200	ADSB_2	1500	0.880	0.809	0.009	353
sq1_041	15	1200	none	250	0.739	0.743	0.003	314
sq1_042	15	1200	radar	250	0.927	0.904	0.022	220
sq1_043	15	1200	ADSB_1	250	0.911	0.878	0.011	274
sq1_044	15	1200	ADSB_2	250	0.874	0.809	0.010	347
sq1_045	15	1200	none	50	0.573	0.803	0.004	215
sq1_046	15	1200	radar	50	0.863	0.909	0.022	169
sq1_047	15	1200	ADSB_1	50	0.831	0.886	0.013	203
sq1_048	15	1200	ADSB_2	50	0.731	0.836	0.008	234
sq1_049	15	600	none	1500	0.644	0.624	0.003	246
sq1_050	15	600	radar	1500	0.901	0.834	0.025	202
sq1_051	15	600	ADSB_1	1500	0.878	0.793	0.014	236
sq1_052	15	600	ADSB_2	1500	0.815	0.687	0.010	274
sq1_053	15	600	none	250	0.644	0.624	0.003	246
sq1_054	15	600	radar	250	0.901	0.835	0.022	203
sq1_055	15	600	ADSB_1	250	0.879	0.793	0.014	237
sq1_056	15	600	ADSB_2	250	0.815	0.687	0.010	275
sq1_057	15	600	none	50	0.519	0.677	0.004	196
sq1_058	15	600	radar	50	0.852	0.842	0.024	166
sq1_059	15	600	ADSB_1	50	0.814	0.805	0.012	193
sq1_060	15	600	ADSB_2	50	0.696	0.721	0.009	214
sq1_061	15	300	none	1500	0.479	0.460	0.004	171
sq1_062	15	300	radar	1500	0.849	0.708	0.023	154
sq1_063	15	300	ADSB_1	1500	0.812	0.640	0.013	173
sq1_064	15	300	ADSB_2	1500	0.701	0.502	0.010	186
sq1_065	15	300	none	250	0.479	0.460	0.004	171
sq1_066	15	300	radar	250	0.849	0.707	0.025	155
sq1_067	15	300	ADSB_1	250	0.813	0.640	0.015	174
sq1_068	15	300	ADSB_2	250	0.701	0.503	0.009	184
sq1_069	15	300	none	50	0.427	0.481	0.004	160
sq1_070	15	300	radar	50	0.827	0.713	0.024	146
sq1_071	15	300	ADSB_1	50	0.781	0.649	0.016	163
sq1_072	15	300	ADSB_2	50	0.639	0.522	0.010	172

Table 18. Surveillance quality run data with asymmetric predictions and 60 second CD cycle period.

Run	T_{det} [s]	T_{pred} [s]	SQ_{model}	R_s [NM]	P_{FA}	P_{MA}	P_{MD}	$\Delta t_{LOS,mean}$ [s]
sq1_073	60	1200	none	1500	0.557	0.586	0.039	420
sq1_074	60	1200	radar	1500	0.896	0.850	0.151	303
sq1_075	60	1200	ADSB_1	1500	0.864	0.797	0.050	354
sq1_076	60	1200	ADSB_2	1500	0.812	0.696	0.038	420
sq1_077	60	1200	none	250	0.544	0.589	0.039	416
sq1_078	60	1200	radar	250	0.892	0.849	0.150	299
sq1_079	60	1200	ADSB_1	250	0.858	0.797	0.049	350
sq1_080	60	1200	ADSB_2	250	0.801	0.698	0.039	414
sq1_081	60	1200	none	50	0.416	0.724	0.042	263
sq1_082	60	1200	radar	50	0.808	0.872	0.166	198
sq1_083	60	1200	ADSB_1	50	0.749	0.831	0.056	227
sq1_084	60	1200	ADSB_2	50	0.612	0.770	0.045	261
sq1_085	60	600	none	1500	0.446	0.456	0.040	297
sq1_086	60	600	radar	1500	0.857	0.754	0.157	230
sq1_087	60	600	ADSB_1	1500	0.814	0.679	0.053	252
sq1_088	60	600	ADSB_2	1500	0.721	0.543	0.040	294
sq1_089	60	600	none	250	0.446	0.456	0.040	297
sq1_090	60	600	radar	250	0.857	0.756	0.159	230
sq1_091	60	600	ADSB_1	250	0.814	0.679	0.052	253
sq1_092	60	600	ADSB_2	250	0.721	0.544	0.041	293
sq1_093	60	600	none	50	0.357	0.569	0.042	227
sq1_094	60	600	radar	50	0.792	0.784	0.171	177
sq1_095	60	600	ADSB_1	50	0.725	0.717	0.056	194
sq1_096	60	600	ADSB_2	50	0.562	0.621	0.043	221
sq1_097	60	300	none	1500	0.311	0.310	0.043	185
sq1_098	60	300	radar	1500	0.796	0.614	0.178	148
sq1_099	60	300	ADSB_1	1500	0.734	0.507	0.061	158
sq1_100	60	300	ADSB_2	1500	0.589	0.361	0.046	182
sq1_101	60	300	none	250	0.311	0.310	0.043	185
sq1_102	60	300	radar	250	0.796	0.614	0.181	149
sq1_103	60	300	ADSB_1	250	0.736	0.511	0.062	156
sq1_104	60	300	ADSB_2	250	0.589	0.363	0.046	181
sq1_105	60	300	none	50	0.278	0.354	0.043	170
sq1_106	60	300	radar	50	0.766	0.632	0.187	137
sq1_107	60	300	ADSB_1	50	0.691	0.528	0.064	146
sq1_108	60	300	ADSB_2	50	0.511	0.400	0.049	167

Table 19. Surveillance quality run data with asymmetric predictions and 15 second CD cycle period.

Run	T_{det} [s]	T_{pred} [s]	SQ_{model}	R_s [NM]	P_{FA}	P_{MA}	P_{MD}	$\Delta t_{LOS,mean}$ [s]
sq1_109	15	1200	none	1500	0.555	0.585	0.002	458
sq1_110	15	1200	radar	1500	0.895	0.849	0.049	472
sq1_111	15	1200	ADSB_1	1500	0.864	0.797	0.007	515
sq1_112	15	1200	ADSB_2	1500	0.811	0.696	0.006	522
sq1_113	15	1200	none	250	0.542	0.588	0.002	453
sq1_114	15	1200	radar	250	0.891	0.848	0.049	464
sq1_115	15	1200	ADSB_1	250	0.858	0.797	0.007	508
sq1_116	15	1200	ADSB_2	250	0.800	0.697	0.006	513
sq1_117	15	1200	none	50	0.414	0.724	0.002	293
sq1_118	15	1200	radar	50	0.809	0.872	0.051	297
sq1_119	15	1200	ADSB_1	50	0.748	0.831	0.006	327
sq1_120	15	1200	ADSB_2	50	0.609	0.769	0.006	324
sq1_121	15	600	none	1500	0.444	0.455	0.002	325
sq1_122	15	600	radar	1500	0.856	0.754	0.053	332
sq1_123	15	600	ADSB_1	1500	0.814	0.679	0.007	351
sq1_124	15	600	ADSB_2	1500	0.720	0.544	0.006	354
sq1_125	15	600	none	250	0.444	0.455	0.002	325
sq1_126	15	600	radar	250	0.856	0.754	0.049	331
sq1_127	15	600	ADSB_1	250	0.813	0.678	0.007	352
sq1_128	15	600	ADSB_2	250	0.720	0.544	0.006	353
sq1_129	15	600	none	50	0.355	0.568	0.002	252
sq1_130	15	600	radar	50	0.791	0.783	0.052	251
sq1_131	15	600	ADSB_1	50	0.724	0.716	0.008	269
sq1_132	15	600	ADSB_2	50	0.562	0.621	0.007	268
sq1_133	15	300	none	1500	0.308	0.309	0.002	206
sq1_134	15	300	radar	1500	0.793	0.612	0.067	203
sq1_135	15	300	ADSB_1	1500	0.734	0.506	0.008	211
sq1_136	15	300	ADSB_2	1500	0.586	0.361	0.007	214
sq1_137	15	300	none	250	0.308	0.309	0.002	206
sq1_138	15	300	radar	250	0.794	0.613	0.064	202
sq1_139	15	300	ADSB_1	250	0.733	0.506	0.009	212
sq1_140	15	300	ADSB_2	250	0.587	0.361	0.007	214
sq1_141	15	300	none	50	0.274	0.353	0.002	191
sq1_142	15	300	radar	50	0.764	0.630	0.065	187
sq1_143	15	300	ADSB_1	50	0.690	0.528	0.007	195
sq1_144	15	300	ADSB_2	50	0.508	0.398	0.007	198

Table 20. Surveillance quality sensitivity run data with symmetric predictions and no baseline surveillance error.

Run	T_{det} [s]	T_{pred} [s]	R_s [NM]	t_{sl} [s]	σ_r [NM]	σ_a [ft]	σ_{gs} [knots]	σ_{vs} [ft/min]	σ_{trk} [deg]	*Same X*	P_{FA}	P_{MA}	P_{MD}	$\Delta t_{LOS,mean}$ [s]
sq2_001	60	600	1500	0	0	0	0	0	0	1	0.647	0.624	0.064	214
sq2_002	15	600	1500	0	0	0	0	0	0	1	0.644	0.624	0.003	246
sq2_003	30	600	1500	0	0	0	0	0	0	1	0.645	0.624	0.016	230
sq2_004	120	600	1500	0	0	0	0	0	0	1	0.650	0.624	0.193	205
sq2_005	300	600	1500	0	0	0	0	0	0	1	0.666	0.633	0.463	203
sq2_006	60	60	1500	0	0	0	0	0	0	1	0.146	0.138	0.138	30
sq2_007	60	120	1500	0	0	0	0	0	0	1	0.257	0.245	0.083	70
sq2_008	60	300	1500	0	0	0	0	0	0	1	0.483	0.460	0.069	148
sq2_009	60	900	1500	0	0	0	0	0	0	1	0.712	0.698	0.064	251
sq2_010	60	1200	1500	0	0	0	0	0	0	1	0.752	0.742	0.063	277
sq2_011	60	600	20	0	0	0	0	0	0	1	0.478	0.771	0.081	114
sq2_012	60	600	40	0	0	0	0	0	0	1	0.507	0.699	0.071	158
sq2_013	60	600	80	0	0	0	0	0	0	1	0.573	0.642	0.067	197
sq2_014	60	600	100	0	0	0	0	0	0	1	0.601	0.632	0.065	206
sq2_015	60	600	200	0	0	0	0	0	0	1	0.647	0.624	0.064	214
sq2_016	60	600	300	0	0	0	0	0	0	1	0.647	0.624	0.064	214
sq2_017	60	600	500	0	0	0	0	0	0	1	0.647	0.624	0.064	214
sq2_018	60	600	1500	1	0	0	0	0	0	1	0.647	0.625	0.068	214
sq2_019	60	600	1500	2	0	0	0	0	0	1	0.649	0.627	0.071	213
sq2_020	60	600	1500	5	0	0	0	0	0	1	0.659	0.634	0.083	213
sq2_021	60	600	1500	10	0	0	0	0	0	1	0.670	0.643	0.106	212
sq2_022	60	600	1500	15	0	0	0	0	0	1	0.680	0.652	0.126	212
sq2_023	60	600	1500	0	0.001	0	0	0	0	1	0.647	0.624	0.064	214
sq2_024	60	600	1500	0	0.01	0	0	0	0	1	0.647	0.624	0.064	214
sq2_025	60	600	1500	0	0.1	0	0	0	0	1	0.648	0.626	0.068	215
sq2_026	60	600	1500	0	0.5	0	0	0	0	1	0.663	0.642	0.084	217
sq2_027	60	600	1500	0	0	1	0	0	0	1	0.647	0.624	0.064	213
sq2_028	60	600	1500	0	0	10	0	0	0	1	0.648	0.624	0.066	213
sq2_029	60	600	1500	0	0	25	0	0	0	1	0.648	0.625	0.068	214
sq2_030	60	600	1500	0	0	50	0	0	0	1	0.652	0.626	0.071	215
sq2_031	60	600	1500	0	0	100	0	0	0	1	0.688	0.625	0.070	220
sq2_032	60	600	1500	0	0	150	0	0	0	1	0.724	0.626	0.075	223
sq2_033	60	600	1500	0	0	0	0.1	0	0	1	0.647	0.624	0.065	214
sq2_034	60	600	1500	0	0	0	1	0	0	1	0.647	0.624	0.065	214
sq2_035	60	600	1500	0	0	0	5	0	0	1	0.653	0.630	0.066	213
sq2_036	60	600	1500	0	0	0	10	0	0	1	0.665	0.641	0.069	210
sq2_037	60	600	1500	0	0	0	20	0	0	1	0.691	0.663	0.073	205
sq2_038	60	600	1500	0	0	0	50	0	0	1	0.758	0.717	0.091	187
sq2_039	60	600	1500	0	0	0	0	10	0	1	0.657	0.623	0.064	216
sq2_040	60	600	1500	0	0	0	0	25	0	1	0.703	0.619	0.057	222
sq2_041	60	600	1500	0	0	0	0	50	0	1	0.744	0.624	0.054	222
sq2_042	60	600	1500	0	0	0	0	100	0	1	0.785	0.650	0.052	221
sq2_043	60	600	1500	0	0	0	0	500	0	1	0.877	0.792	0.090	147
sq2_044	60	600	1500	0	0	0	0	1000	0	1	0.912	0.860	0.199	101
sq2_045	60	600	1500	0	0	0	0	0	0.1	1	0.647	0.624	0.064	214
sq2_046	60	600	1500	0	0	0	0	0	0.5	1	0.648	0.626	0.064	213
sq2_047	60	600	1500	0	0	0	0	0	1	1	0.653	0.632	0.065	212
sq2_048	60	600	1500	0	0	0	0	0	2	1	0.664	0.647	0.069	209
sq2_049	60	600	1500	0	0	0	0	0	5	1	0.706	0.698	0.081	190
sq2_050	60	600	1500	0	0	0	0	0	0	0.5	0.684	0.664	0.086	188
sq2_051	60	600	1500	0	0	0	0	0	0	2	0.624	0.595	0.049	234
sq2_052	60	600	1500	0	0	0	0	0	0	Inf.	0.606	0.560	0.036	277

Table 21. Surveillance quality sensitivity run data with symmetric predictions and ADSB_2 baseline surveillance error.

Run	T_{det} [s]	T_{pred} [s]	R_s [NM]	t_{sl} [s]	σ_r [NM]	σ_a [ft]	σ_{gs} [knots]	σ_{vs} [ft/min]	σ_{trk} [deg]	Same X	P_{FA}	P_{MA}	P_{MD}	$\Delta t_{LOS,mean}$ [s]
sq2_053	60	600	1500	1	0.0081	73.8	1	150	1	1	0.815	0.684	0.061	211
sq2_054	15	600	1500	1	0.0081	73.8	1	150	1	1	0.815	0.687	0.008	275
sq2_055	30	600	1500	1	0.0081	73.8	1	150	1	1	0.814	0.686	0.021	243
sq2_056	120	600	1500	1	0.0081	73.8	1	150	1	1	0.818	0.689	0.193	182
sq2_057	300	600	1500	1	0.0081	73.8	1	150	1	1	0.826	0.698	0.496	157
sq2_058	60	60	1500	1	0.0081	73.8	1	150	1	1	0.416	0.183	0.183	30
sq2_059	60	120	1500	1	0.0081	73.8	1	150	1	1	0.519	0.275	0.094	69
sq2_060	60	300	1500	1	0.0081	73.8	1	150	1	1	0.703	0.503	0.070	146
sq2_061	60	900	1500	1	0.0081	73.8	1	150	1	1	0.858	0.766	0.066	242
sq2_062	60	1200	1500	1	0.0081	73.8	1	150	1	1	0.881	0.809	0.065	258
sq2_063	60	600	20	1	0.0081	73.8	1	150	1	1	0.622	0.795	0.092	111
sq2_064	60	600	40	1	0.0081	73.8	1	150	1	1	0.673	0.737	0.074	153
sq2_065	60	600	80	1	0.0081	73.8	1	150	1	1	0.754	0.699	0.067	192
sq2_066	60	600	100	1	0.0081	73.8	1	150	1	1	0.780	0.692	0.066	202
sq2_067	60	600	200	1	0.0081	73.8	1	150	1	1	0.816	0.687	0.065	212
sq2_068	60	600	300	1	0.0081	73.8	1	150	1	1	0.816	0.687	0.065	212
sq2_069	60	600	500	1	0.0081	73.8	1	150	1	1	0.816	0.687	0.064	210
sq2_070	60	600	1500	1	0.0081	73.8	1	150	1	1	0.816	0.687	0.064	210
sq2_071	60	600	1500	2	0.0081	73.8	1	150	1	1	0.817	0.689	0.067	209
sq2_072	60	600	1500	5	0.0081	73.8	1	150	1	1	0.821	0.695	0.077	208
sq2_073	60	600	1500	10	0.0081	73.8	1	150	1	1	0.827	0.703	0.092	207
sq2_074	60	600	1500	15	0.0081	73.8	1	150	1	1	0.833	0.712	0.108	205
sq2_075	60	600	1500	1	0.001	73.8	1	150	1	1	0.815	0.686	0.064	211
sq2_076	60	600	1500	1	0.01	73.8	1	150	1	1	0.815	0.685	0.064	211
sq2_077	60	600	1500	1	0.1	73.8	1	150	1	1	0.816	0.687	0.067	211
sq2_078	60	600	1500	1	0.5	73.8	1	150	1	1	0.825	0.701	0.083	211
sq2_079	60	600	1500	1	0.0081	1	1	150	1	1	0.812	0.683	0.058	208
sq2_080	60	600	1500	1	0.0081	10	1	150	1	1	0.814	0.684	0.058	209
sq2_081	60	600	1500	1	0.0081	25	1	150	1	1	0.814	0.684	0.061	208
sq2_082	60	600	1500	1	0.0081	50	1	150	1	1	0.813	0.685	0.063	212
sq2_083	60	600	1500	1	0.0081	100	1	150	1	1	0.818	0.688	0.066	210
sq2_084	60	600	1500	1	0.0081	150	1	150	1	1	0.820	0.693	0.076	213
sq2_085	60	600	1500	1	0.0081	73.8	0.1	150	1	1	0.815	0.686	0.063	210
sq2_086	60	600	1500	1	0.0081	73.8	1	150	1	1	0.817	0.689	0.067	210
sq2_087	60	600	1500	1	0.0081	73.8	5	150	1	1	0.818	0.690	0.065	209
sq2_088	60	600	1500	1	0.0081	73.8	10	150	1	1	0.821	0.695	0.065	206
sq2_089	60	600	1500	1	0.0081	73.8	20	150	1	1	0.830	0.708	0.074	200
sq2_090	60	600	1500	1	0.0081	73.8	50	150	1	1	0.858	0.747	0.094	180
sq2_091	60	600	1500	1	0.0081	73.8	1	10	1	1	0.690	0.635	0.072	216
sq2_092	60	600	1500	1	0.0081	73.8	1	25	1	1	0.725	0.634	0.071	221
sq2_093	60	600	1500	1	0.0081	73.8	1	50	1	1	0.757	0.638	0.063	222
sq2_094	60	600	1500	1	0.0081	73.8	1	100	1	1	0.794	0.661	0.063	220
sq2_095	60	600	1500	1	0.0081	73.8	1	500	1	1	0.881	0.798	0.100	144
sq2_096	60	600	1500	1	0.0081	73.8	1	1000	1	1	0.915	0.865	0.214	99
sq2_097	60	600	1500	1	0.0081	73.8	1	150	0.1	1	0.813	0.681	0.060	212
sq2_098	60	600	1500	1	0.0081	73.8	1	150	0.5	1	0.814	0.684	0.061	212
sq2_099	60	600	1500	1	0.0081	73.8	1	150	1	1	0.815	0.686	0.066	212
sq2_100	60	600	1500	1	0.0081	73.8	1	150	2	1	0.820	0.696	0.066	205
sq2_101	60	600	1500	1	0.0081	73.8	1	150	5	1	0.836	0.733	0.082	184
sq2_102	60	600	1500	1	0.0081	73.8	1	150	1	0.5	0.847	0.741	0.096	166
sq2_103	60	600	1500	1	0.0081	73.8	1	150	1	2	0.799	0.656	0.047	240
sq2_104	60	600	1500	1	0.0081	73.8	1	150	1	Inf.	0.786	0.615	0.026	288

Table 22. Surveillance quality sensitivity run data with asymmetric predictions and no baseline surveillance error.

Run	T_{det} [s]	T_{pred} [s]	R_s [NM]	t_{sl} [s]	σ_r [NM]	σ_a [ft]	σ_{gs} [knots]	σ_{vs} [ft/min]	σ_{trk} [deg]	*Same X*	P_{FA}	P_{MA}	P_{MD}	$\Delta t_{LOS,mean}$ [s]
sq2_105	60	600	1500	0	0	0	0	0	0	1	0.446	0.456	0.040	297
sq2_106	15	600	1500	0	0	0	0	0	0	1	0.444	0.455	0.002	325
sq2_107	30	600	1500	0	0	0	0	0	0	1	0.445	0.455	0.010	311
sq2_108	120	600	1500	0	0	0	0	0	0	1	0.450	0.458	0.121	286
sq2_109	300	600	1500	0	0	0	0	0	0	1	0.465	0.463	0.309	269
sq2_110	60	60	1500	0	0	0	0	0	0	1	0.087	0.084	0.084	31
sq2_111	60	120	1500	0	0	0	0	0	0	1	0.158	0.154	0.051	78
sq2_112	60	300	1500	0	0	0	0	0	0	1	0.311	0.310	0.043	185
sq2_113	60	900	1500	0	0	0	0	0	0	1	0.511	0.534	0.039	369
sq2_114	60	1200	1500	0	0	0	0	0	0	1	0.557	0.586	0.039	420
sq2_115	60	600	20	0	0	0	0	0	0	1	0.338	0.699	0.048	151
sq2_116	60	600	40	0	0	0	0	0	0	1	0.349	0.602	0.043	207
sq2_117	60	600	80	0	0	0	0	0	0	1	0.388	0.505	0.041	266
sq2_118	60	600	100	0	0	0	0	0	0	1	0.409	0.481	0.040	281
sq2_119	60	600	200	0	0	0	0	0	0	1	0.446	0.456	0.040	297
sq2_120	60	600	300	0	0	0	0	0	0	1	0.446	0.456	0.040	297
sq2_121	60	600	500	0	0	0	0	0	0	1	0.446	0.456	0.040	297
sq2_122	60	600	1500	1	0	0	0	0	0	1	0.449	0.459	0.045	298
sq2_123	60	600	1500	2	0	0	0	0	0	1	0.455	0.465	0.057	300
sq2_124	60	600	1500	5	0	0	0	0	0	1	0.482	0.487	0.089	303
sq2_125	60	600	1500	10	0	0	0	0	0	1	0.523	0.526	0.154	307
sq2_126	60	600	1500	15	0	0	0	0	0	1	0.561	0.562	0.213	309
sq2_127	60	600	1500	0	0.001	0	0	0	0	1	0.446	0.456	0.040	297
sq2_128	60	600	1500	0	0.01	0	0	0	0	1	0.446	0.456	0.040	297
sq2_129	60	600	1500	0	0.1	0	0	0	0	1	0.448	0.458	0.042	298
sq2_130	60	600	1500	0	0.5	0	0	0	0	1	0.462	0.471	0.048	300
sq2_131	60	600	1500	0	0	1	0	0	0	1	0.446	0.456	0.040	297
sq2_132	60	600	1500	0	0	10	0	0	0	1	0.447	0.456	0.040	297
sq2_133	60	600	1500	0	0	25	0	0	0	1	0.448	0.457	0.041	298
sq2_134	60	600	1500	0	0	50	0	0	0	1	0.450	0.459	0.043	299
sq2_135	60	600	1500	0	0	100	0	0	0	1	0.479	0.461	0.046	301
sq2_136	60	600	1500	0	0	150	0	0	0	1	0.537	0.464	0.047	303
sq2_137	60	600	1500	0	0	0	0.1	0	0	1	0.446	0.456	0.040	297
sq2_138	60	600	1500	0	0	0	1	0	0	1	0.447	0.456	0.040	297
sq2_139	60	600	1500	0	0	0	5	0	0	1	0.454	0.462	0.040	297
sq2_140	60	600	1500	0	0	0	10	0	0	1	0.467	0.475	0.040	296
sq2_141	60	600	1500	0	0	0	20	0	0	1	0.501	0.503	0.043	290
sq2_142	60	600	1500	0	0	0	50	0	0	1	0.594	0.574	0.052	272
sq2_143	60	600	1500	0	0	0	0	10	0	1	0.453	0.457	0.039	298
sq2_144	60	600	1500	0	0	0	0	25	0	1	0.523	0.457	0.035	302
sq2_145	60	600	1500	0	0	0	0	50	0	1	0.600	0.463	0.033	303
sq2_146	60	600	1500	0	0	0	0	100	0	1	0.672	0.496	0.032	299
sq2_147	60	600	1500	0	0	0	0	500	0	1	0.814	0.681	0.043	247
sq2_148	60	600	1500	0	0	0	0	1000	0	1	0.860	0.772	0.084	199
sq2_149	60	600	1500	0	0	0	0	0	0.1	1	0.446	0.456	0.040	297
sq2_150	60	600	1500	0	0	0	0	0	0.5	1	0.449	0.459	0.040	297
sq2_151	60	600	1500	0	0	0	0	0	1	1	0.456	0.466	0.040	296
sq2_152	60	600	1500	0	0	0	0	0	2	1	0.472	0.484	0.041	294
sq2_153	60	600	1500	0	0	0	0	0	5	1	0.527	0.545	0.045	281
sq2_154	60	600	1500	0	0	0	0	0	0	0.5	0.481	0.491	0.051	278
sq2_155	60	600	1500	0	0	0	0	0	0	2	0.425	0.432	0.031	312
sq2_156	60	600	1500	0	0	0	0	0	0	Inf.	0.409	0.400	0.024	341

Table 23. Surveillance quality sensitivity run data with asymmetric predictions and ADSB_2 baseline surveillance error.

Run	T_{det} [s]	T_{pred} [s]	R_s [NM]	t_{sl} [s]	σ_r [NM]	σ_a [ft]	σ_{gs} [knots]	σ_{vs} [ft/min]	σ_{trk} [deg]	*Same X*	P_{FA}	P_{MA}	P_{MD}	$\Delta t_{LOS,mean}$ [s]
sq2_157	60	600	1500	1	0.0081	73.8	1	150	1	1	0.720	0.543	0.040	294
sq2_158	15	600	1500	1	0.0081	73.8	1	150	1	1	0.719	0.543	0.006	353
sq2_159	30	600	1500	1	0.0081	73.8	1	150	1	1	0.720	0.544	0.014	325
sq2_160	120	600	1500	1	0.0081	73.8	1	150	1	1	0.721	0.545	0.118	261
sq2_161	300	600	1500	1	0.0081	73.8	1	150	1	1	0.732	0.555	0.342	220
sq2_162	60	60	1500	1	0.0081	73.8	1	150	1	1	0.299	0.151	0.151	31
sq2_163	60	120	1500	1	0.0081	73.8	1	150	1	1	0.406	0.199	0.069	76
sq2_164	60	300	1500	1	0.0081	73.8	1	150	1	1	0.587	0.362	0.046	181
sq2_165	60	900	1500	1	0.0081	73.8	1	150	1	1	0.778	0.639	0.040	369
sq2_166	60	1200	1500	1	0.0081	73.8	1	150	1	1	0.812	0.695	0.038	420
sq2_167	60	600	20	1	0.0081	73.8	1	150	1	1	0.480	0.728	0.063	151
sq2_168	60	600	40	1	0.0081	73.8	1	150	1	1	0.534	0.646	0.047	204
sq2_169	60	600	80	1	0.0081	73.8	1	150	1	1	0.632	0.574	0.042	260
sq2_170	60	600	100	1	0.0081	73.8	1	150	1	1	0.667	0.560	0.040	275
sq2_171	60	600	200	1	0.0081	73.8	1	150	1	1	0.721	0.545	0.040	294
sq2_172	60	600	300	1	0.0081	73.8	1	150	1	1	0.721	0.544	0.039	293
sq2_173	60	600	500	1	0.0081	73.8	1	150	1	1	0.721	0.544	0.040	294
sq2_174	60	600	1500	1	0.0081	73.8	1	150	1	1	0.721	0.544	0.040	294
sq2_175	60	600	1500	2	0.0081	73.8	1	150	1	1	0.724	0.549	0.047	294
sq2_176	60	600	1500	5	0.0081	73.8	1	150	1	1	0.736	0.567	0.075	296
sq2_177	60	600	1500	10	0.0081	73.8	1	150	1	1	0.755	0.597	0.134	300
sq2_178	60	600	1500	15	0.0081	73.8	1	150	1	1	0.774	0.628	0.190	301
sq2_179	60	600	1500	1	0.001	73.8	1	150	1	1	0.721	0.544	0.041	294
sq2_180	60	600	1500	1	0.01	73.8	1	150	1	1	0.721	0.543	0.042	295
sq2_181	60	600	1500	1	0.1	73.8	1	150	1	1	0.722	0.546	0.042	293
sq2_182	60	600	1500	1	0.5	73.8	1	150	1	1	0.728	0.555	0.045	293
sq2_183	60	600	1500	1	0.0081	1	1	150	1	1	0.718	0.541	0.038	293
sq2_184	60	600	1500	1	0.0081	10	1	150	1	1	0.718	0.541	0.038	293
sq2_185	60	600	1500	1	0.0081	25	1	150	1	1	0.718	0.542	0.038	293
sq2_186	60	600	1500	1	0.0081	50	1	150	1	1	0.719	0.542	0.040	294
sq2_187	60	600	1500	1	0.0081	100	1	150	1	1	0.722	0.544	0.043	294
sq2_188	60	600	1500	1	0.0081	150	1	150	1	1	0.727	0.547	0.045	295
sq2_189	60	600	1500	1	0.0081	73.8	0.1	150	1	1	0.721	0.543	0.041	294
sq2_190	60	600	1500	1	0.0081	73.8	1	150	1	1	0.721	0.544	0.042	295
sq2_191	60	600	1500	1	0.0081	73.8	5	150	1	1	0.723	0.548	0.041	292
sq2_192	60	600	1500	1	0.0081	73.8	10	150	1	1	0.728	0.555	0.040	291
sq2_193	60	600	1500	1	0.0081	73.8	20	150	1	1	0.740	0.571	0.045	284
sq2_194	60	600	1500	1	0.0081	73.8	50	150	1	1	0.778	0.625	0.054	263
sq2_195	60	600	1500	1	0.0081	73.8	1	10	1	1	0.486	0.473	0.048	300
sq2_196	60	600	1500	1	0.0081	73.8	1	25	1	1	0.551	0.474	0.045	302
sq2_197	60	600	1500	1	0.0081	73.8	1	50	1	1	0.617	0.478	0.043	304
sq2_198	60	600	1500	1	0.0081	73.8	1	100	1	1	0.684	0.510	0.040	299
sq2_199	60	600	1500	1	0.0081	73.8	1	500	1	1	0.819	0.689	0.052	248
sq2_200	60	600	1500	1	0.0081	73.8	1	1000	1	1	0.864	0.777	0.096	199
sq2_201	60	600	1500	1	0.0081	73.8	1	150	0.1	1	0.717	0.538	0.041	295
sq2_202	60	600	1500	1	0.0081	73.8	1	150	0.5	1	0.718	0.540	0.039	294
sq2_203	60	600	1500	1	0.0081	73.8	1	150	1	1	0.721	0.545	0.041	294
sq2_204	60	600	1500	1	0.0081	73.8	1	150	2	1	0.727	0.556	0.041	289
sq2_205	60	600	1500	1	0.0081	73.8	1	150	5	1	0.750	0.601	0.046	272
sq2_206	60	600	1500	1	0.0081	73.8	1	150	1	0.5	0.750	0.592	0.059	266
sq2_207	60	600	1500	1	0.0081	73.8	1	150	1	2	0.706	0.517	0.029	311
sq2_208	60	600	1500	1	0.0081	73.8	1	150	1	Inf.	0.693	0.482	0.018	340

Table 24. Comparison sensitivity run data from circular scenarios and analysis method 2, with symmetric predictions, no baseline surveillance error and with ADSB_2 error (no surveillance lag).

T_{det} [s]	T_{pred} [s]	R_s [NM]	t_{sl} [s]	σ_r [NM]	σ_a [ft]	σ_{gs} [knots]	σ_{vs} [ft/min]	σ_{trk} [deg]	Same X	P_{FA}	P_{MA}	P_{MD}	$\Delta t_{LOS,mean}$ [s]
60	60	500	0	0	0	0	0	0	1	0.052	0.061	0.062	31
60	120	500	0	0	0	0	0	0	1	0.107	0.109	0.053	76
60	300	500	0	0	0	0	0	0	1	0.260	0.229	0.044	157
60	600	500	0	0	0	0	0	0	1	0.444	0.373	0.039	218
60	900	500	0	0	0	0	0	0	1	0.560	0.469	0.037	245
60	1200	500	0	0	0	0	0	0	1	0.638	0.534	0.037	258
60	600	500	0	0	0	0	0	0	1	0.425	0.361	0.037	227
60	600	500	1	0	0	0	0	0	1	0.430	0.365	0.041	228
60	600	500	2	0	0	0	0	0	1	0.436	0.371	0.046	228
60	600	500	5	0	0	0	0	0	1	0.450	0.385	0.056	228
60	600	500	10	0	0	0	0	0	1	0.475	0.411	0.073	227
60	600	500	15	0	0	0	0	0	1	0.499	0.437	0.089	226
60	60	500	0	0.0081	73.8	1	150	1	1	0.148	0.074	0.077	31
60	120	500	0	0.0081	73.8	1	150	1	1	0.226	0.117	0.045	75
60	300	500	0	0.0081	73.8	1	150	1	1	0.376	0.258	0.025	159
60	600	500	0	0.0081	73.8	1	150	1	1	0.528	0.440	0.019	226
60	900	500	0	0.0081	73.8	1	150	1	1	0.608	0.545	0.019	256
60	1200	500	0	0.0081	73.8	1	150	1	1	0.656	0.610	0.018	269

Table 25. Surveillance quality run data with 10 different traffic scenarios, no surveillance error or ADSB_2 error, and symmetric and asymmetric predictions.

Run	Scenario Number	SQ_{model}	Symmetric/ Asymmetric	P_{FA}	P_{MA}	P_{MD}	$\Delta t_{LOS,mean}$ [s]
sq3_001	1	none	symmetric	0.644	0.624	0.069	217
sq3_002	2	none	symmetric	0.645	0.620	0.068	217
sq3_003	3	none	symmetric	0.648	0.624	0.062	214
sq3_004	4	none	symmetric	0.641	0.623	0.068	216
sq3_005	5	none	symmetric	0.647	0.624	0.064	214
sq3_006	6	none	symmetric	0.645	0.625	0.066	214
sq3_007	7	none	symmetric	0.651	0.624	0.063	213
sq3_008	8	none	symmetric	0.644	0.619	0.069	218
sq3_009	9	none	symmetric	0.650	0.618	0.059	218
sq3_010	10	none	symmetric	0.648	0.625	0.066	213
sq3_011	1	none	asymmetric	0.450	0.457	0.043	302
sq3_012	2	none	asymmetric	0.448	0.454	0.041	299
sq3_013	3	none	asymmetric	0.450	0.456	0.039	298
sq3_014	4	none	asymmetric	0.446	0.457	0.039	299
sq3_015	5	none	asymmetric	0.446	0.456	0.040	297
sq3_016	6	none	asymmetric	0.448	0.456	0.041	299
sq3_017	7	none	asymmetric	0.453	0.454	0.038	299
sq3_018	8	none	asymmetric	0.449	0.454	0.039	299
sq3_019	9	none	asymmetric	0.453	0.451	0.035	300
sq3_020	10	none	asymmetric	0.451	0.458	0.039	297
sq3_021	1	ADSB_2	symmetric	0.813	0.688	0.066	212
sq3_022	2	ADSB_2	symmetric	0.814	0.685	0.070	215
sq3_023	3	ADSB_2	symmetric	0.814	0.687	0.060	211
sq3_024	4	ADSB_2	symmetric	0.810	0.686	0.070	214
sq3_025	5	ADSB_2	symmetric	0.816	0.688	0.064	210
sq3_026	6	ADSB_2	symmetric	0.814	0.687	0.067	211
sq3_027	7	ADSB_2	symmetric	0.815	0.684	0.062	214
sq3_028	8	ADSB_2	symmetric	0.813	0.683	0.072	215
sq3_029	9	ADSB_2	symmetric	0.814	0.678	0.060	216
sq3_030	10	ADSB_2	symmetric	0.815	0.687	0.061	210
sq3_031	1	ADSB_2	asymmetric	0.718	0.544	0.042	300
sq3_032	2	ADSB_2	asymmetric	0.719	0.542	0.040	297
sq3_033	3	ADSB_2	asymmetric	0.720	0.544	0.040	295
sq3_034	4	ADSB_2	asymmetric	0.717	0.544	0.038	296
sq3_035	5	ADSB_2	asymmetric	0.721	0.545	0.039	294
sq3_036	6	ADSB_2	asymmetric	0.719	0.544	0.041	295
sq3_037	7	ADSB_2	asymmetric	0.723	0.544	0.038	296
sq3_038	8	ADSB_2	asymmetric	0.719	0.542	0.039	295
sq3_039	9	ADSB_2	asymmetric	0.721	0.539	0.035	298
sq3_040	10	ADSB_2	asymmetric	0.723	0.546	0.041	295

Table 26. Surveillance quality run data with the same scenario and 10 different random seeds, the ADSB_2 error model, and symmetric and asymmetric predictions.

Run	SQ_{model}	Symmetric/ Asymmetric	P_{FA}	P_{MA}	P_{MD}	$\Delta t_{LOS,mean}$ [s]
sq3_061	ADSB_2	symmetric	0.816	0.688	0.066	209
sq3_062	ADSB_2	symmetric	0.816	0.688	0.066	209
sq3_063	ADSB_2	symmetric	0.816	0.688	0.066	209
sq3_064	ADSB_2	symmetric	0.816	0.687	0.063	211
sq3_065	ADSB_2	symmetric	0.815	0.686	0.068	212
sq3_066	ADSB_2	symmetric	0.815	0.686	0.068	212
sq3_067	ADSB_2	symmetric	0.816	0.688	0.064	210
sq3_068	ADSB_2	symmetric	0.816	0.687	0.062	209
sq3_069	ADSB_2	symmetric	0.816	0.688	0.062	210
sq3_070	ADSB_2	symmetric	0.816	0.687	0.062	211
sq3_071	ADSB_2	asymmetric	0.721	0.544	0.039	293
sq3_072	ADSB_2	asymmetric	0.721	0.544	0.039	293
sq3_073	ADSB_2	asymmetric	0.721	0.544	0.039	293
sq3_074	ADSB_2	asymmetric	0.720	0.543	0.042	294
sq3_075	ADSB_2	asymmetric	0.722	0.544	0.041	295
sq3_076	ADSB_2	asymmetric	0.721	0.543	0.039	295
sq3_077	ADSB_2	asymmetric	0.721	0.545	0.040	293
sq3_078	ADSB_2	asymmetric	0.721	0.545	0.043	293
sq3_079	ADSB_2	asymmetric	0.721	0.544	0.038	295
sq3_080	ADSB_2	asymmetric	0.722	0.544	0.042	295

Table 27. CD performance metric variability to different scenario randomizations with no surveillance error and with the ADSB_2 error model, symmetric and asymmetric predictions.

	P_{FA}		P_{MA}		P_{MD}		$\Delta t_{LOS,mean}$ [s]	
Case	**Mean**	**Std. Dev.**	**Mean**	**Std. Dev.**	**Mean**	**Std. Dev.**	**Mean**	**Std. Dev.**
None - Symmetric	0.646	0.00303	0.623	0.00262	0.065	0.00328	215	2.02
None - Symmetric - Circular	0.434	0.00342	0.368	0.00232	0.039	0.00200	223	1.39
None - Asymmetric	0.449	0.00269	0.455	0.00207	0.039	0.00209	299	1.45
ADSB_2 - Symmetric	0.814	0.00154	0.685	0.00299	0.065	0.00459	213	2.15
ADSB_2 - Asymmetric	0.720	0.00192	0.543	0.00190	0.039	0.00202	296	1.71

Table 28. CD performance metric variability to surveillance error model Monte Carlo sampling with the ADSB_2 error model, symmetric and asymmetric predictions.

	P_{FA}		P_{MA}		P_{MD}		$\Delta t_{LOS,mean}$ [s]	
Case	**Mean**	**Std. Dev.**	**Mean**	**Std. Dev.**	**Mean**	**Std. Dev.**	**Mean**	**Std. Dev.**
ADSB_2 - Symmetric	0.816	0.00055	0.687	0.00090	0.065	0.00243	210	1.27
ADSB_2 - Asymmetric	0.721	0.00052	0.544	0.00057	0.040	0.00140	294	0.83

Surveillance Quality Results Figures

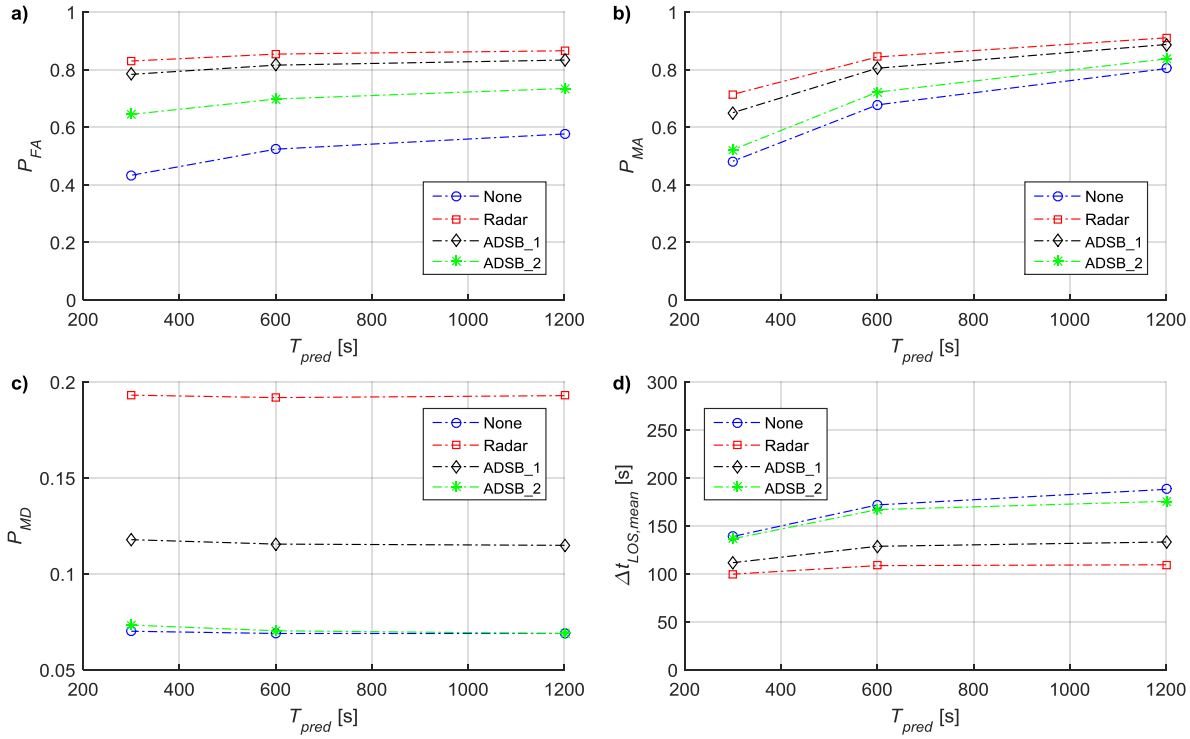

Figure 24. CD performance metrics as a function of the prediction and detection horizon for the 4 surveillance models, using symmetric predictions and short surveillance range (50 NM).

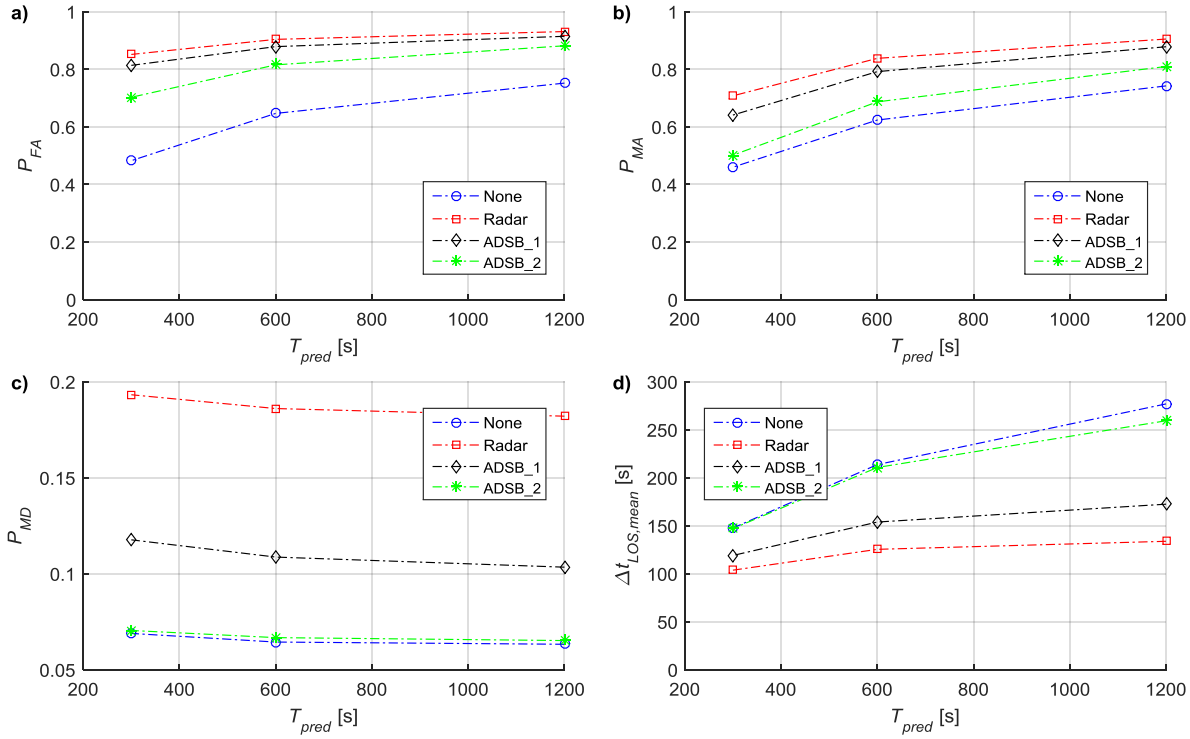

Figure 25. CD performance metrics as a function of the prediction and detection horizon for the 4 surveillance models, using symmetric predictions and infinite surveillance range (1500 NM).

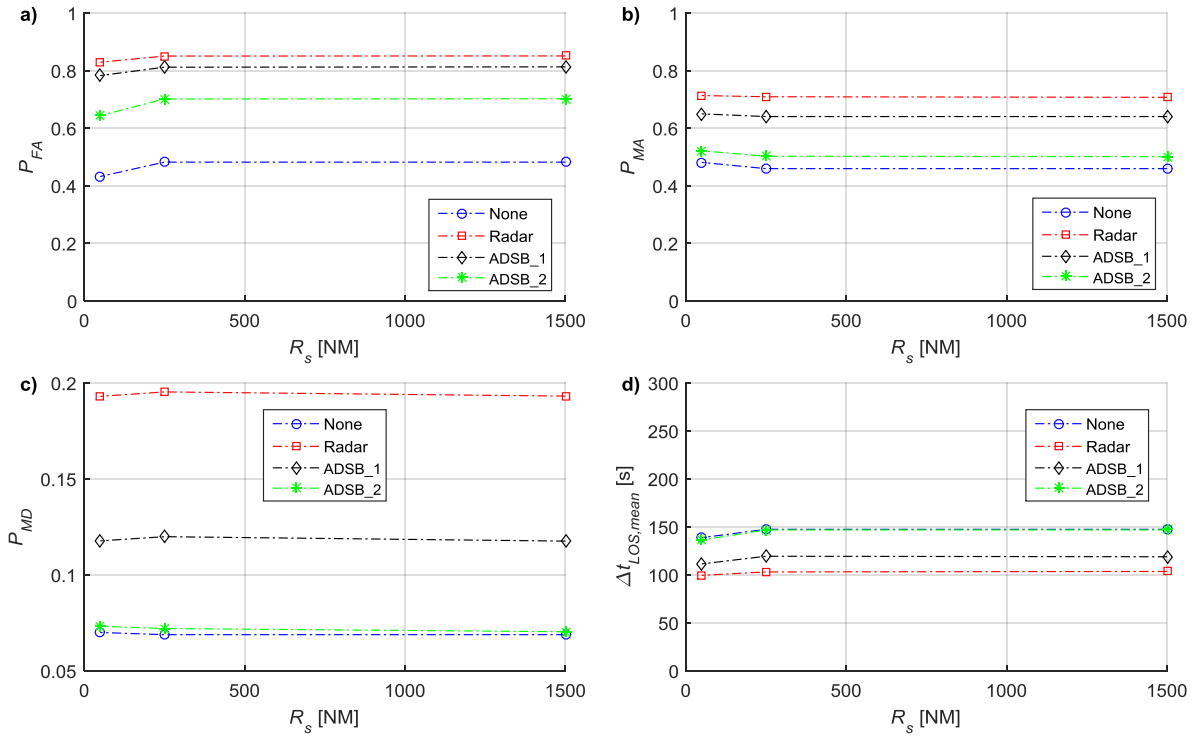

Figure 26. CD performance metrics as a function of the surveillance range parameter for the 4 surveillance models, using symmetric predictions and short CD horizon (300 seconds).

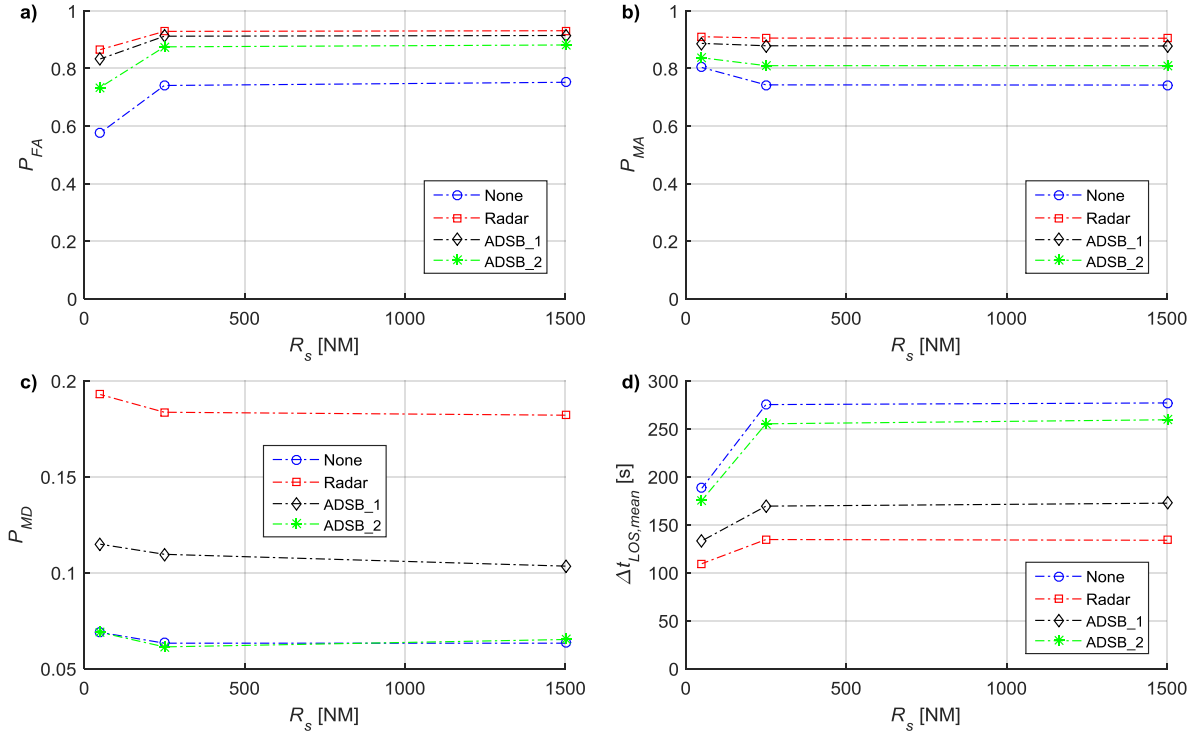

Figure 27. CD performance metrics as a function of the surveillance range parameter for the 4 surveillance models, using symmetric predictions and long CD horizon (1200 seconds).

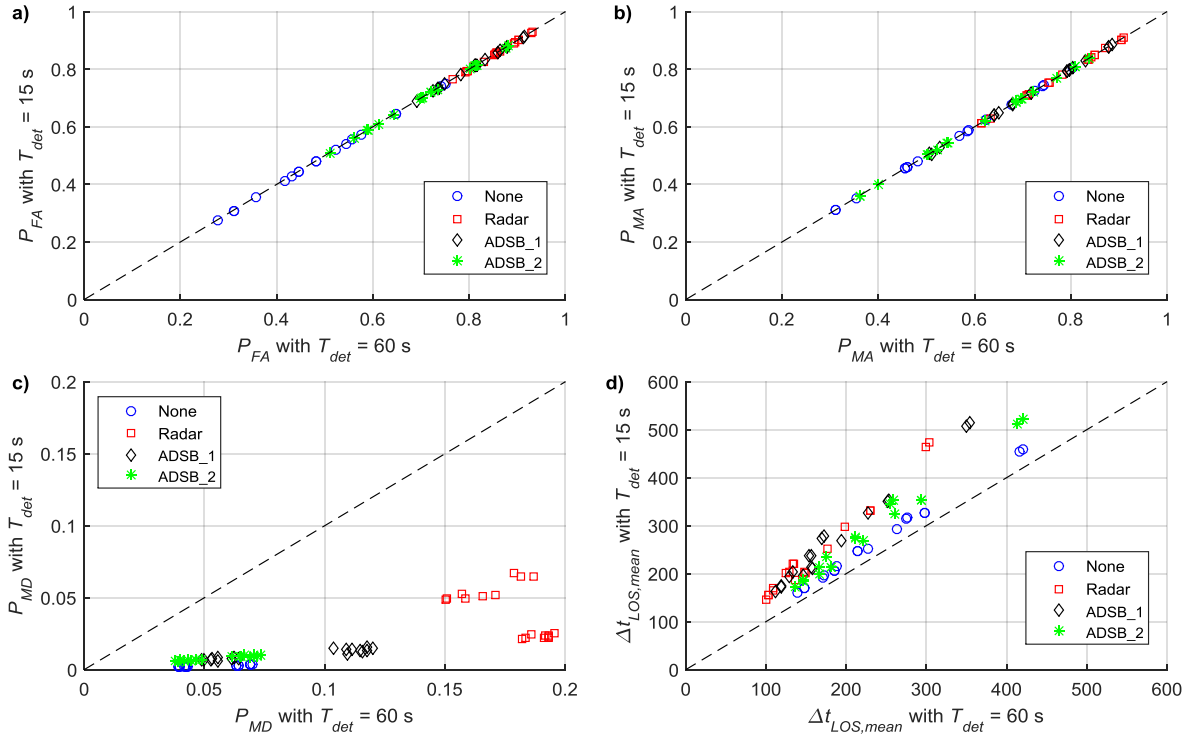

Figure 28. Difference in CD performance metrics between a CD cycle period of 15 seconds and a CD cycle period of 60 seconds over all SQ1 surveillance quality analysis runs.

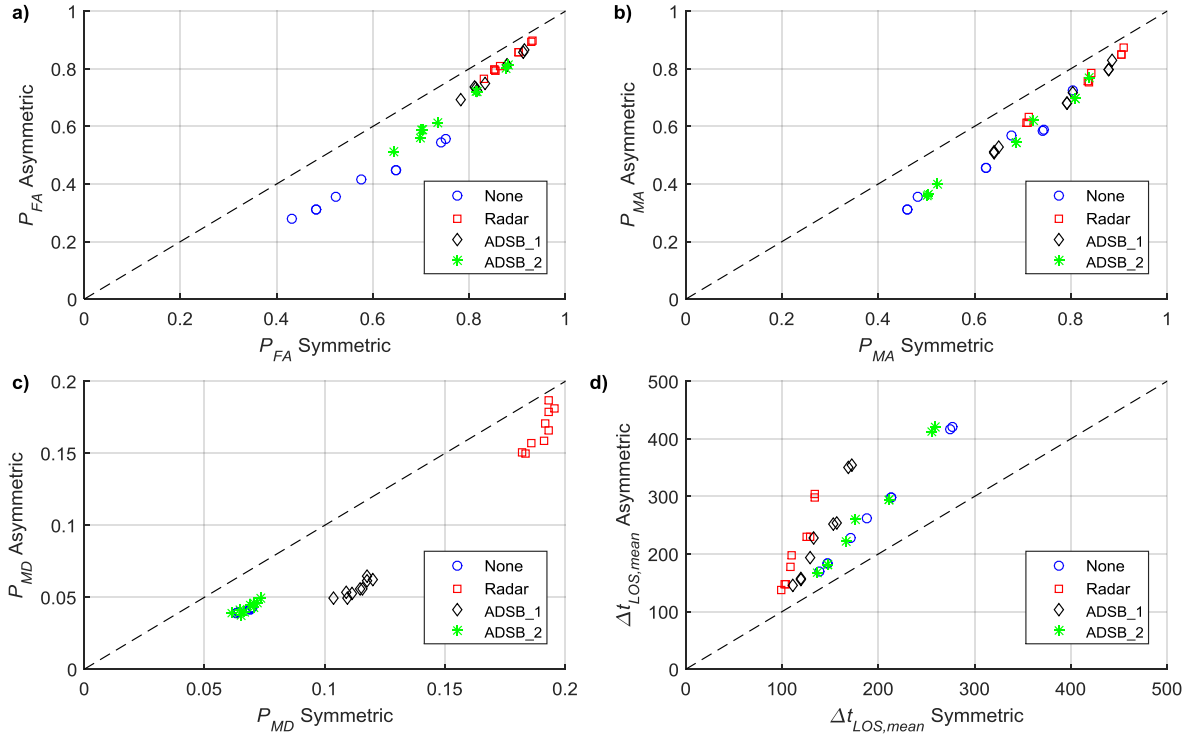

Figure 29. Difference in CD performance metrics between symmetric and asymmetric trajectory predictions over all SQ1 surveillance quality analysis runs with CD cycle period of 60 seconds.

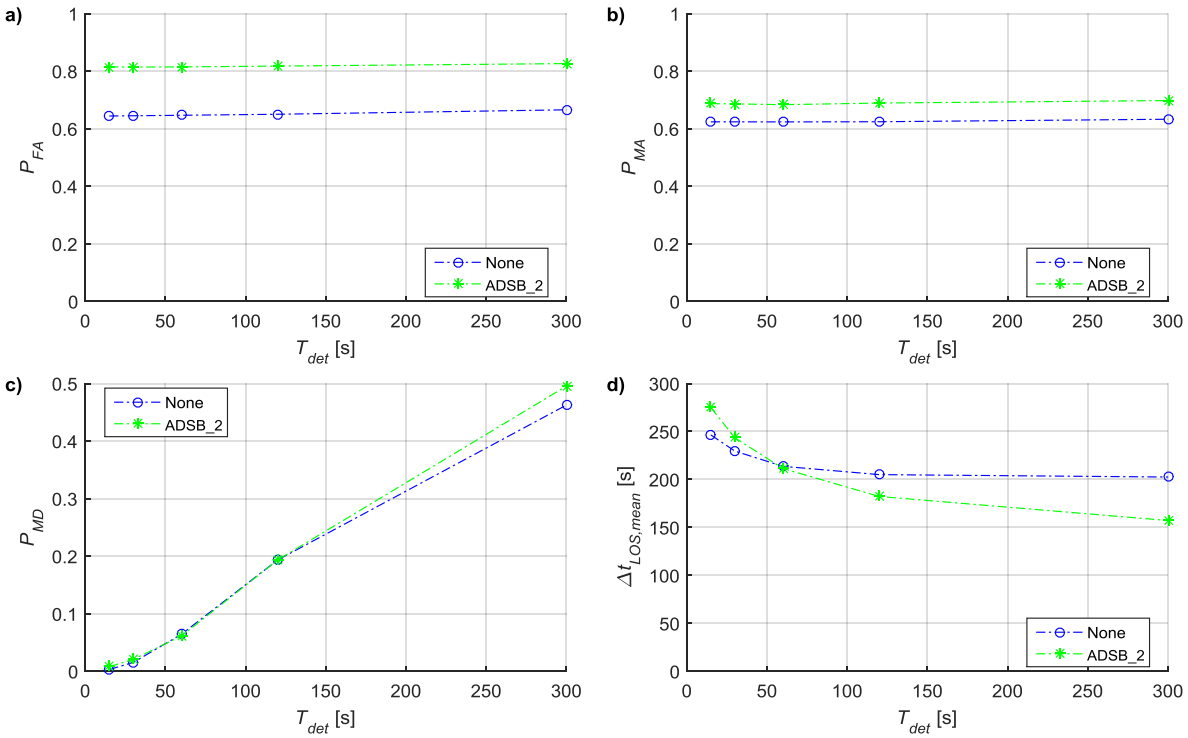

Figure 30. CD performance metric sensitivities to CD cycle period with no surveillance error (None) and with the ADSB_2 surveillance error model.

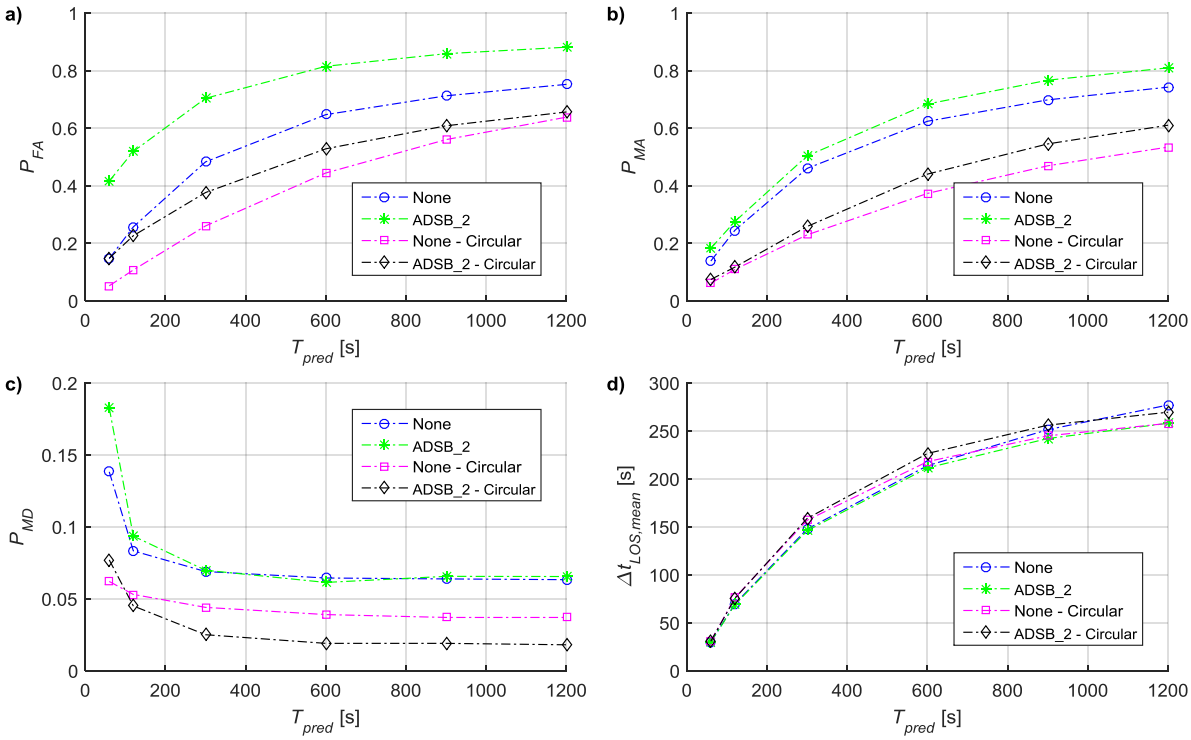

Figure 31. CD performance metric sensitivities to conflict detection and trajectory prediction time horizon with no surveillance error (None), with the ADSB_2 surveillance error model, from a circular scenario with no surveillance error (None – Circular), and from a circular scenario with ABDS_2 surveillance error (ADSB_2 – Circular).

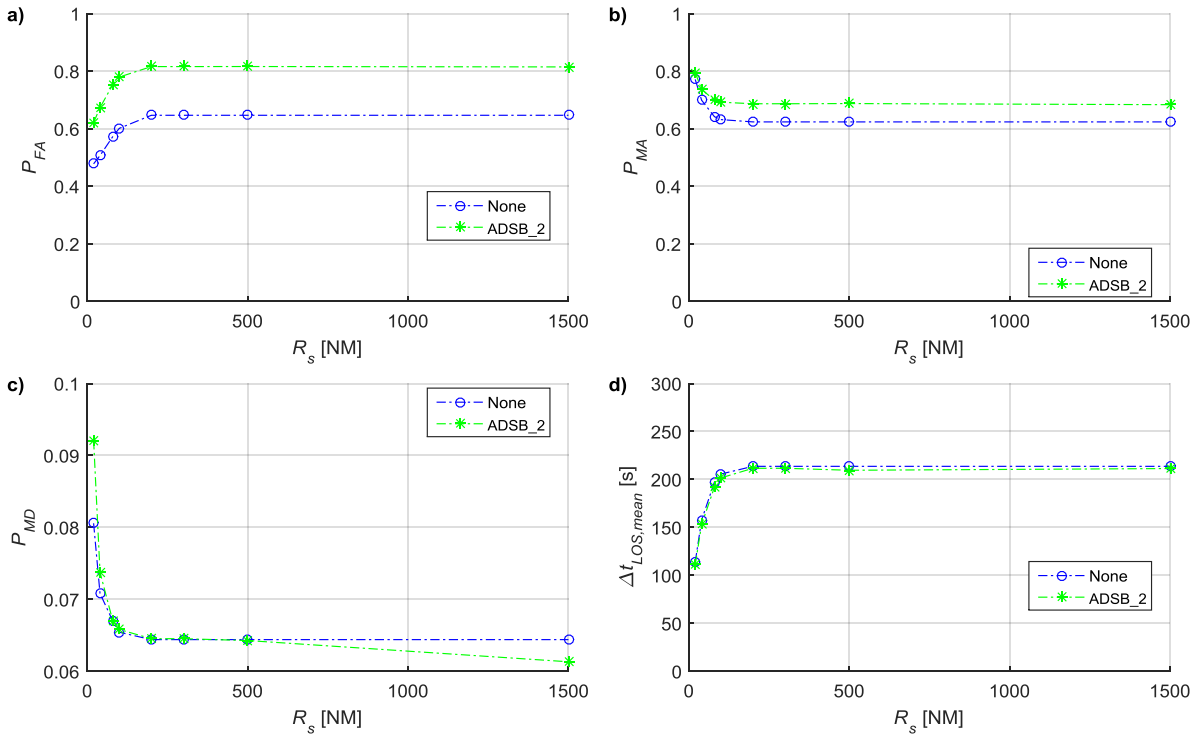

Figure 32. CD performance metric sensitivities to the surveillance range parameters with no surveillance error (None) and with the ADSB_2 surveillance error model.

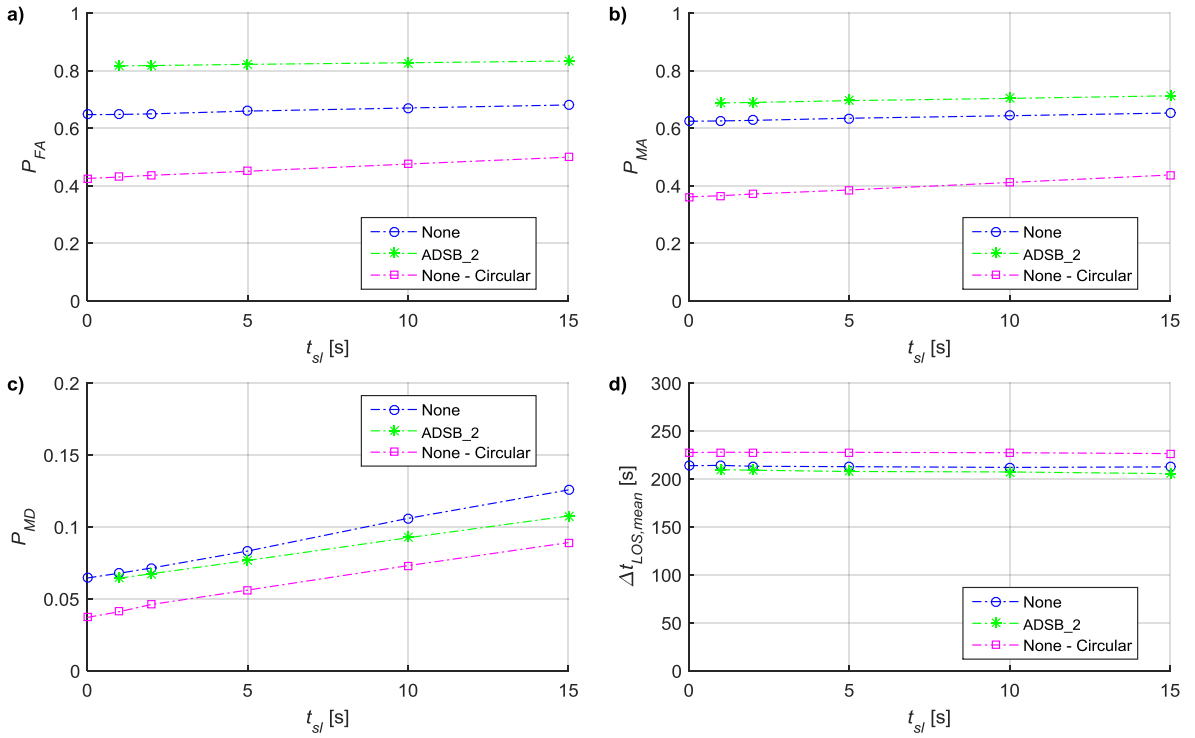

Figure 33. CD performance metric sensitivities to the surveillance lag time parameter with no surveillance error (None), with the ADSB_2 surveillance error model, and from a circular scenario with no surveillance error (None – Circular).

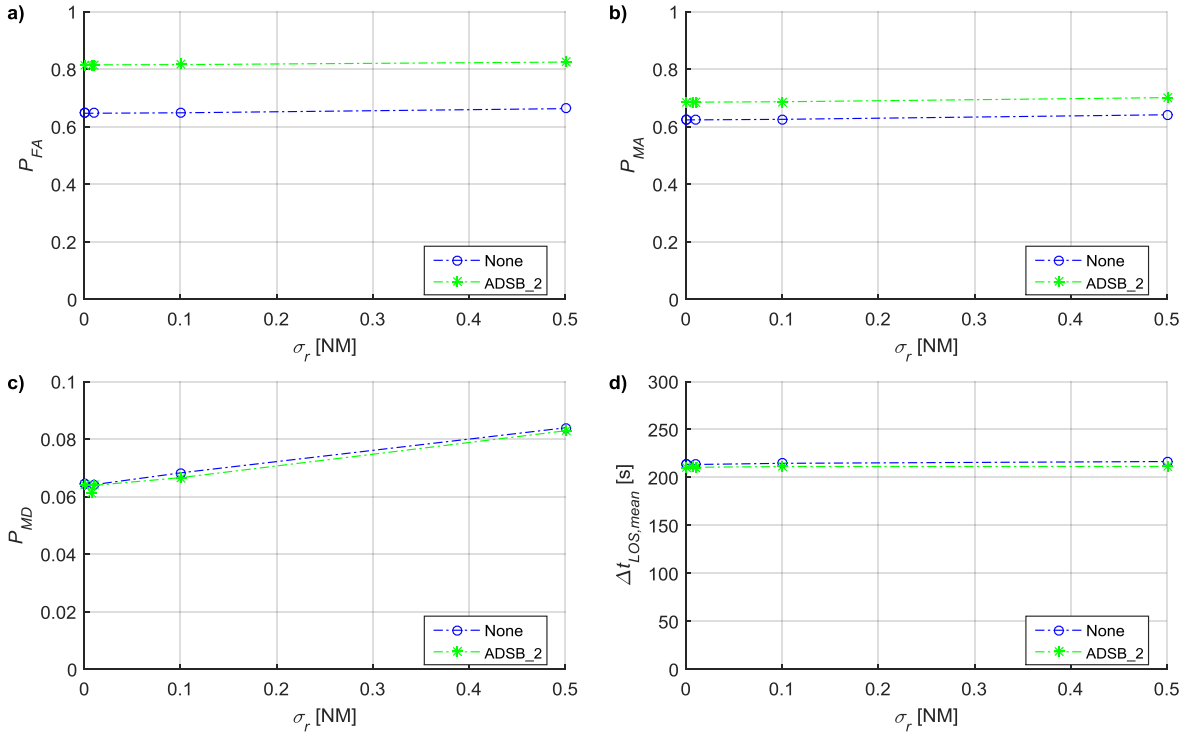

Figure 34. CD performance metric sensitivities to surveillance horizontal position error standard deviation with no other surveillance error (None) and with the ADSB_2 surveillance error model.

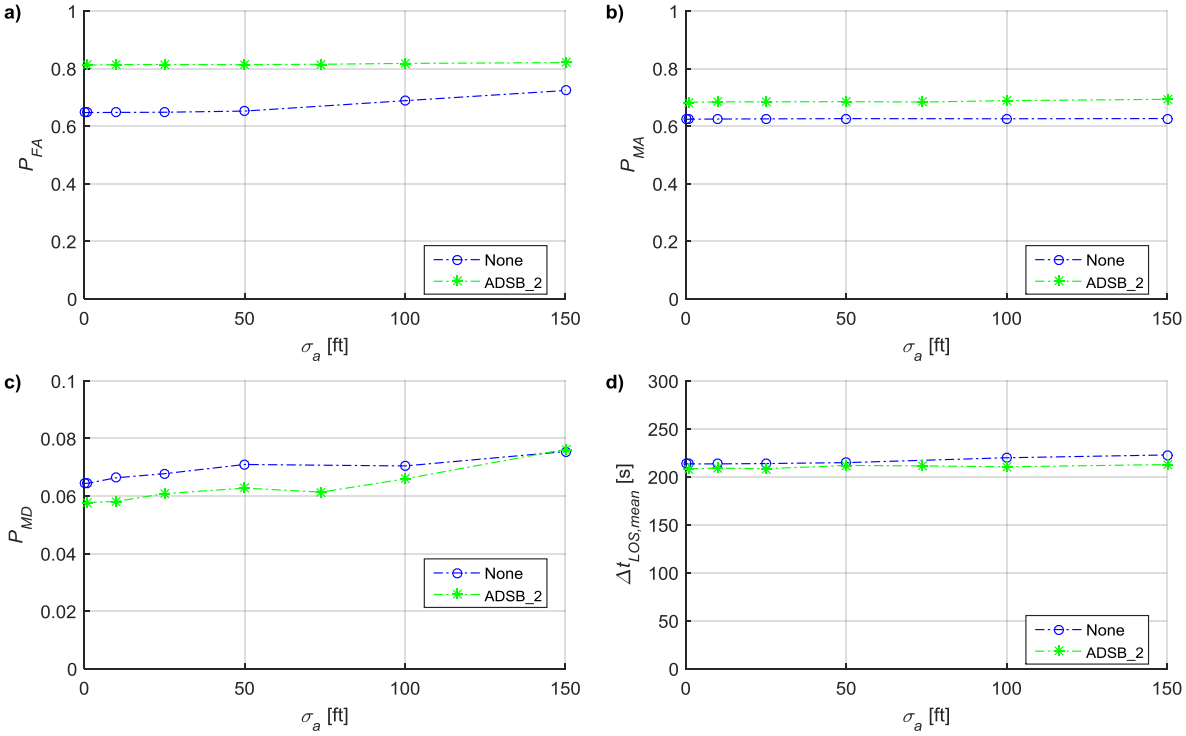

Figure 35. CD performance metric sensitivities to surveillance vertical position error standard deviation with no other surveillance error (None) and with the ADSB_2 surveillance error model.

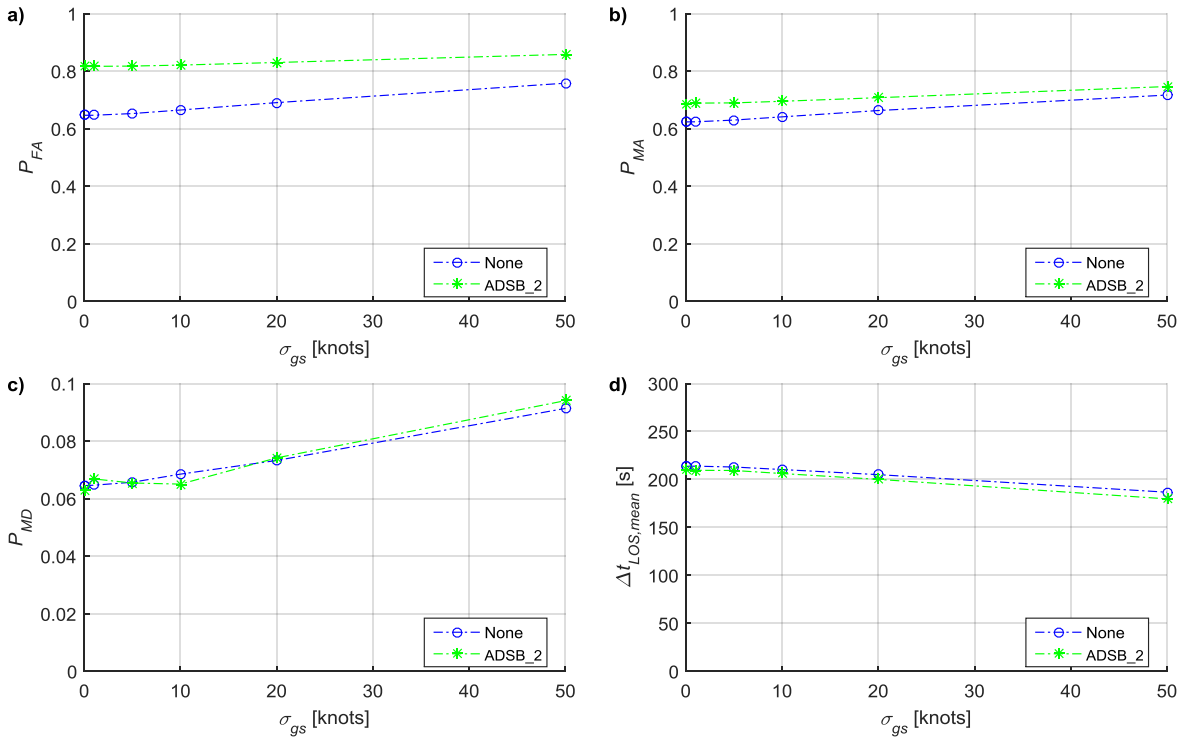

Figure 36. CD performance metric sensitivities to surveillance groundspeed error standard deviation with no other surveillance error (None) and with the ADSB_2 surveillance error model.

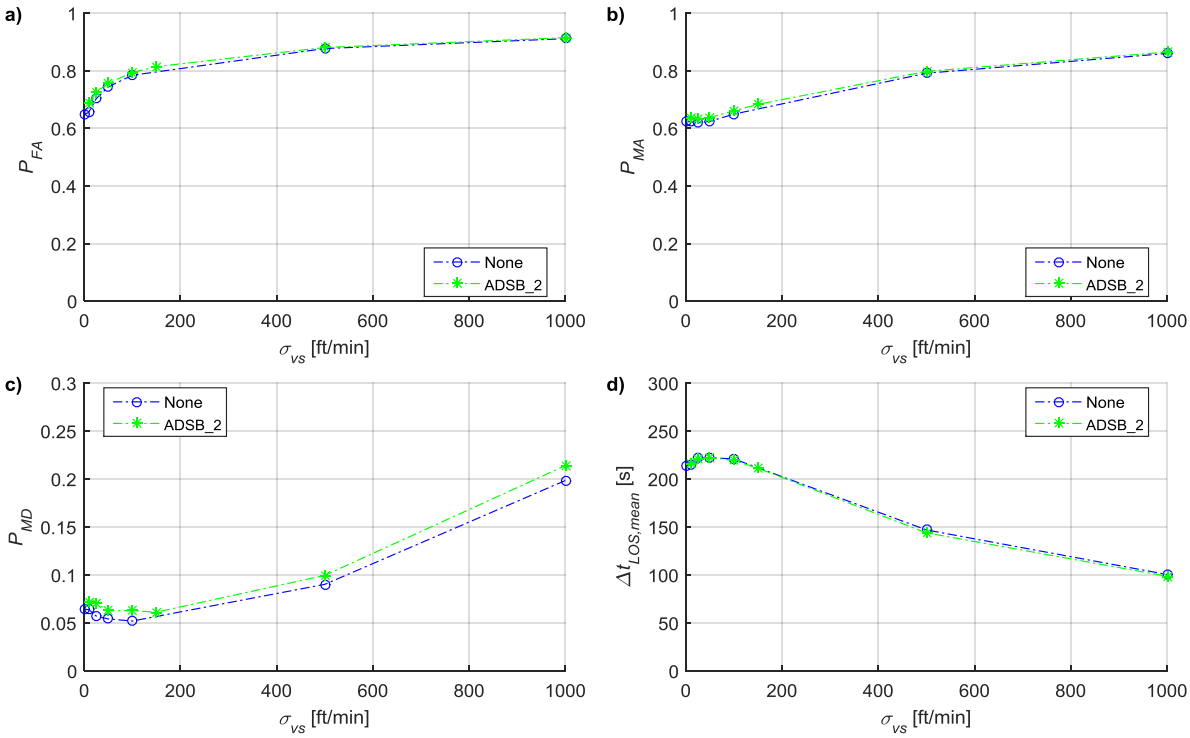

Figure 37. CD performance metric sensitivities to surveillance vertical speed error standard deviation with no other surveillance error (None) and with the ADSB_2 surveillance error model.

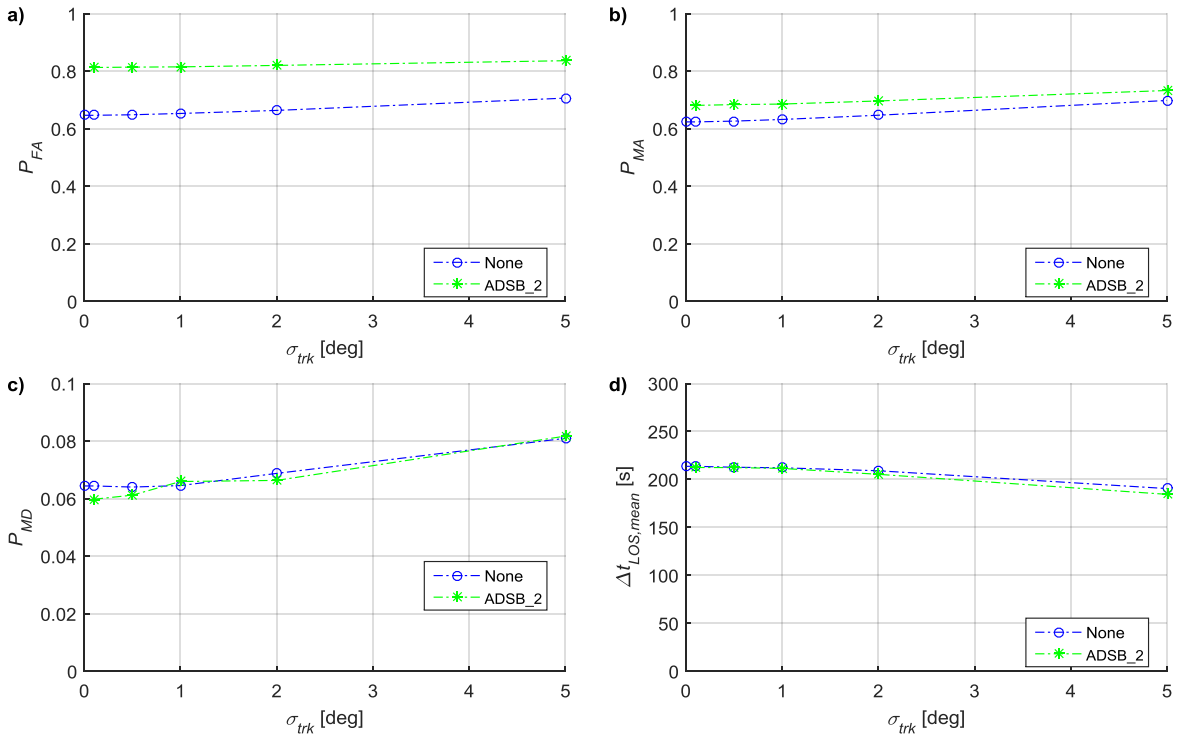

Figure 38. CD performance metric sensitivities to surveillance track angle error standard deviation with no other surveillance error (None) and with the ADSB_2 surveillance error model.

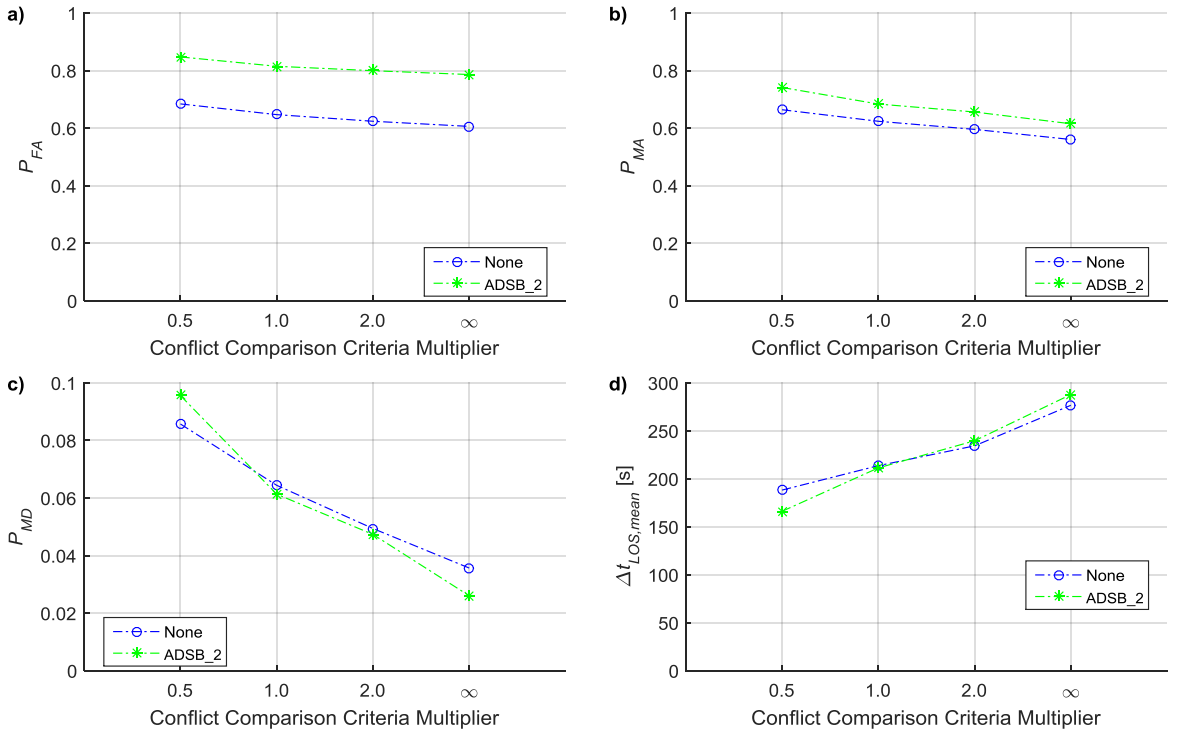

Figure 39. CD performance metric sensitivities to the conflict comparison criterion with no other surveillance error (None) and with the ADSB_2 surveillance error model.

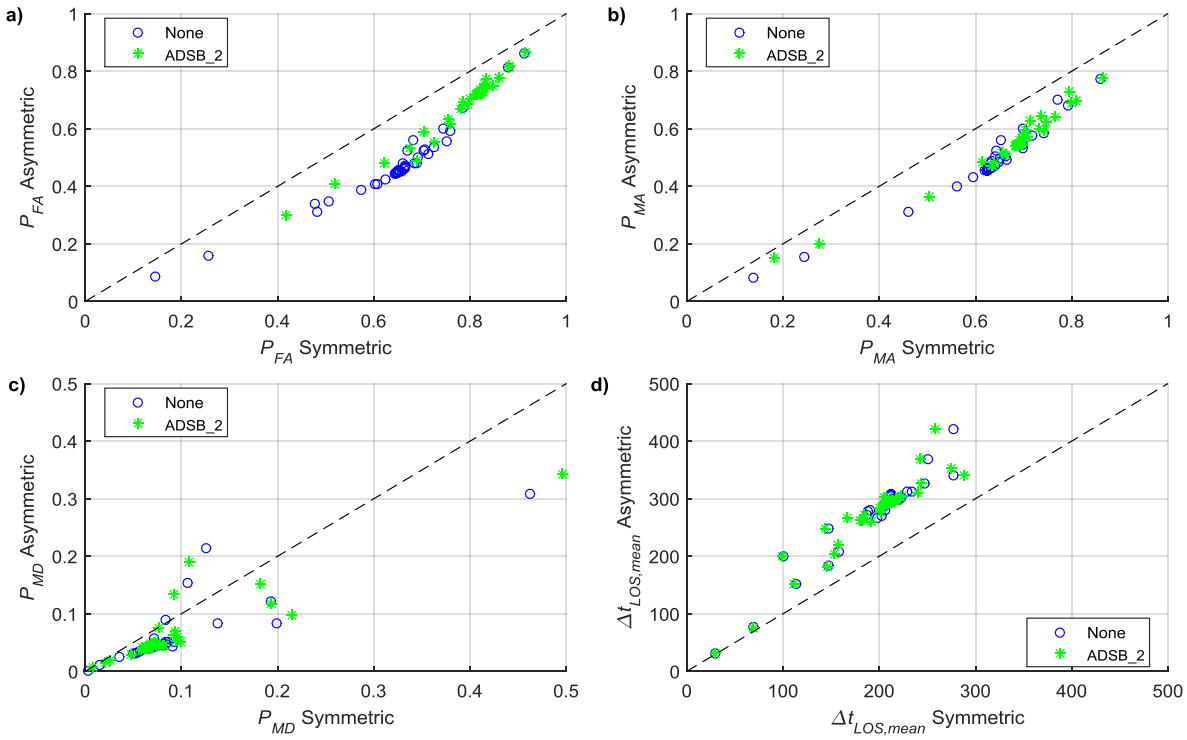

Figure 40. Difference in CD performance metrics between symmetric and asymmetric trajectory prediction over all SQ2 sensitivity runs (with no other surveillance error (None) and with the ADSB_2 surveillance error model).

B. Level and Quality of Intent Information Results and Discussion

The results of the analysis runs for the level and quality of intent information test matrix 1 (IQ1) are listed in Table 29-Table 32. Table 33 shows the results of some comparison runs performed using the circular scenarios and analysis method 2. The figures associated with test matrix IQ1 are Figure 41-Figure 45. The intent information quality trends indicate that conflict detection performance is improved as the intent horizon approaches the trajectory prediction and conflict detection horizon. This is expected because, for intent horizons shorter than the CD horizon, the trajectory predictions are less accurate due to the lack of complete intent information. Comparing the results where the CD horizon is equal to the intent horizon (e.g., $T_{pred} = T_{int}$), CD performance is improved by a shorter detection horizon (e.g., T_{pred} = 300 s and T_{int} = 300s) for the metrics of false alerts, missed alerts, and missed detections but there is a negative impact to the mean time-to-LOS metric.

In general, conflict detection performance is improved as the quality of intent information is increased. Reduced false alerts, missed alerts, and missed detections and increased mean time-to-LOS are the trends observed as the intent quality increases from none (IQ_V = 0, IQ_H = 0) to maximum information (IQ_V = 4, IQ_H = 4). One exception to these trends are the cases where the vertical and horizontal intent information quality is of quality 1. These cases show better CD performance compared to the cases where horizontal intent information quality is of quality 2. This exception is likely due to the assumptions made in trajectory prediction for this analysis where, in absence of a turn radius and turn rate, the turn rate is assumed to be 0.2 deg/s, based on observations of the recorded data, and the turn radius is computed using the average speed of the previous leg and this assumed turn rate. CD performance is shown to be better when only the turn reference point is provided (IQ_H = 1) and reasonable values are assumed for the turn rate and turn radius as compared to the cases were a partially specified turn is provided (IQ_H = 2) and other turn parameters have to be assumed. However, a fully specified turn geometry (IQ_H = 3) still produces better

CD performance. Notably, one example of a partially specified turn geometry is the definition proposed by the ADS-B DO-242 MASPS.

The analysis runs conducted using analysis method 2 and shown in Figure 41-Figure 43 provide an upper bound on CD performance for false alerts, missed alerts and missed detections. Because method 2 uses perfect trajectory prediction, as the intent horizon approaches the trajectory prediction and conflict detection horizon, the false alert and missed alert probabilities approach zero. The missed detection probabilities are always zero because, as long as there is some intent horizon larger than the conflict detection cycle period, there is always at least one CD cycle in which to correctly detect a LOS. The mean time-to-LOS parameter, however, does not represent an upper limit on performance because of the random nature of the circular scenarios and the fact that some LOS were introduced into the scenarios with a time-to-LOS that was less than the trajectory prediction and conflict detection horizon; the conflict detector never had the opportunity to detect those losses at the full detection horizon.

The use of shorter conflict detection cycle period has a positive impact on CD performance, primarily by reducing the missed detection rate. For all intent information qualities of 1-4, there was approximately a 40 percent reduction of the missed detection probabilities when using CD cycle period of 15 seconds versus 60 seconds and little or no change to the other metrics (Figure 44). The shorter cycle period provides four times as many detection cycles over which to successfully detect a LOS.

Similar to the surveillance analysis runs, conflict detection performance using asymmetric predictions (perfect prediction for aircraft 1 in a pair) versus symmetric prediction had a positive impact on CD performance for all metrics (Figure 45).

The results of the analysis runs for the level and quality of intent information test matrix 2 (IQ2) are listed in Table 34 and Table 35. Table 34 presents the results of the analysis runs for the variability due to different traffic scenarios; those results are summarized in Table 36. The variability of the CD performance metrics due to different traffic scenarios is small with 0.33% or less of standard deviation in the false alert probability, 0.38% or less of standard deviation in the missed alert probability, 0.27% or less of standard deviation in the missed detection probability, and less than 7 seconds of standard deviation in the mean time-to-loss.

Table 35 shows the results of the analysis runs for the sensitivity of the time and altitude interval for the intent information quality 4 horizontal and vertical points. The associated figures are shown in Figure 46 and Figure 47. The sensitivities indicate that the choice of the time and altitude interval for the quality 4 intent points can be chosen within a fairly wide range with only a small impact to the CD performance. The choice of time interval for the additional horizontal points is less critical than the choice of the altitude interval for the additional vertical points due to the flatter sensitivity profiles. As expected, all of the intent information quality 4 analysis runs showed better CD performance when compared to the equivalent intent quality 3 runs.

It can be noted that one problem with intent information in the form used in this study arises from considering the horizontal and vertical trajectory profiles to be, aside from the initial and end points, completely independent. Because both horizontal and vertical intent points are indexed only by time, variations in groundspeed, especially in long segments between turns, can result in a vertical profile that is insufficiently synchronized with the horizontal profile to allow for accurate four-dimensional conflict detection. This can have the apparent effect of introducing along-track errors, which can be emphasized from a detection standpoint for predicted climb and descent segments. Intent information quality 4 tends to mitigate this by introducing additional points that allow for localized speed corrections in the absence of speed intent information.

Level and Quality of Intent Results Tables

Table 29. Intent quality run data with symmetric predictions and 60 second CD cycle period.

Run	T_{det} [s]	T_{pred} [s]	T_{int} [s]	IQ_V	IQ_H	P_{FA}	P_{MA}	P_{MD}	$\Delta t_{LOS,mean}$ [s]
iq1_001	60	1200	1200	4	4	0.037	0.053	0.029	882
iq1_002	60	1200	1200	3	3	0.086	0.109	0.037	871
iq1_003	60	1200	1200	2	2	0.280	0.220	0.067	854
iq1_004	60	1200	1200	1	2	0.308	0.253	0.070	849
iq1_005	60	1200	1200	1	1	0.172	0.195	0.056	851
iq1_006	60	1200	600	4	4	0.191	0.282	0.020	672
iq1_007	60	1200	600	3	3	0.214	0.309	0.027	665
iq1_008	60	1200	600	2	2	0.395	0.395	0.046	635
iq1_009	60	1200	600	1	2	0.405	0.406	0.046	633
iq1_010	60	1200	600	1	1	0.262	0.353	0.040	655
iq1_011	60	1200	300	4	4	0.386	0.486	0.018	484
iq1_012	60	1200	300	3	3	0.393	0.499	0.023	476
iq1_013	60	1200	300	2	2	0.529	0.558	0.034	440
iq1_014	60	1200	300	1	2	0.531	0.559	0.030	438
iq1_015	60	1200	300	1	1	0.414	0.517	0.027	467
iq1_016	60	600	600	4	4	0.038	0.053	0.026	500
iq1_017	60	600	600	3	3	0.072	0.095	0.033	496
iq1_018	60	600	600	2	2	0.251	0.184	0.057	489
iq1_019	60	600	600	1	2	0.264	0.202	0.058	489
iq1_020	60	600	600	1	1	0.133	0.156	0.047	490
iq1_021	60	600	300	4	4	0.206	0.241	0.018	399
iq1_022	60	600	300	3	3	0.220	0.261	0.023	395
iq1_023	60	600	300	2	2	0.393	0.335	0.034	374
iq1_024	60	600	300	1	2	0.388	0.338	0.031	371
iq1_025	60	600	300	1	1	0.250	0.290	0.028	387
iq1_026	60	300	300	4	4	0.036	0.051	0.025	253
iq1_027	60	300	300	3	3	0.054	0.080	0.031	252
iq1_028	60	300	300	2	2	0.218	0.136	0.050	250
iq1_029	60	300	300	1	2	0.213	0.136	0.044	250
iq1_030	60	300	300	1	1	0.083	0.107	0.038	251
iq1_031	60	1200	1200	0	0	0.559	0.710	0.122	301
iq1_032	60	600	600	0	0	0.410	0.590	0.122	232
iq1_033	60	300	300	0	0	0.269	0.440	0.123	157

Table 30. Intent quality run data with symmetric predictions and 15 second CD cycle period.

Run	T_{det} [s]	T_{pred} [s]	T_{int} [s]	IQ_V	IQ_H	P_{FA}	P_{MA}	P_{MD}	$\Delta t_{LOS,mean}$ [s]
iq1_034	15	1200	1200	4	4	0.037	0.053	0.016	889
iq1_035	15	1200	1200	3	3	0.086	0.110	0.021	880
iq1_036	15	1200	1200	2	2	0.280	0.220	0.040	859
iq1_037	15	1200	1200	1	2	0.308	0.253	0.039	851
iq1_038	15	1200	1200	1	1	0.173	0.195	0.030	855
iq1_039	15	1200	600	4	4	0.191	0.282	0.011	691
iq1_040	15	1200	600	3	3	0.215	0.310	0.016	681
iq1_041	15	1200	600	2	2	0.395	0.395	0.027	651
iq1_042	15	1200	600	1	2	0.405	0.406	0.026	648
iq1_043	15	1200	600	1	1	0.261	0.353	0.023	670
iq1_044	15	1200	300	4	4	0.386	0.486	0.010	511
iq1_045	15	1200	300	3	3	0.393	0.499	0.012	499
iq1_046	15	1200	300	2	2	0.530	0.558	0.018	462
iq1_047	15	1200	300	1	2	0.531	0.559	0.019	463
iq1_048	15	1200	300	1	1	0.414	0.517	0.017	492
iq1_049	15	600	600	4	4	0.038	0.052	0.014	514
iq1_050	15	600	600	3	3	0.072	0.095	0.018	512
iq1_051	15	600	600	2	2	0.251	0.184	0.033	505
iq1_052	15	600	600	1	2	0.263	0.201	0.030	505
iq1_053	15	600	600	1	1	0.133	0.155	0.025	506
iq1_054	15	600	300	4	4	0.207	0.241	0.010	421
iq1_055	15	600	300	3	3	0.221	0.261	0.012	415
iq1_056	15	600	300	2	2	0.395	0.335	0.018	395
iq1_057	15	600	300	1	2	0.389	0.337	0.019	394
iq1_058	15	600	300	1	1	0.250	0.290	0.017	408
iq1_059	15	300	300	4	4	0.036	0.051	0.013	272
iq1_060	15	300	300	3	3	0.055	0.080	0.015	271
iq1_061	15	300	300	2	2	0.219	0.137	0.026	269
iq1_062	15	300	300	1	2	0.213	0.136	0.023	271
iq1_063	15	300	300	1	1	0.083	0.106	0.019	271
iq1_064	15	1200	1200	0	0	0.553	0.709	0.020	300
iq1_065	15	600	600	0	0	0.402	0.588	0.020	232
iq1_066	15	300	300	0	0	0.261	0.437	0.020	163

Table 31. Intent quality run data with asymmetric predictions and 60 second CD cycle period.

Run	T_{det} [s]	T_{pred} [s]	T_{int} [s]	IQ_V	IQ_H	P_{FA}	P_{MA}	P_{MD}	$\Delta t_{LOS,mean}$ [s]
iq1_067	60	1200	1200	4	4	0.024	0.031	0.017	886
iq1_068	60	1200	1200	3	3	0.065	0.075	0.022	878
iq1_069	60	1200	1200	2	2	0.219	0.169	0.050	864
iq1_070	60	1200	1200	1	2	0.243	0.192	0.051	859
iq1_071	60	1200	1200	1	1	0.130	0.137	0.038	865
iq1_072	60	1200	600	4	4	0.133	0.199	0.011	737
iq1_073	60	1200	600	3	3	0.154	0.221	0.016	730
iq1_074	60	1200	600	2	2	0.295	0.295	0.033	703
iq1_075	60	1200	600	1	2	0.307	0.304	0.032	701
iq1_076	60	1200	600	1	1	0.192	0.255	0.027	723
iq1_077	60	1200	300	4	4	0.269	0.364	0.010	589
iq1_078	60	1200	300	3	3	0.278	0.374	0.013	581
iq1_079	60	1200	300	2	2	0.393	0.430	0.022	548
iq1_080	60	1200	300	1	2	0.397	0.432	0.018	546
iq1_081	60	1200	300	1	1	0.296	0.391	0.015	574
iq1_082	60	600	600	4	4	0.024	0.031	0.015	502
iq1_083	60	600	600	3	3	0.051	0.060	0.020	500
iq1_084	60	600	600	2	2	0.186	0.131	0.041	494
iq1_085	60	600	600	1	2	0.201	0.144	0.040	494
iq1_086	60	600	600	1	1	0.101	0.106	0.032	495
iq1_087	60	600	300	4	4	0.133	0.157	0.010	436
iq1_088	60	600	300	3	3	0.146	0.171	0.013	433
iq1_089	60	600	300	2	2	0.276	0.232	0.022	416
iq1_090	60	600	300	1	2	0.277	0.234	0.018	414
iq1_091	60	600	300	1	1	0.172	0.195	0.015	426
iq1_092	60	300	300	4	4	0.023	0.030	0.014	255
iq1_093	60	300	300	3	3	0.038	0.050	0.018	254
iq1_094	60	300	300	2	2	0.154	0.092	0.032	252
iq1_095	60	300	300	1	2	0.154	0.091	0.028	252
iq1_096	60	300	300	1	1	0.062	0.069	0.022	253
iq1_097	60	1200	1200	0	0	0.405	0.540	0.062	453
iq1_098	60	600	600	0	0	0.294	0.410	0.062	318
iq1_099	60	300	300	0	0	0.204	0.282	0.064	193

Table 32. Intent quality run data with asymmetric predictions and 15 second CD cycle period.

Run	T_{det} [s]	T_{pred} [s]	T_{int} [s]	IQ_V	IQ_H	P_{FA}	P_{MA}	P_{MD}	$\Delta t_{LOS,mean}$ [s]
iq1_100	15	1200	1200	4	4	0.024	0.031	0.008	894
iq1_101	15	1200	1200	3	3	0.065	0.075	0.011	887
iq1_102	15	1200	1200	2	2	0.219	0.168	0.029	871
iq1_103	15	1200	1200	1	2	0.243	0.192	0.029	867
iq1_104	15	1200	1200	1	1	0.130	0.137	0.021	873
iq1_105	15	1200	600	4	4	0.133	0.200	0.006	753
iq1_106	15	1200	600	3	3	0.154	0.221	0.008	744
iq1_107	15	1200	600	2	2	0.295	0.295	0.019	716
iq1_108	15	1200	600	1	2	0.307	0.304	0.020	717
iq1_109	15	1200	600	1	1	0.193	0.256	0.016	740
iq1_110	15	1200	300	4	4	0.270	0.365	0.005	613
iq1_111	15	1200	300	3	3	0.278	0.375	0.006	602
iq1_112	15	1200	300	2	2	0.394	0.430	0.012	567
iq1_113	15	1200	300	1	2	0.397	0.432	0.011	569
iq1_114	15	1200	300	1	1	0.296	0.391	0.009	599
iq1_115	15	600	600	4	4	0.024	0.031	0.007	517
iq1_116	15	600	600	3	3	0.051	0.060	0.009	515
iq1_117	15	600	600	2	2	0.187	0.130	0.023	510
iq1_118	15	600	600	1	2	0.201	0.144	0.022	510
iq1_119	15	600	600	1	1	0.101	0.106	0.018	511
iq1_120	15	600	300	4	4	0.134	0.157	0.005	456
iq1_121	15	600	300	3	3	0.147	0.171	0.007	452
iq1_122	15	600	300	2	2	0.278	0.232	0.012	435
iq1_123	15	600	300	1	2	0.277	0.234	0.011	435
iq1_124	15	600	300	1	1	0.172	0.195	0.009	447
iq1_125	15	300	300	4	4	0.023	0.029	0.007	274
iq1_126	15	300	300	3	3	0.039	0.049	0.008	273
iq1_127	15	300	300	2	2	0.154	0.091	0.017	271
iq1_128	15	300	300	1	2	0.154	0.091	0.014	272
iq1_129	15	300	300	1	1	0.062	0.068	0.010	273
iq1_130	15	1200	1200	0	0	0.402	0.539	0.012	457
iq1_131	15	600	600	0	0	0.291	0.408	0.012	325
iq1_132	15	300	300	0	0	0.200	0.280	0.012	205

Table 33. Comparison level of intent run data using circular method 2 with symmetric predictions, 60 second CD cycle period, and 3 CD horizons.

T_{det} [s]	T_{pred} [s]	T_{int} [s]	IQ_V	IQ_H	P_{FA}	P_{MA}	P_{MD}	$\Delta t_{LOS,mean}$ [s]
60	300	60	3	3	0.160	0.158	0.000	167
60	300	120	3	3	0.086	0.098	0.000	180
60	300	300	3	3	0.002	0.000	0.000	202
60	300	600	3	3	0.003	0.000	0.000	202
60	300	900	3	3	0.003	0.000	0.000	202
60	300	1200	3	3	0.003	0.000	0.000	202
60	600	60	3	3	0.354	0.323	0.000	228
60	600	120	3	3	0.270	0.269	0.000	244
60	600	300	3	3	0.097	0.121	0.000	293
60	600	600	3	3	0.003	0.000	0.000	335
60	600	900	3	3	0.003	0.000	0.000	335
60	600	1200	3	3	0.004	0.000	0.000	335
60	1200	60	3	3	0.569	0.493	0.000	266
60	1200	120	3	3	0.500	0.451	0.000	284
60	1200	300	3	3	0.318	0.328	0.000	341
60	1200	600	3	3	0.135	0.163	0.000	422
60	1200	900	3	3	0.038	0.050	0.000	479
60	1200	1200	3	3	0.002	0.000	0.000	505

Table 34. Intent quality run data with 10 different traffic scenarios, 3 intent horizons, and symmetric and asymmetric predictions.

Run	Scenario Number	T_{pred} [s]	T_{int} [s]	Symmetric/ Asymmetric	P_{FA}	P_{MA}	P_{MD}	$\Delta t_{LOS,mean}$ [s]
iq2_001	1	1200	1200	symmetric	0.087	0.111	0.034	894
iq2_002	2	1200	1200	symmetric	0.081	0.111	0.038	879
iq2_003	3	1200	1200	symmetric	0.085	0.102	0.031	876
iq2_004	4	1200	1200	symmetric	0.087	0.115	0.033	881
iq2_005	5	1200	1200	symmetric	0.086	0.109	0.037	871
iq2_006	6	1200	1200	symmetric	0.089	0.106	0.034	879
iq2_007	7	1200	1200	symmetric	0.088	0.104	0.031	879
iq2_008	8	1200	1200	symmetric	0.084	0.110	0.034	880
iq2_009	9	1200	1200	symmetric	0.086	0.108	0.032	874
iq2_010	10	1200	1200	symmetric	0.092	0.107	0.030	881
iq2_011	1	1200	600	symmetric	0.216	0.314	0.026	675
iq2_012	2	1200	600	symmetric	0.217	0.312	0.028	666
iq2_013	3	1200	600	symmetric	0.217	0.309	0.024	664
iq2_014	4	1200	600	symmetric	0.214	0.312	0.023	669
iq2_015	5	1200	600	symmetric	0.214	0.309	0.027	665
iq2_016	6	1200	600	symmetric	0.218	0.310	0.023	666
iq2_017	7	1200	600	symmetric	0.218	0.307	0.023	666
iq2_018	8	1200	600	symmetric	0.214	0.309	0.022	669
iq2_019	9	1200	600	symmetric	0.219	0.306	0.021	669
iq2_020	10	1200	600	symmetric	0.219	0.310	0.021	668
iq2_021	1	1200	300	symmetric	0.394	0.503	0.022	481
iq2_022	2	1200	300	symmetric	0.397	0.500	0.021	476
iq2_023	3	1200	300	symmetric	0.400	0.500	0.019	474
iq2_024	4	1200	300	symmetric	0.392	0.499	0.019	479
iq2_025	5	1200	300	symmetric	0.393	0.499	0.023	476
iq2_026	6	1200	300	symmetric	0.396	0.500	0.019	475
iq2_027	7	1200	300	symmetric	0.398	0.498	0.019	476
iq2_028	8	1200	300	symmetric	0.393	0.497	0.020	478
iq2_029	9	1200	300	symmetric	0.401	0.492	0.019	482
iq2_030	10	1200	300	symmetric	0.397	0.499	0.017	476
iq2_031	1	1200	1200	asymmetric	0.068	0.076	0.021	900
iq2_032	2	1200	1200	asymmetric	0.061	0.074	0.022	883
iq2_033	3	1200	1200	asymmetric	0.064	0.069	0.020	884
iq2_034	4	1200	1200	asymmetric	0.067	0.075	0.020	888
iq2_035	5	1200	1200	asymmetric	0.065	0.075	0.022	878
iq2_036	6	1200	1200	asymmetric	0.066	0.068	0.020	887
iq2_037	7	1200	1200	asymmetric	0.065	0.070	0.020	885
iq2_038	8	1200	1200	asymmetric	0.062	0.075	0.020	883
iq2_039	9	1200	1200	asymmetric	0.063	0.071	0.020	881
iq2_040	10	1200	1200	asymmetric	0.068	0.071	0.018	889
iq2_041	1	1200	600	asymmetric	0.157	0.224	0.016	743
iq2_042	2	1200	600	asymmetric	0.156	0.222	0.017	732
iq2_043	3	1200	600	asymmetric	0.157	0.219	0.015	731
iq2_044	4	1200	600	asymmetric	0.155	0.222	0.014	737
iq2_045	5	1200	600	asymmetric	0.154	0.221	0.016	730
iq2_046	6	1200	600	asymmetric	0.157	0.218	0.015	735
iq2_047	7	1200	600	asymmetric	0.158	0.218	0.014	734
iq2_048	8	1200	600	asymmetric	0.156	0.222	0.013	732
iq2_049	9	1200	600	asymmetric	0.158	0.217	0.013	734
iq2_050	10	1200	600	asymmetric	0.159	0.222	0.012	735
iq2_051	1	1200	300	asymmetric	0.281	0.379	0.013	591
iq2_052	2	1200	300	asymmetric	0.282	0.376	0.013	584
iq2_053	3	1200	300	asymmetric	0.284	0.375	0.012	582
iq2_054	4	1200	300	asymmetric	0.280	0.376	0.011	587
iq2_055	5	1200	300	asymmetric	0.278	0.374	0.013	581
iq2_056	6	1200	300	asymmetric	0.281	0.374	0.012	585
iq2_057	7	1200	300	asymmetric	0.285	0.372	0.012	586
iq2_058	8	1200	300	asymmetric	0.282	0.376	0.011	583
iq2_059	9	1200	300	asymmetric	0.286	0.369	0.011	588
iq2_060	10	1200	300	asymmetric	0.284	0.377	0.010	584

Table 35. Intent quality 4 time and altitude interval parameter sensitivity runs with symmetric and asymmetric trajectory predictions.

Run	T_{pred} [s]	T_{int} [s]	Symmetric/ Asymmetric	Δt_{Q4}	Δalt_{Q4}	P_{FA}	P_{MA}	P_{MD}	$\Delta t_{LOS,mean}$ [s]
iq2_061	600	600	symmetric	15	1000	0.037	0.049	0.025	501
iq2_062	600	600	symmetric	30	1000	0.037	0.050	0.026	500
iq2_063	600	600	symmetric	45	1000	0.037	0.050	0.026	500
iq2_064	600	600	symmetric	60	1000	0.038	0.051	0.026	500
iq2_065	600	600	symmetric	75	1000	0.038	0.051	0.026	500
iq2_066	600	600	symmetric	90	1000	0.038	0.052	0.026	500
iq2_067	600	600	symmetric	120	1000	0.038	0.053	0.026	500
iq2_068	600	600	symmetric	180	1000	0.039	0.054	0.027	500
iq2_069	600	600	symmetric	300	1000	0.044	0.058	0.028	500
iq2_070	600	600	symmetric	120	100	0.037	0.047	0.022	500
iq2_071	600	600	symmetric	120	200	0.037	0.047	0.023	500
iq2_072	600	600	symmetric	120	300	0.037	0.048	0.024	500
iq2_073	600	600	symmetric	120	400	0.037	0.049	0.024	500
iq2_074	600	600	symmetric	120	500	0.037	0.050	0.025	500
iq2_075	600	600	symmetric	120	750	0.038	0.050	0.025	500
iq2_076	600	600	symmetric	120	1000	0.038	0.053	0.026	500
iq2_077	600	600	symmetric	120	2000	0.040	0.059	0.028	500
iq2_078	600	600	symmetric	120	5000	0.047	0.068	0.030	498
iq2_079	600	600	asymmetric	15	1000	0.023	0.028	0.014	503
iq2_080	600	600	asymmetric	30	1000	0.023	0.029	0.014	503
iq2_081	600	600	asymmetric	45	1000	0.023	0.029	0.015	502
iq2_082	600	600	asymmetric	60	1000	0.024	0.029	0.015	503
iq2_083	600	600	asymmetric	75	1000	0.024	0.030	0.015	502
iq2_084	600	600	asymmetric	90	1000	0.024	0.030	0.015	502
iq2_085	600	600	asymmetric	120	1000	0.024	0.031	0.015	502
iq2_086	600	600	asymmetric	180	1000	0.025	0.032	0.015	502
iq2_087	600	600	asymmetric	300	1000	0.029	0.035	0.016	502
iq2_088	600	600	asymmetric	120	100	0.023	0.027	0.013	502
iq2_089	600	600	asymmetric	120	200	0.023	0.027	0.013	502
iq2_090	600	600	asymmetric	120	300	0.023	0.028	0.013	502
iq2_091	600	600	asymmetric	120	400	0.023	0.028	0.013	502
iq2_092	600	600	asymmetric	120	500	0.023	0.029	0.014	502
iq2_093	600	600	asymmetric	120	750	0.024	0.029	0.014	502
iq2_094	600	600	asymmetric	120	1000	0.024	0.031	0.015	502
iq2_095	600	600	asymmetric	120	2000	0.026	0.035	0.016	502
iq2_096	600	600	asymmetric	120	5000	0.030	0.041	0.017	501

Table 36. CD performance metric variability to different scenario randomizations with 1200s CD horizon, horizontal and vertical intent quality levels of 3, and 3 intent horizons – symmetric and asymmetric predictions.

	P_{FA}		P_{MA}		P_{MD}		$\Delta t_{LOS,mean}$ [s]	
Case	**Mean**	**Std. Dev.**	**Mean**	**Std. Dev.**	**Mean**	**Std. Dev.**	**Mean**	**Std. Dev.**
1200 s Intent Horizon - Symmetric	0.086	0.00284	0.108	0.00376	0.033	0.00261	879	6.12
1200 s Intent Horizon - Asymmetric	0.065	0.00245	0.072	0.00285	0.020	0.00109	886	5.89
600 s Intent Horizon - Symmetric	0.217	0.00205	0.310	0.00245	0.024	0.00226	668	3.21
600 s Intent Horizon - Asymmetric	0.157	0.00153	0.221	0.00234	0.014	0.00142	734	3.74
300 s Intent Horizon - Symmetric	0.396	0.00322	0.499	0.00287	0.020	0.00163	477	2.61
300 s Intent Horizon - Asymmetric	0.282	0.00246	0.375	0.00277	0.012	0.00106	585	2.86

Level and Quality of Intent Information Results Figures

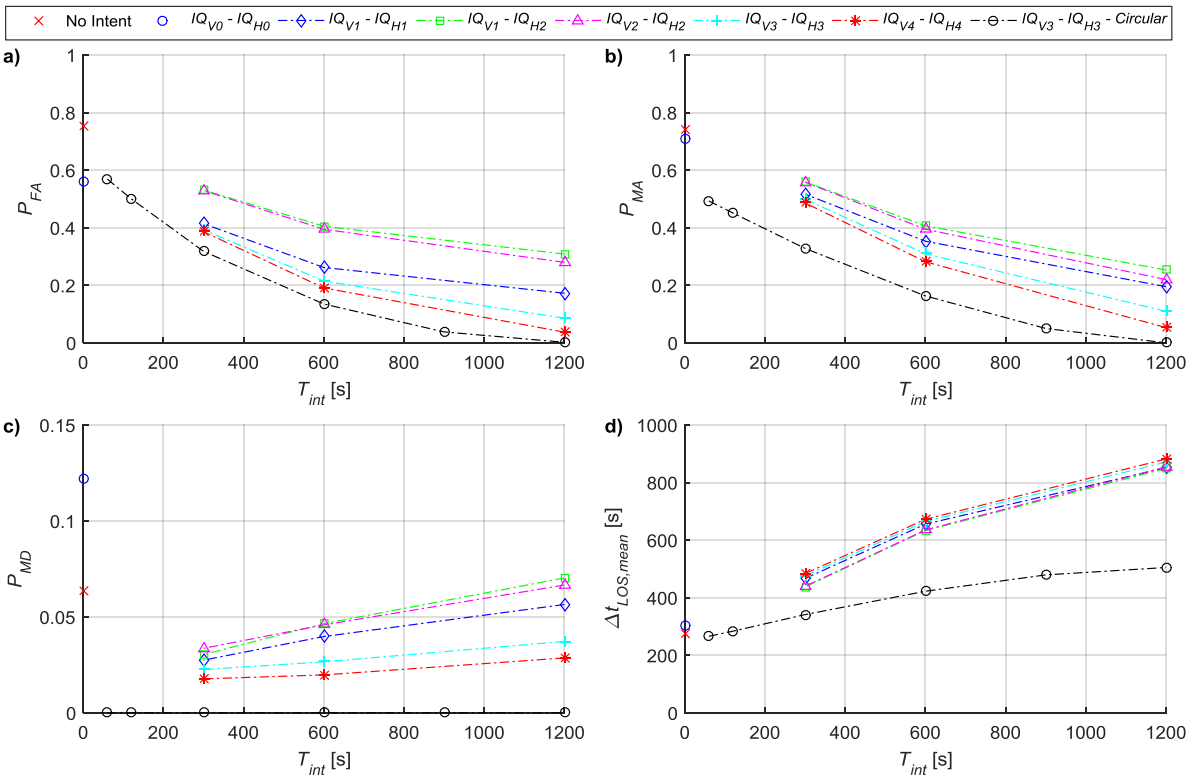

Figure 41. CD performance metrics versus intent horizon for various intent quality levels, with long CD and trajectory prediction horizon (1200 s), symmetric predictions, and 60 second CD cycle period.

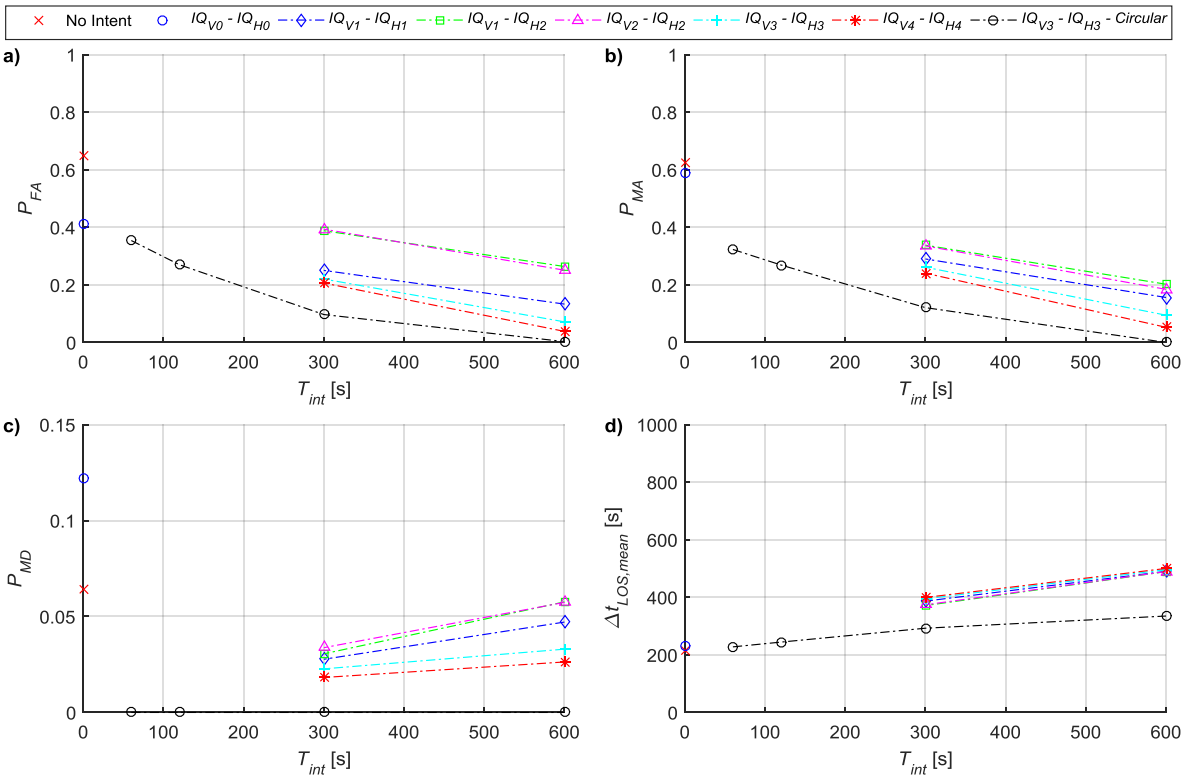

Figure 42. CD performance metrics versus intent horizon for various intent quality levels, with medium CD and trajectory prediction horizon (600 s), symmetric predictions, and 60 second CD cycle period.

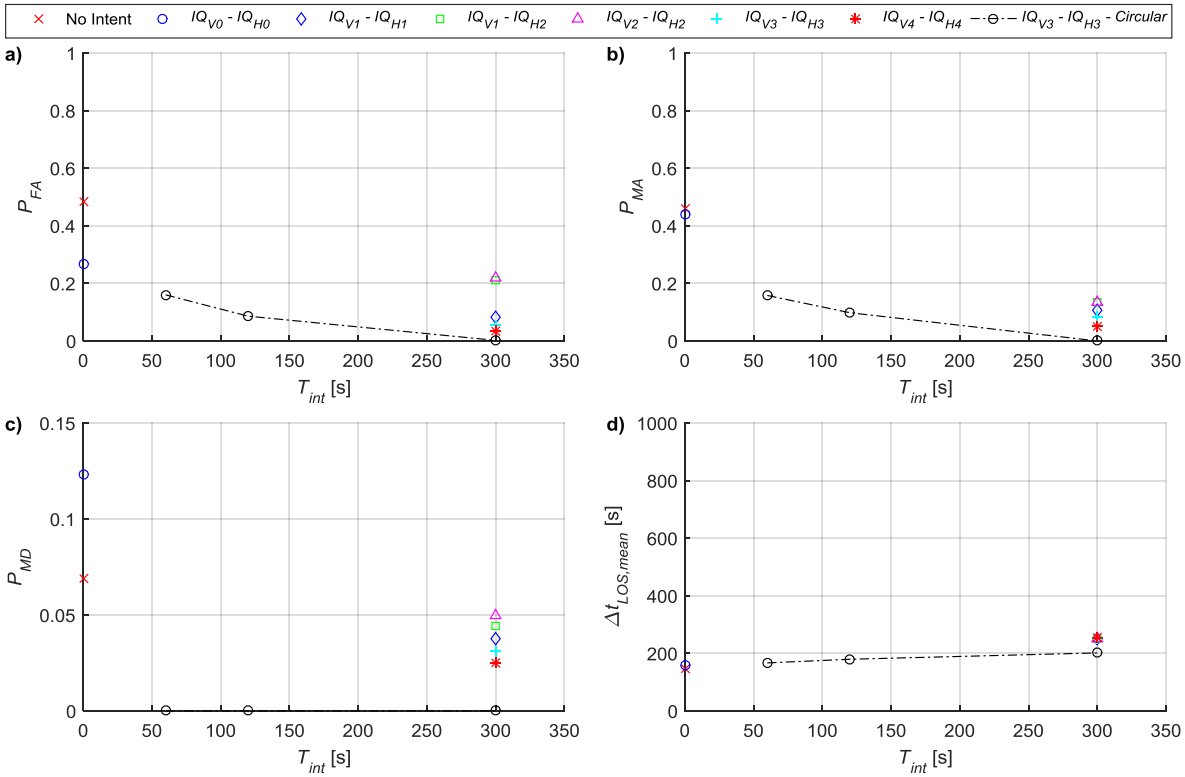

Figure 43. CD performance metrics versus intent horizon for various intent quality levels, with short CD and trajectory prediction horizon (300 s), symmetric predictions, and 60 second CD cycle period.

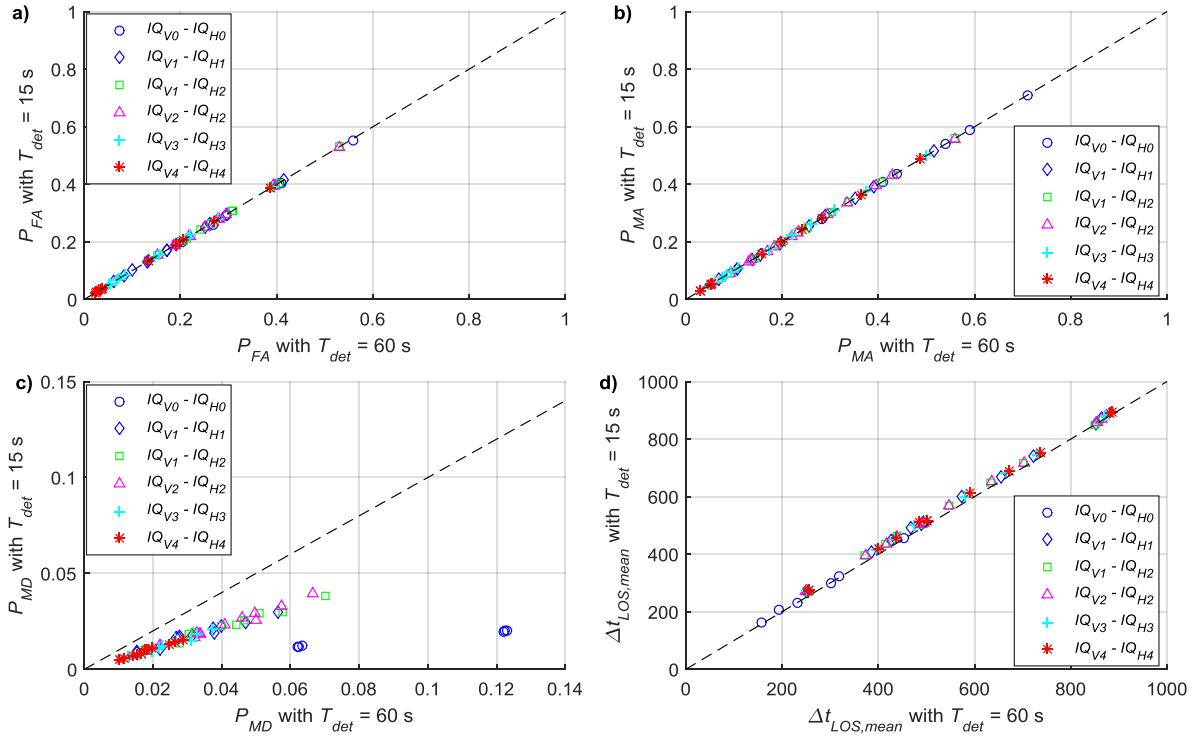

Figure 44. Difference in CD performance metrics between a CD cycle period of 15 seconds and a CD cycle period of 60 seconds over all IQ1 intent quality analysis runs.

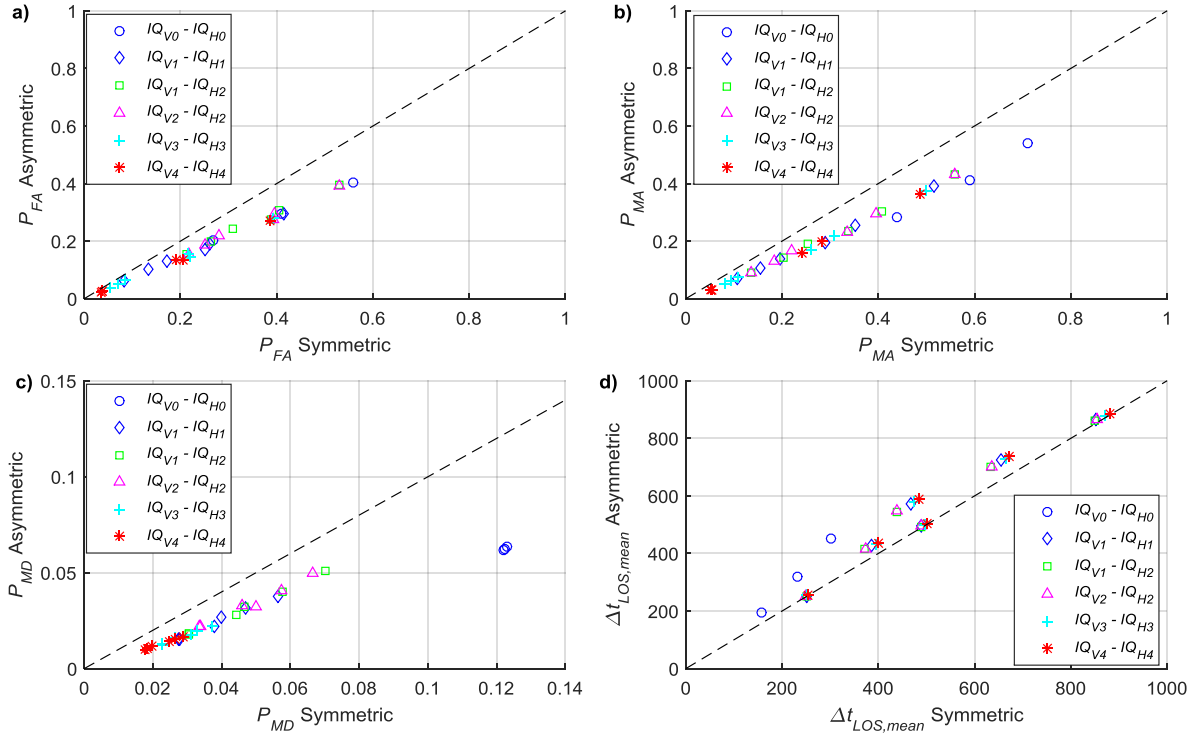

Figure 45. Difference in CD performance metrics between symmetric and asymmetric trajectory predictions over all IQ1 intent quality analysis runs with CD cycle period of 60 seconds.

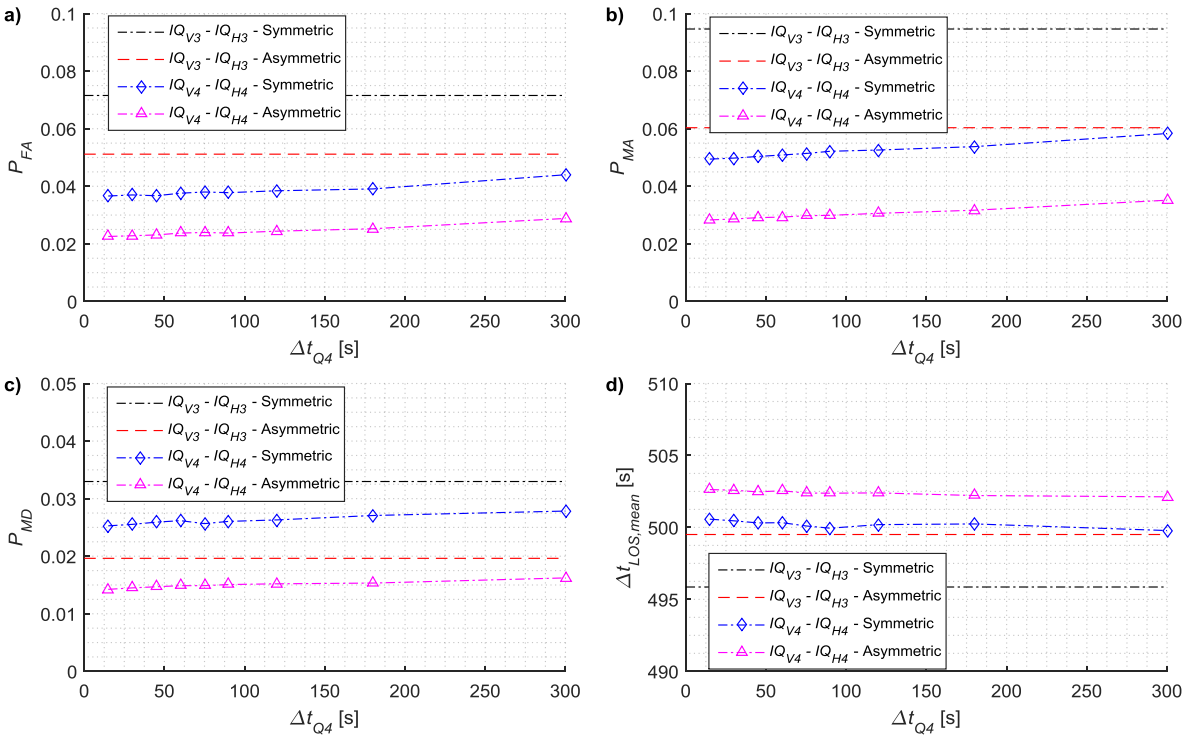

Figure 46. CD performance metrics sensitivity to the time interval for intent quality 4 horizontal points with vertical quality 4 altitude interval of 1000 ft.

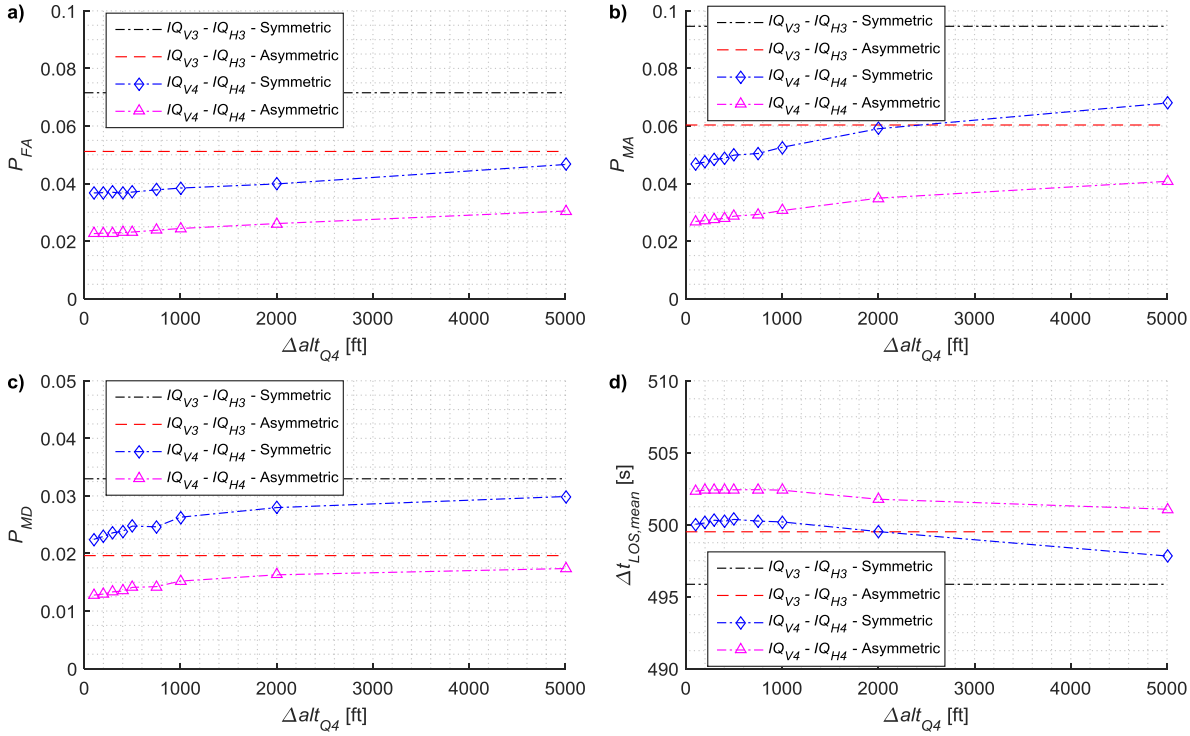

Figure 47. CD performance metrics sensitivity to the altitude interval for intent quality 4 vertical points with horizontal quality 4 time interval of 120 seconds.

References

[1]Bilimoria, K.D., "Survey of Air/Ground and Human/Automation Functional Allocation for Separation Assurance," *12th AIAA Aviation Technology, Integration, and Operations (ATIO) Conference and 17th AIAA/ISSM*, Indianapolis, Indiana, September 17-19, 2012.

[2]Lauderdale, T.A., Cone, A.C., Bowe, A.R., "Relative Significance of Trajectory Prediction Errors on an Automated Separation Assurance Algorithm," *Ninth UAS/Europe Air Traffic Management Research and Development Seminar (ATM2011)*, Berlin, Germany, 14-17 June 2011.

[3]Yang, L.C., Kuchar, J.K., *Aircraft Conflict Analysis and Real-Time Conflict Probing Using Probabilistic Trajectory Modeling*, Dept. of Aeronautics and Astronautics, Massachusetts Institute of Technology, Cambridge, MA, 2000.

[4]Kuchar, J.K., Yang, L.C., "A Review of Conflict Detection and Resolution Modeling Methods," *IEEE Transactions on Intelligent Transportation Systems*, Vol. 1. No. 4, December, 2000.

[5]Krozel, J., Peters, M.E., "Conflict Detection and Resolution for Future Air Transportation Management," *NASA Technical Report, NAS2-14285*, April, 1997.

[6]Karr, D.A., Vivona, R.A., "Conflict Detection Using Variable Four-Dimensional Uncertainty Bounds to Control Missed Alerts," *AIAA Guidance Navigation, and Control Conference and Exhibit*, Keystone, Colorado, August 21-24, 2006.

[7]Wickens, C.D., et.al., "False Alerts in Air Traffic Control Conflict Alerting System: Is There a 'Cry Wolf' Effect?" *HUMAN FACTORS*, Vol. 51, No. 4, August 2009, pp. 446-462.

[8]Thomas, L.C., Wickens, C.D., Rantanen, E.M., "Imperfect Automation in Air Traffic Alerts: A Review of Conflict Detection Algorithms and Their Implications for Human Factors Research," *Proceedings of the 47th Annual Meeting of the Human Factors and Ergonomics Society*, Santa Monica, California, 2003.

[9]Paglione, M.M., Ryan, H.F., Liu, S., "Evaluation of En Route Host Computer System's Tactical Alert Processing: Description and Methodology," Technical Note, US Department of Transportation, Federal Aviation Administration, DOT/FAA/TC/TN07/13, February 2007.

[10]Bilimoria, K.D., "Methodology for the Performance Evaluation of a Conflict Probe," *Journal of Guidance, Control, and Dynamics*, Vol. 24, No. 3, May-June 2001.

[11]Gaydos, T.L., Liao, B., Smith, E.C., Wang, L., "Analysis of Conflict Detection Performance for Trajectory-Based Descent Operations," *Tenth USA/Europe Air Traffic Management Research and Development Seminar (ATM2013)*, Chicago, Illinois, June 10-13, 2013.

[12]Shakarian, A., Haraldsdottir, A., "Required Total System Performance and Results of a Short Term Conflict Alert Simulation Study," *4th US/Europe Air Traffic Management R&D Seminar*, Santa Fe, New Mexico, December 3-7, 2001.

[13]Paielli, R., Erzberger, H., "Improved Conflict Detection for Reducing Operational Errors in Air Traffic Control," *AIAA 4th Aviation Technology, Integration and Operations (ATIO) Forum*, Chicago, Illinois, September 20-22, 2004.

[14]Narkawicz, A., Muñoz, C. "A Formally Verified Conflict Detection Algorithm for Polynomial Trajectories" *Proceedings of the 2015 AIAA Infotech @ Aerospace Conference*, AIAA-2015-0795, January 2015.

[15]Chung, W.W., et. al., "Surveillance and Datalink Communication Performance Analysis for Distributed Separation Assurance System Architectures," *NASA Contractor Report, CR-2012-217590*, July 2012.

[16]Cashion, P., Lozito, S., "The Effects of Different Levels of Intent Information on Pilot Self-Separation Performance," *Proceedings of International Symposium on Aviation Psychology*, 1999.

[17]Lewis, T.A., Phojanamongkolkij, N., Wing, D.J., "The Effects of Limited Intent Information Availability on Self-Separation in Mixed Operations," *2012 Integrated Communications Navigation and Surveillance (ICNS) Conference*, Herndon, Virginia, April 24-26, 2012.

[18]Finkelsztein, D.M., Sturdy, J.L., Alaverdi, O., Hochwarth, J.K., "4D Dynamic Required Navigation Performance Final Report," *NASA Contractor Report, CR-2011-217051*, February, 2011.

[19]Wing, D.J., Barmore, B.E., Krishnamurthy, K., "Use of Traffic Intent Information by Autonomous Aircraft in Constrained Operations," *AIAA Guidance Navigation and Control Conference and Exhibit, AIAA-2002-4555*, Monterey, California, August 5-8, 2002.

[20]Ruigrok, R.C., Clari, M.S., "The Use of Aircraft Intent Information in Airborne Separation Assurance Systems," *FAA-Eurocontrol Third Technical Interchange Meeting (TIM) on Airborne Separation Assurance Systems*, San Francisco, California, October 21-23, 2002.

[21]Paglione, M.M., Oaks, R.D., Bilimoria, K.D., "Methodology for Generating Conflict Scenarios by Time Shifting Recorded Traffic Data," *AIAA's 3rd Annual Aviation Technology, Integration, and Operations (ATIO) Forum*, Denver, Colorado, November 17-19, 2003.

[22]ICAO, *Guidance Material on Comparison of Surveillance Technologies (GMST)*, Edition 1.0, September 2007.

[23]Coppenbarger, R.A., Kanning, G., Salcido, R., "Real-Time Data Link of Aircraft Parameters to the Center-TRACON Automation System (CTAS)," *4th USA/Europe ATM R&D Seminar*, Santa Fe, New Mexico, December 3-7, 2001.

[24]RTCA, Inc., *Minimum Aviation System Performance Standards for Automatic Dependent Surveillance Broadcast (ADS-B)*, RTCA DO-242A, June, 25, 2002.

[25]RTCA, Inc., *Minimum Aviation System Performance Standards for Aircraft Surveillance Applications (ASA)*, RTCA DO-289, Volume I, December 9, 2003.

[26]Federal Aviation Administration, *Aviation System Performance Metrics (ASPM)*, https://aspm.faa.gov/.

[27]Welch, G., Bishop, G., "An Introduction to the Kalman Filter," University of North Carolina at Chapel Hill, UNC-Chapel Hill, TR 95-041, July 24, 2006.

[28]Federal Aviation Administration, *Air Traffic Organizational Policy*, JO 7110.65V, CHG 2, February 19, 2014.

Appendix

A.1. Surveillance Error Modeling

The surveillance error model consisted of standard deviation parameters for a set of Gaussian distributions relating to the level of error on the position and velocity states of an aircraft. Each surveillance technology has its own unique error signature and the choice of Gaussian distributions was chosen for convenience as the simple compromise amongst the many possible error distributions.

A fixed surveillance lag parameter, t_{sl}, was applied equally over all aircraft tracks to simulate the un-compensated time delay that may exist between surveillance sampling time and the time of trajectory prediction. At any conflict detection cycle time, t_{cd}, the true track position states of an aircraft were given by $\boldsymbol{s}(t_{cd})$, where,

$$\boldsymbol{s}(t) = [lat, lon, alt] \tag{13}$$

and the velocity states were given by $\boldsymbol{v}(t_{cd})$, where,

$$\boldsymbol{v}(t) = [gs, vs, trk] \tag{14}$$

Linear interpolation was used to compute a true track data point at the surveillance time when the surveillance lag time was not an integer increment of the recorded track data. During the same conflict detection cycle, the surveillance position estimate used for trajectory prediction, $\hat{\boldsymbol{s}}(t_{cd})$, was given by the true position at surveillance time, $\boldsymbol{s}(t_s) = \boldsymbol{s}(t_{cd} - t_{sl})$, plus the surveillance error components in position and velocity, $\boldsymbol{\varepsilon}_s$ and $\boldsymbol{\varepsilon}_v$, respectively. The surveillance error components were computed using equations (15)-(19) as,

$$[\varepsilon_{lat}(t_s), \varepsilon_{lon}(t_s)] = \boldsymbol{f}_{GCD}\big(lat(t_s), lon(t_s), N(0, \sigma_r), U(0{,}360)\big) - [lat(t_s), lon(t_s)] \tag{15}$$

$$\varepsilon_{alt}(t_s) = N(0, \sigma_a) \tag{16}$$

$$\varepsilon_{gs}(t_s) = N(0, \sigma_{gs}) \tag{17}$$

$$\varepsilon_{vs}(t_s) = N(0, \sigma_{vs}) \tag{18}$$

$$\varepsilon_{trk}(t_s) = N(0, \sigma_{trk}) \tag{19}$$

where the horizontal position error components, $\varepsilon_{lat}(t_s)$ and $\varepsilon_{lon}(t_s)$, were computed using a great-circle projection from the true position at surveillance time, $lat(t_s)$ and $lon(t_s)$, with a radial distance error sampled from a Gaussian distribution, $N(0, \sigma_r)$, and an azimuth sampled from a Uniform distribution, $U(0{,}360)$. The great-circle projection function, $\boldsymbol{f}_{GCD}$, computes a latitude and longitude position projected some arc-distance along an initial track on the surface of a sphere from a starting latitude and longitude position. Finally, the surveillance position and velocity states used at conflict detection time were given by:

$$\hat{\boldsymbol{s}}(t_{cd}) = [lat(t_s) + \varepsilon_{lat}(t_s), lon(t_s) + \varepsilon_{lon}(t_s), alt(t_s) + \varepsilon_{alt}(t_s)] \tag{20}$$

$$\hat{\boldsymbol{v}}(t_{cd}) = [gs(t_s) + \varepsilon_{gs}(t_s), vs(t_s) + \varepsilon_{vs}(t_s), trk(t_s) + \varepsilon_{trk}(t_s)] \tag{21}$$

Figure 2 shows a diagram of the surveillance error modeling described above.

A.2. Some Metrics Issues Associated with Intent

In measuring the performance of an intent-based conflict detector, the problem of deciding whether a specific detected conflict matches a true LOS is more complicated than with a state-based conflict detector. There are several reasons for this complication. The first reason is that, an intent-based conflict detector can return a prediction of more than one future losses-of-separation (multiple detected conflicts with the same aircraft pair within the conflict detection horizon). The second reason is that, there may be several true LOS between a pair of aircraft and a smaller number of predicted LOS. The question arises: which predicted LOS correspond to which true LOS, if any?

Figure 48 illustrates the case where a single loss-of-separation exists but where the intent-based conflict detector predicts multiple conflicts. In this figure, the x-axis represents time and the transition up represents an entry into LOS while a transition down is an exit from LOS, with both the true and predicted cases shown for the same time horizon. It is clear that, at least in some sense, the prediction is incorrect. The times do not match exactly and the prediction goes in and out of loss several times. But in an abstract sense it is really pretty close. An assumption in our metrics is to analyze each predicted loss separately since each LOS is characterized by the entry time into that LOS. In the example below there would be 3 detections and, after applying the same conflict comparison criterion, any number of those could be could be identified as correct alerts. Consequently, the remaining conflicts in a group like this would be labeled as false alerts because they would fail to meet the same conflict comparison criterion. For example, the first two predicted losses could be considered correct alerts to the true LOS if they both satisfy the same conflict comparison criterion whereas, the last predicted conflict does not satisfy the same conflict comparison criterion and is labeled as a false alert.

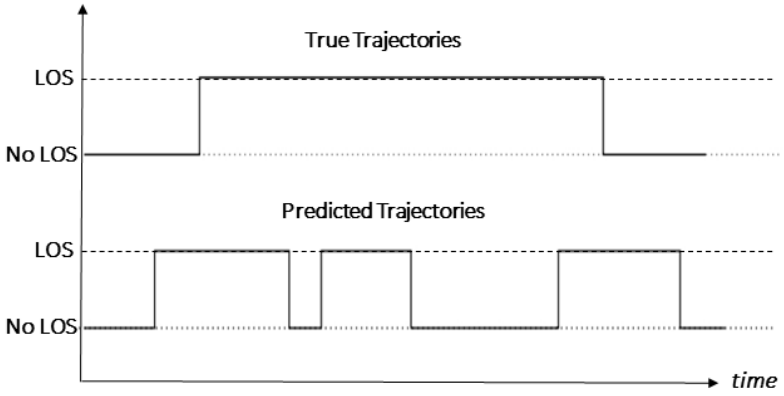

Figure 48. Example single true LOS and multiple predicted LOS.

Figure 49 illustrates the case where multiple losses of separation exist but the intent-based conflict detector predicts only a single conflict. A similar application of the same conflict comparison criteria is used to categorize the predicted and true LOS here. Each predicted LOS is compared sequentially against each true LOS and multiple true LOS could be considered "the same" as a single predicted LOS. In this example, one possibility is that the first true LOS meets the same conflict comparison criterion with respect to the predicted LOS whereas, the second true LOS does not. In this case, the second true LOS would be label as a missed alert and the predicted LOS would be labeled as a correct alert. Another possibility is that neither true LOS meets the same conflict comparison criterion with respect to the predicted LOS. In that case, both true LOS would be labeled as missed alerts and the predicted LOS would be labeled a false alert.

There are many possible and complicated approaches that one could use to try and group the multiple predicted or multiple true LOS together but those were not pursued in this study.

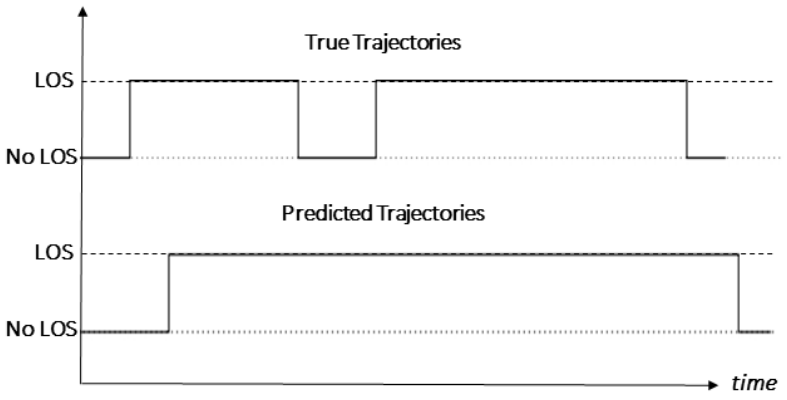

Figure 49. Example multiple true LOS and single predicted LOS.

REPORT DOCUMENTATION PAGE

Form Approved
OMB No. 0704-0188

1. REPORT DATE *(DD-MM-YYYY)*	2. REPORT TYPE	3. DATES COVERED *(From - To)*
01-03-2016	Technical Memorandum	

4. TITLE AND SUBTITLE

Parametric Analysis of Surveillance Quality and Level and Quality of Intent Information and their Impact on Conflict Detection Performance

5a. CONTRACT NUMBER

5b. GRANT NUMBER

5c. PROGRAM ELEMENT NUMBER

6. AUTHOR(S)

Guerreiro, Nelson M.; Butler, Ricky W.; Hagen, George E.; Maddalon, Jeffrey M.; Lewis, Timothy A.

5d. PROJECT NUMBER

5e. TASK NUMBER

5f. WORK UNIT NUMBER

999182.02.20.07.01

7. PERFORMING ORGANIZATION NAME(S) AND ADDRESS(ES)

NASA Langley Research Center
Hampton, VA 23681-2199

8. PERFORMING ORGANIZATION REPORT NUMBER

L-20669

9. SPONSORING/MONITORING AGENCY NAME(S) AND ADDRESS(ES)

National Aeronautics and Space Administration
Washington, DC 20546-0001

10. SPONSOR/MONITOR'S ACRONYM(S)

NASA

11. SPONSOR/MONITOR'S REPORT NUMBER(S)

NASA-TM-2016-219177

12. DISTRIBUTION/AVAILABILITY STATEMENT

Unclassified - Unlimited
Subject Category 03
Availability: NASA STI Program (757) 864-9658

13. SUPPLEMENTARY NOTES

14. ABSTRACT

A loss-of-separation (LOS) is said to occur when two aircraft are spatially too close to one another. A LOS is the fundamental unsafe event to be avoided in air traffic management and conflict detection (CD) is the function that attempts to predict these LOS events. In general, the effectiveness of conflict detection relates to the overall safety and performance of an air traffic management concept. An abstract, parametric analysis was conducted to investigate the impact of surveillance quality, level of intent information, and quality of intent information on conflict detection performance. The data collected in this analysis can be used to estimate the conflict detection performance under alternative future scenarios or alternative allocations of the conflict detection function, based on the quality of the surveillance and intent information under those conditions. Alternatively, this data could also be used to estimate the surveillance and intent information quality required to achieve some desired CD performance as part of the design of a new separation assurance system.

15. SUBJECT TERMS

Conflict detection; Function allocation; Separation assurance; Surveillance intent

16. SECURITY CLASSIFICATION OF:			17. LIMITATION OF ABSTRACT	18. NUMBER OF PAGES	19a. NAME OF RESPONSIBLE PERSON
a. REPORT	b. ABSTRACT	c. THIS PAGE			STI Help Desk (email: help@sti.nasa.gov)
					19b. TELEPHONE NUMBER *(Include area code)*
U	U	U	UU	76	(757) 864-9658